
Ultimate (Resonant) MEMS Sensors

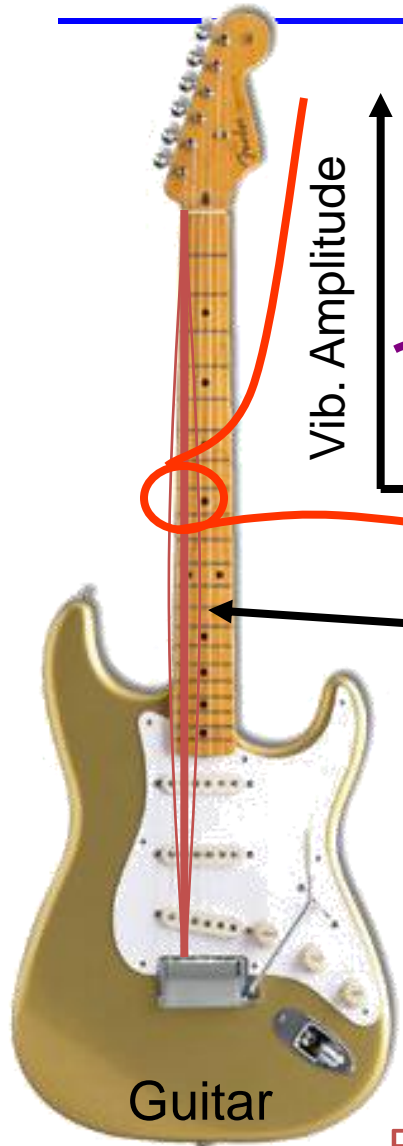
IEEE Sensors 2013 Tutorial Session 1: Novel Trends in Sensing

Siavash Pourkamali

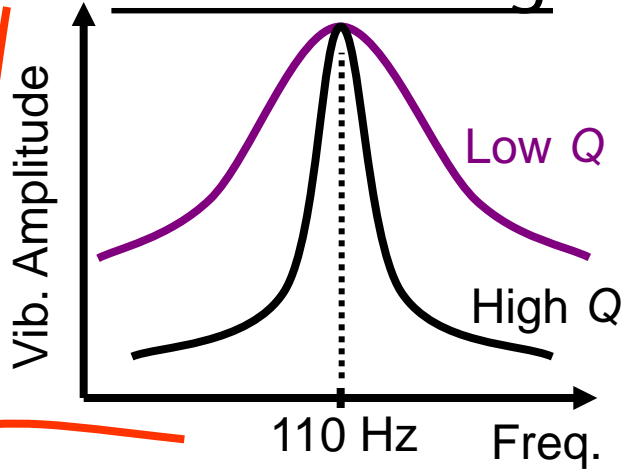
**Department of Electrical Engineering
University of Texas at Dallas**

November 3rd, 2013

What is a MEMS Resonator? Scaling Guitar Strings



Guitar String



Vibrating "A" String (110 Hz)

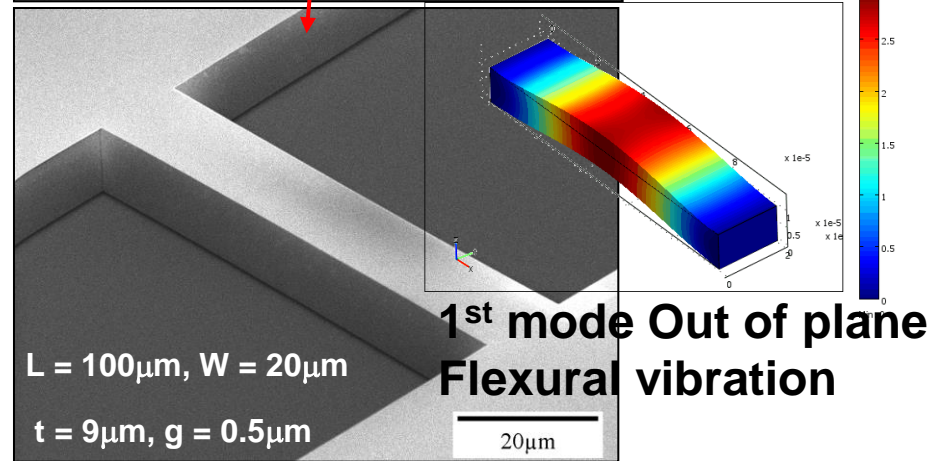
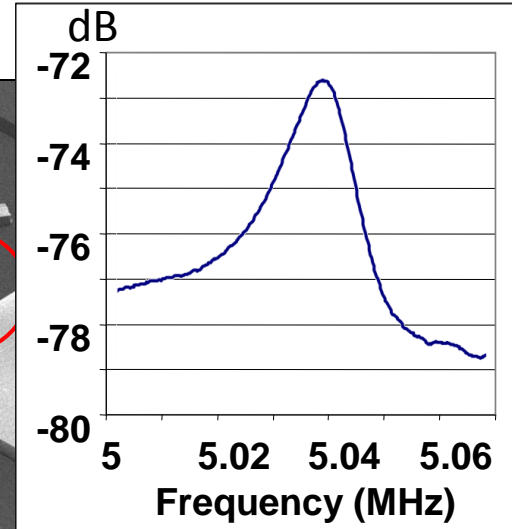
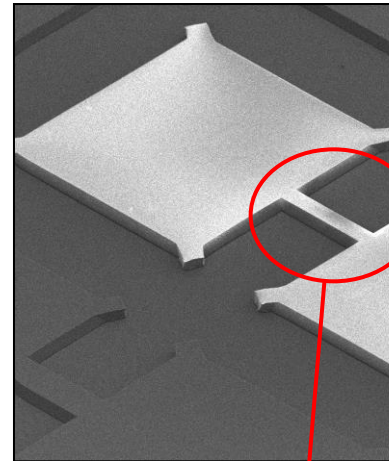
Stiffness

Freq. Equation:

$$f_o = \frac{1}{2\pi} \sqrt{\frac{k_r}{m_r}}$$

Freq.

Mass



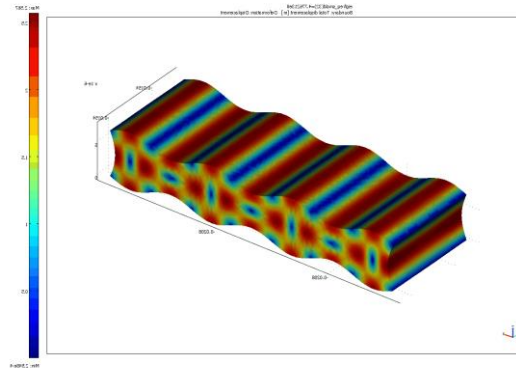
Piezoelectric MEMS Resonators

□ Piezoelectric Actuation

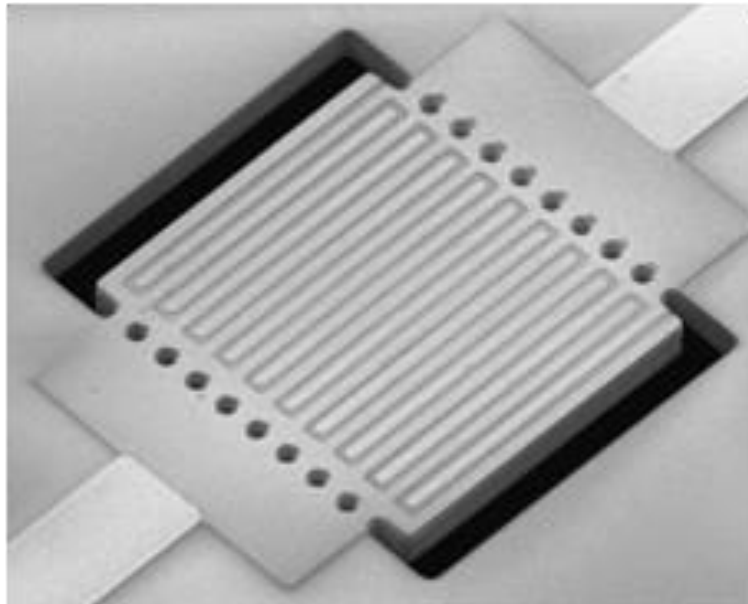
Applied electrical field



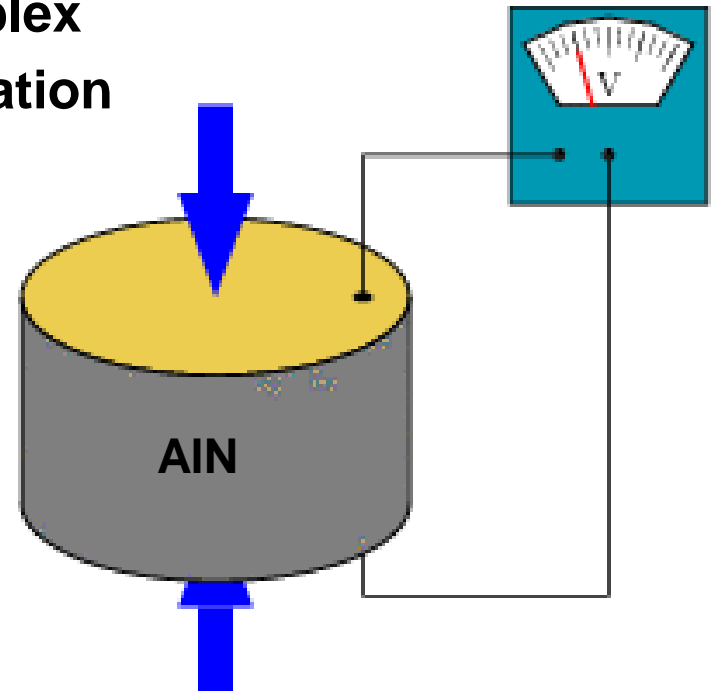
Internal generation of a mechanical force



Finite Element Modal Analysis of a Piezo-Electric Resonator

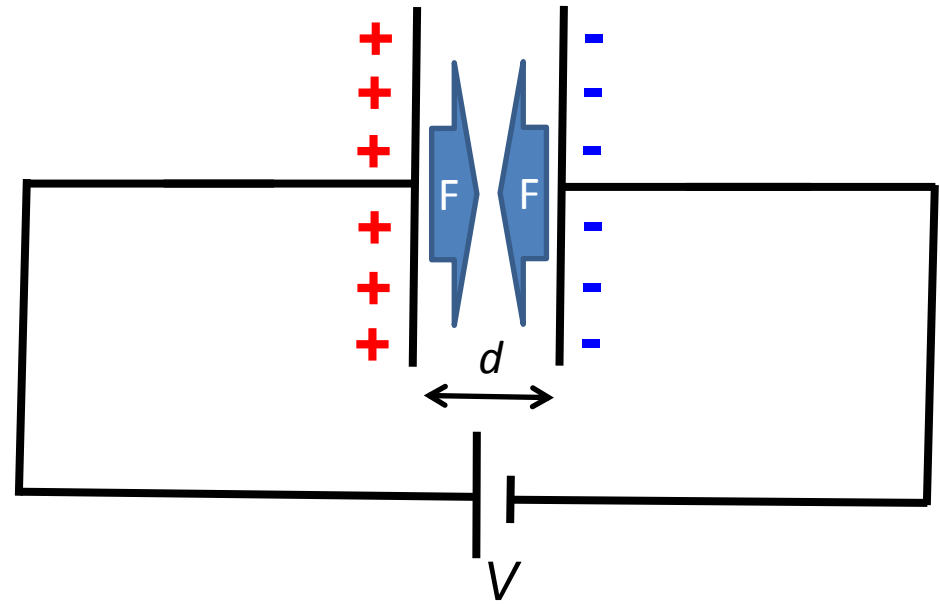
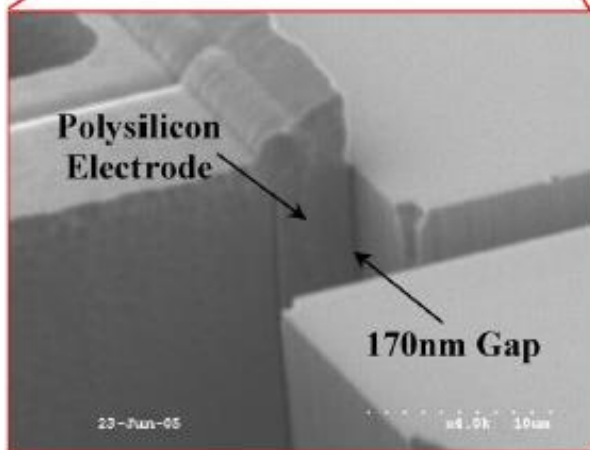
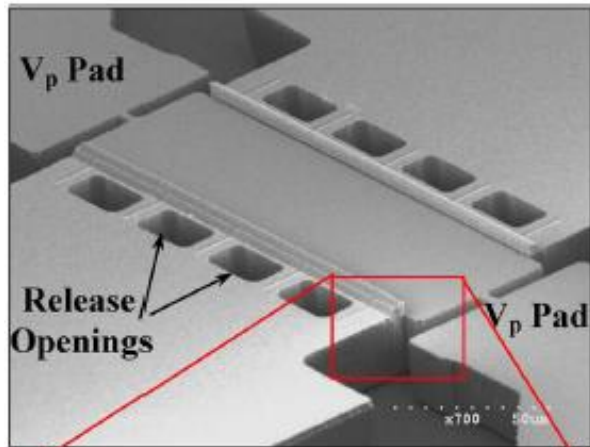


Complex Fabrication



B. Harrington, M. Shahmohammadi, and R. Abdolvand, "Toward Ultimate Performance in GHz MEMS Resonators: Low Impedance and High Q," IEEE MEMS 2010

Electrostatic MEMS Resonators



□ Actuation:

$$F = \frac{V^2 \epsilon_0 A}{2d^2}$$

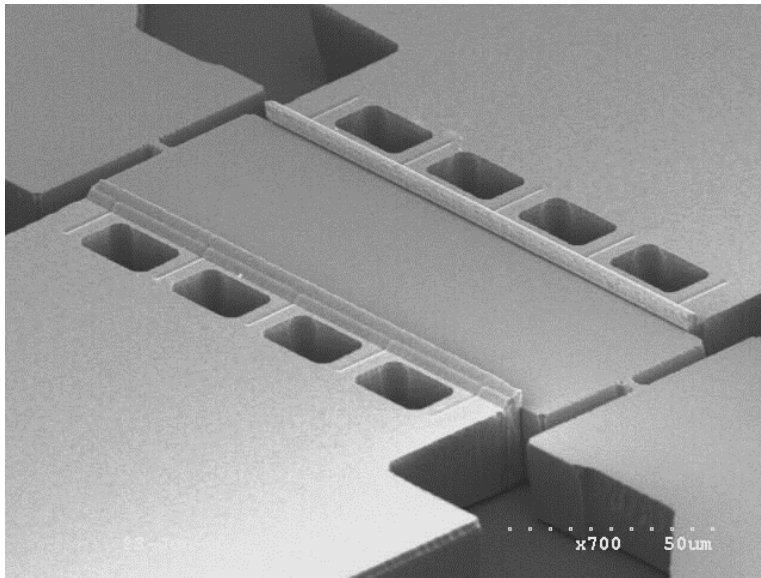
□ Read-out:

$$i_o = V \frac{dC}{dt}$$

Pourkamali et al "Low-Impedance VHF and UHF Capacitive Silicon Bulk Acoustic Wave Resonators-Part I: Concept, IEEE transaction on electron devices

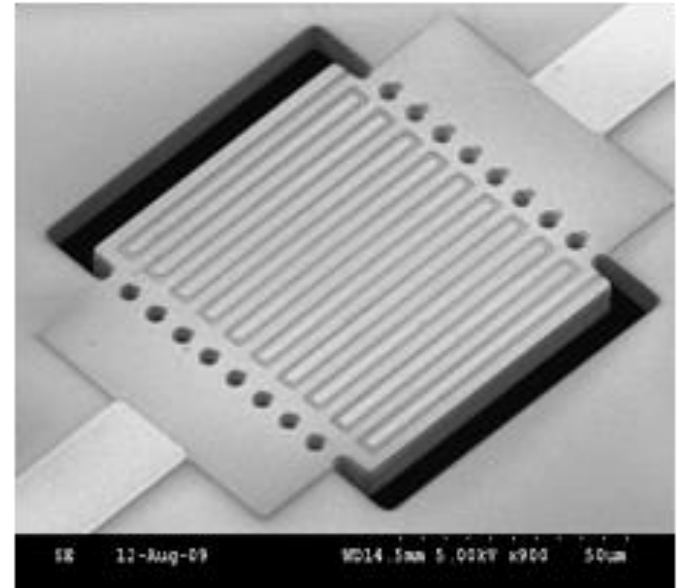
Micro-Resonator Transduction

□ Common Micro-Resonator Transduction Mechanisms:



Capacitive

Piezoelectric



Capacitive Silicon Bulk Acoustic Wave Resonator¹

1GHz AlN on Silicon Piezoelectric Resonator²

¹S. Pourkamali, Z Hao, and F Ayazi, VHF Single Crystal Silicon Capacitive Elliptic Bulk-Mode Disk Resonators—Part I: Implementation and Characterization, JMEMS 2004.

²B. Harrington, M. Shahmohammadi, and R. Abdolvand, "Toward Ultimate Performance in GHz MEMS Resonators: Low Impedance and High Q," IEEE MEMS 2010

Thermal Actuation with Piezo-Resistive Readout

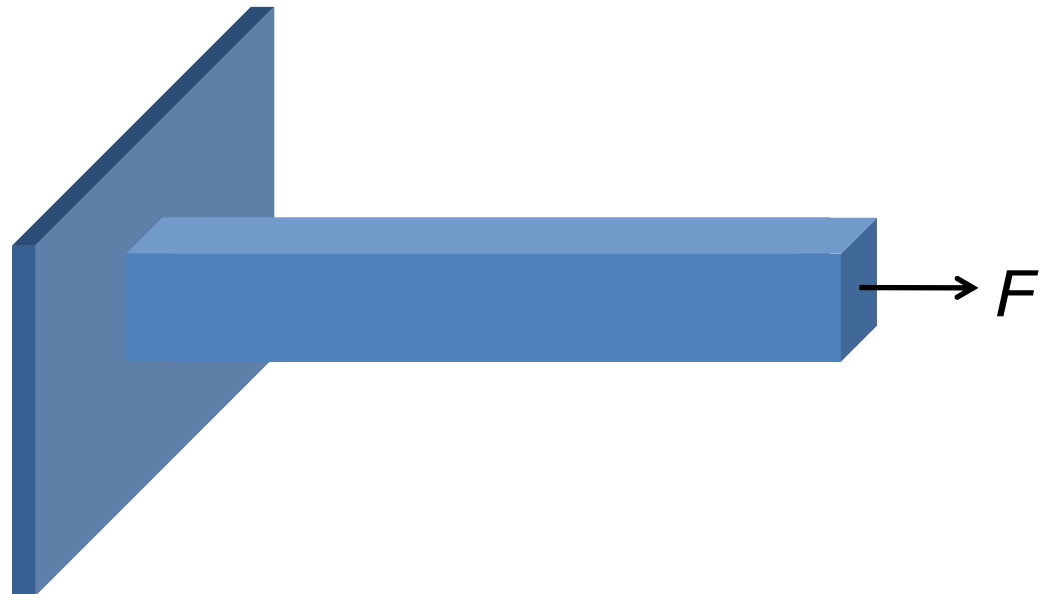
□ Thermal actuation:

$$\Delta L = \alpha L \Delta T$$



□ Piezoresistive Effect:

$$\uparrow \Delta R = R \pi_l \delta_l$$



Thermally Actuated Resonators

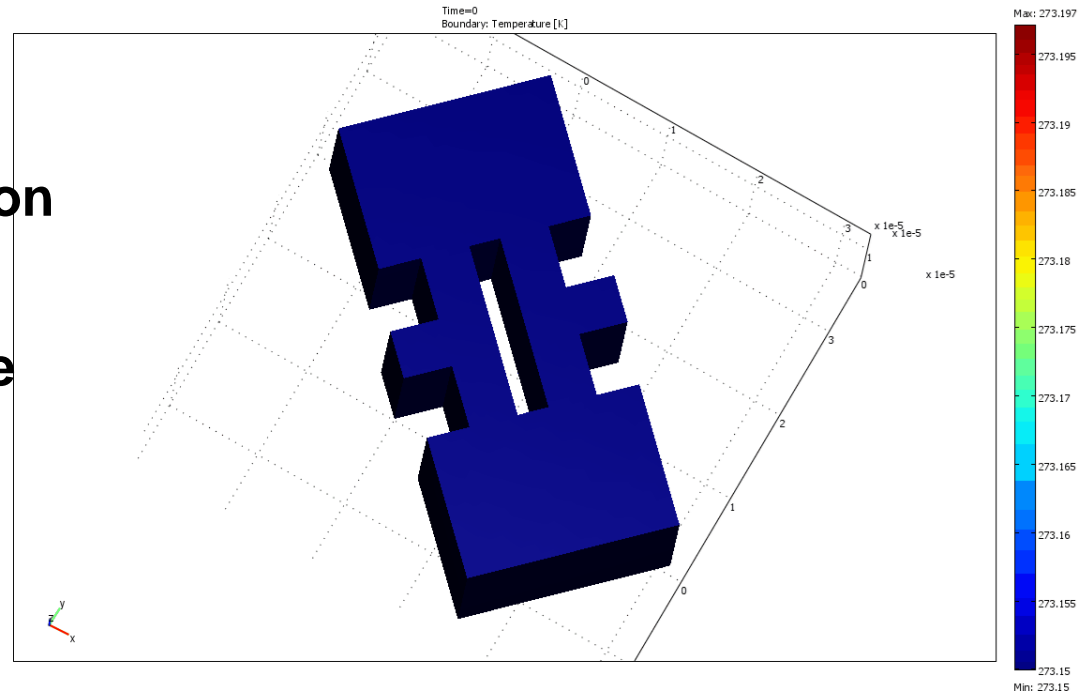
□ Advantages

- Simplicity of fabrication
- Large actuation force
- Low operating voltage
- Robustness

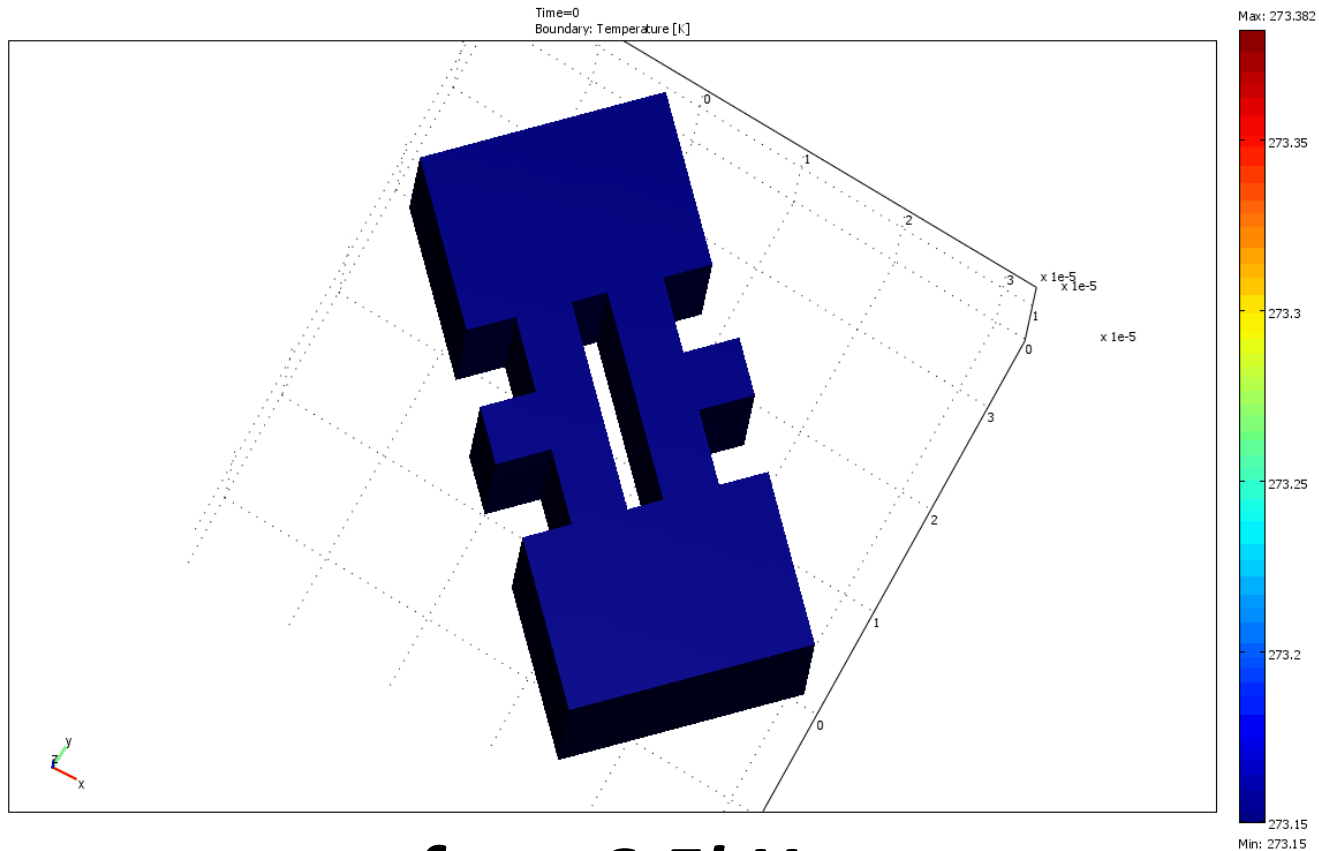
□ Disadvantage

- Power consumption
- Speed?

Usually known as **slow** actuators suitable for **DC** or very **low-frequency** applications



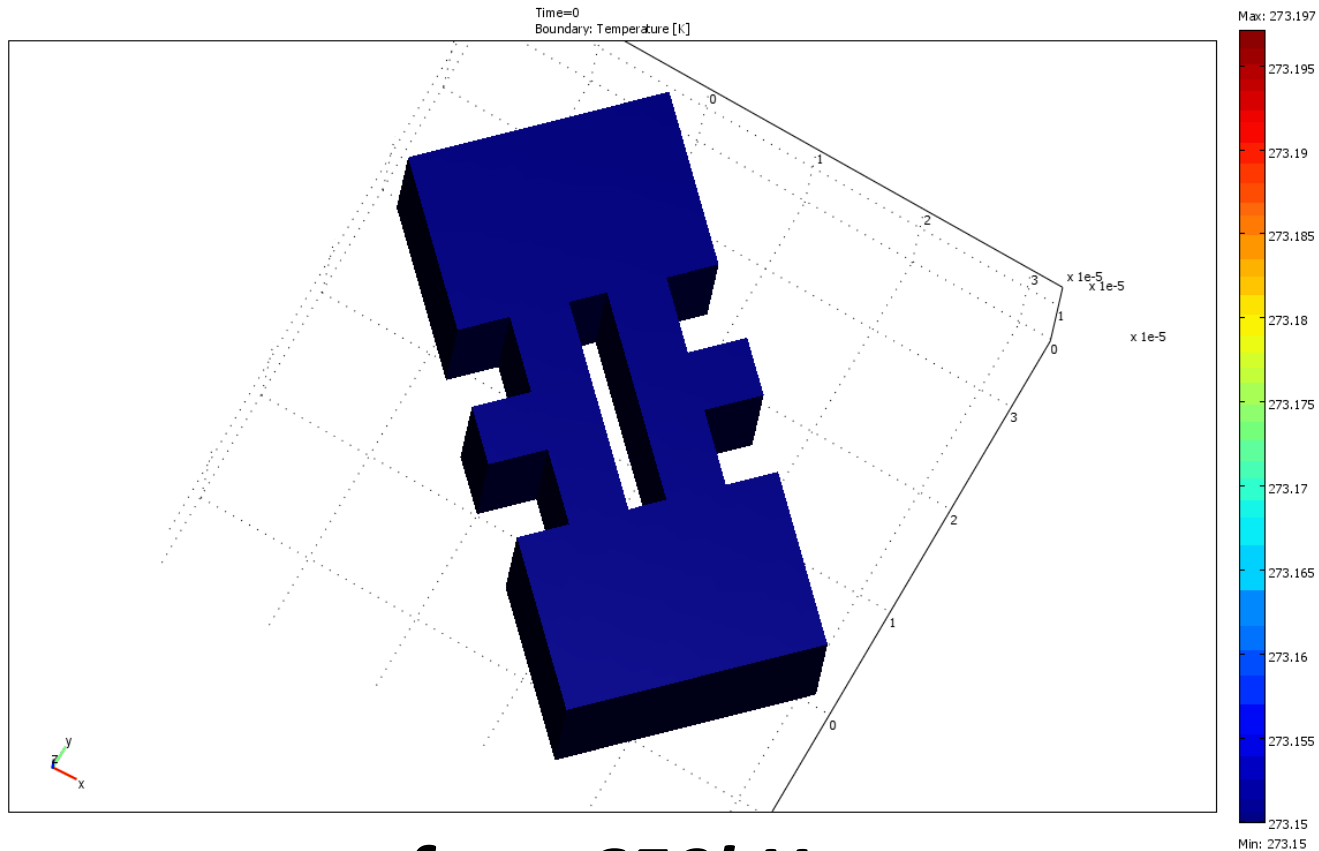
Thermal Time Response



$$f_{act} = 6.5\text{kHz}$$

$$\tau_{Thermal} = 100\mu\text{s} \rightarrow f_{thermal} = 10\text{kHz}$$

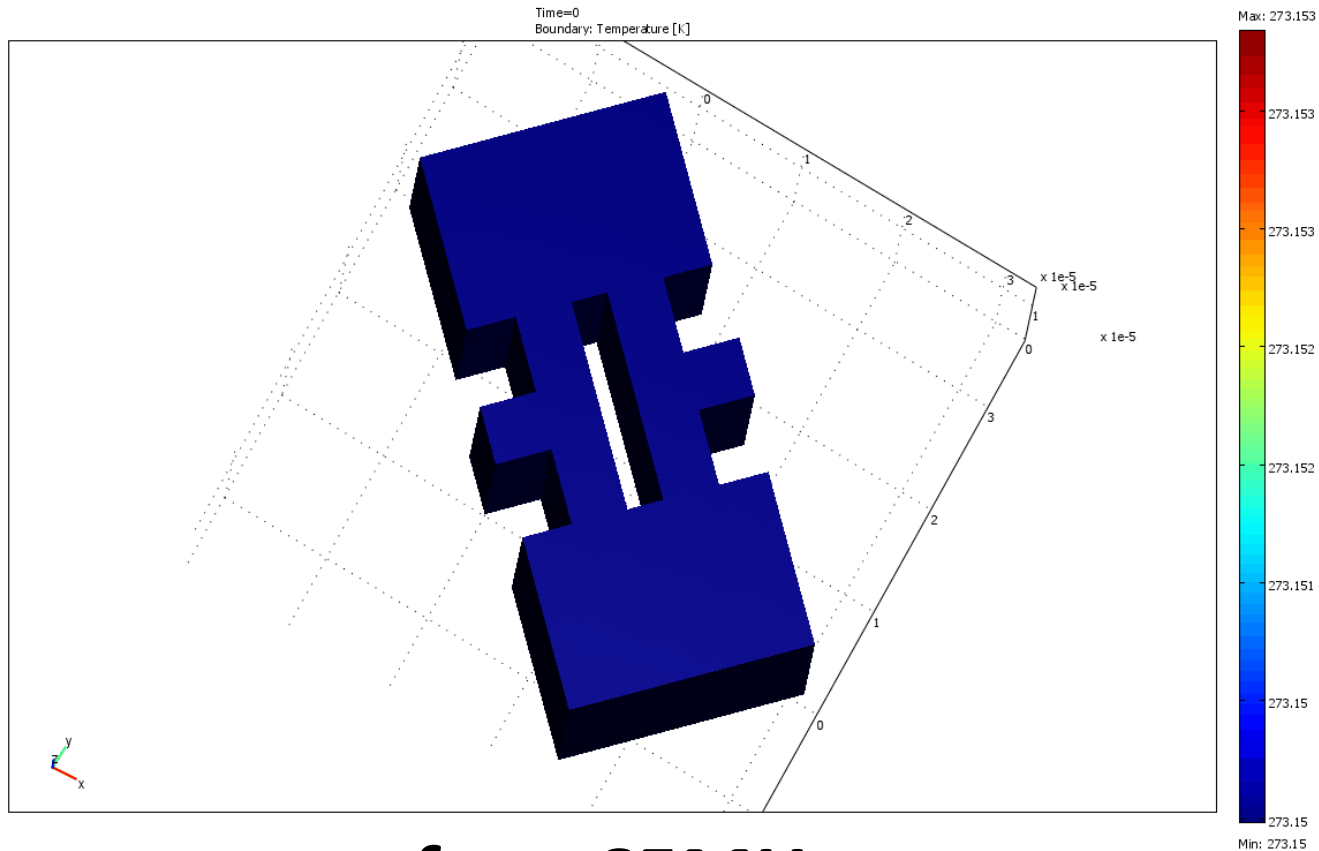
Thermal Time Response



$$f_{act} = 650\text{kHz}$$

$$\tau_{Thermal} = 100\mu\text{s} \rightarrow f_{thermal} = 10\text{kHz}$$

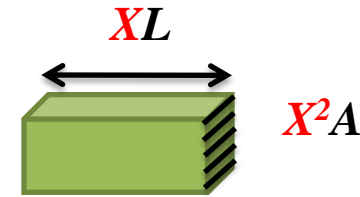
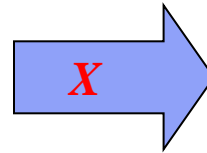
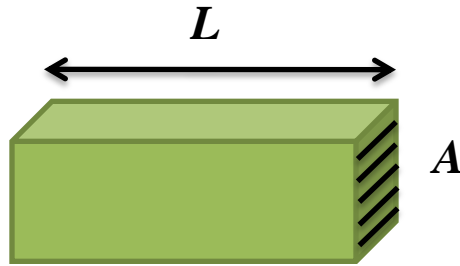
Thermal Time Response



$$f_{act} = 65\text{MHz}$$

$$\tau_{Thermal} = 100\mu\text{s} \rightarrow f_{thermal} = 10\text{kHz}$$

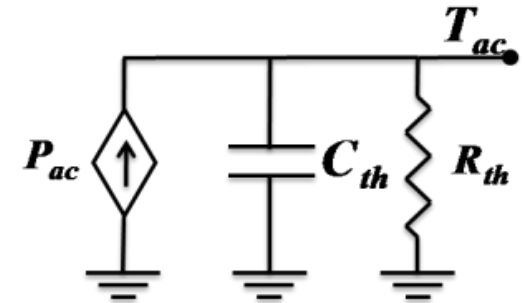
Scaling Behavior of Thermal Actuation



$$\tau_T = R_T C_T \begin{cases} R_T = \rho_T \frac{L}{A} \propto \frac{1}{X} \\ C_T \propto X^3 \end{cases}$$



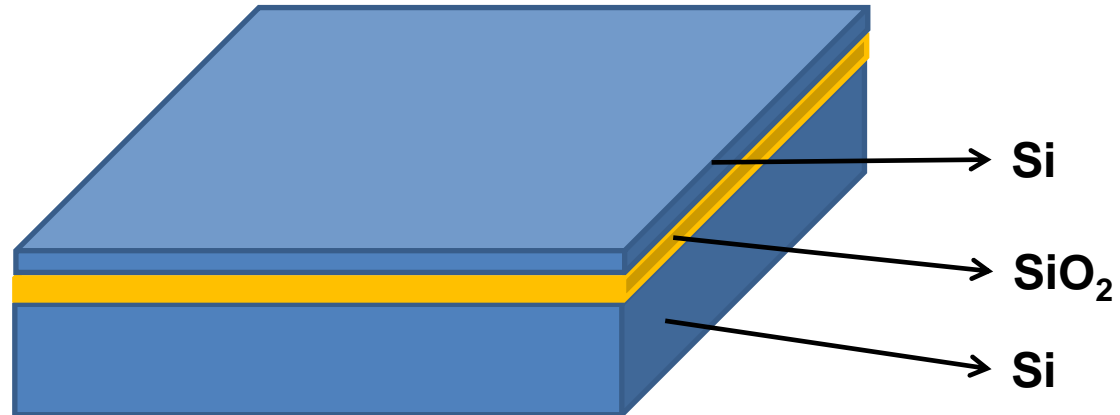
$$\tau_T \propto X^2$$



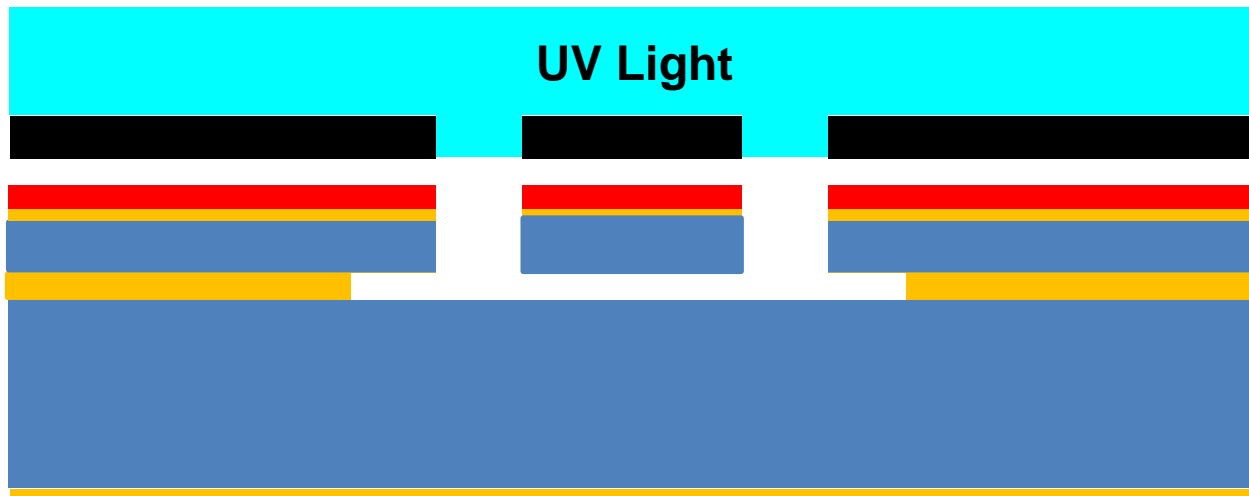
$$\text{Mechanical Time constant} \propto f_m^{-1} \propto X$$

Thermal time constant shrinks faster than mechanical time constant

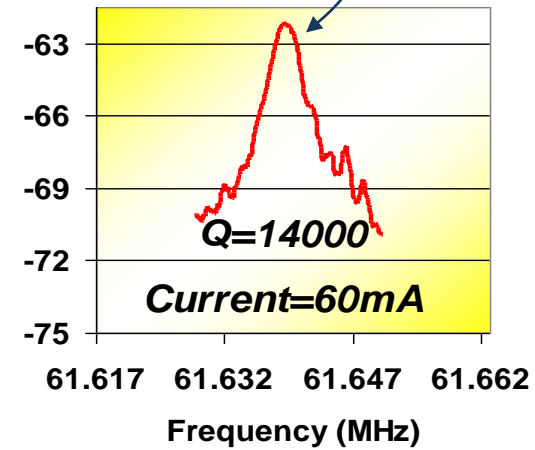
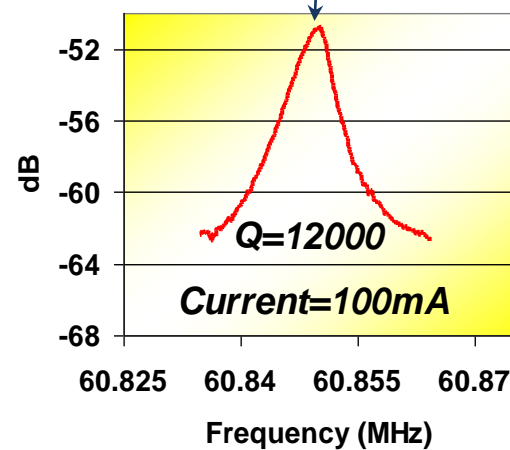
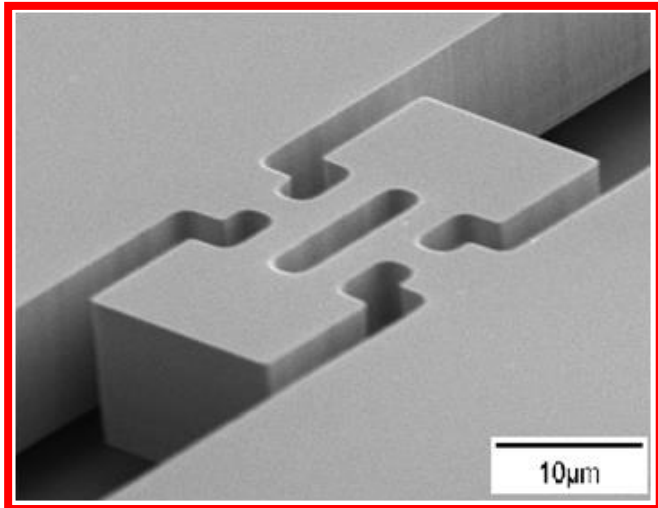
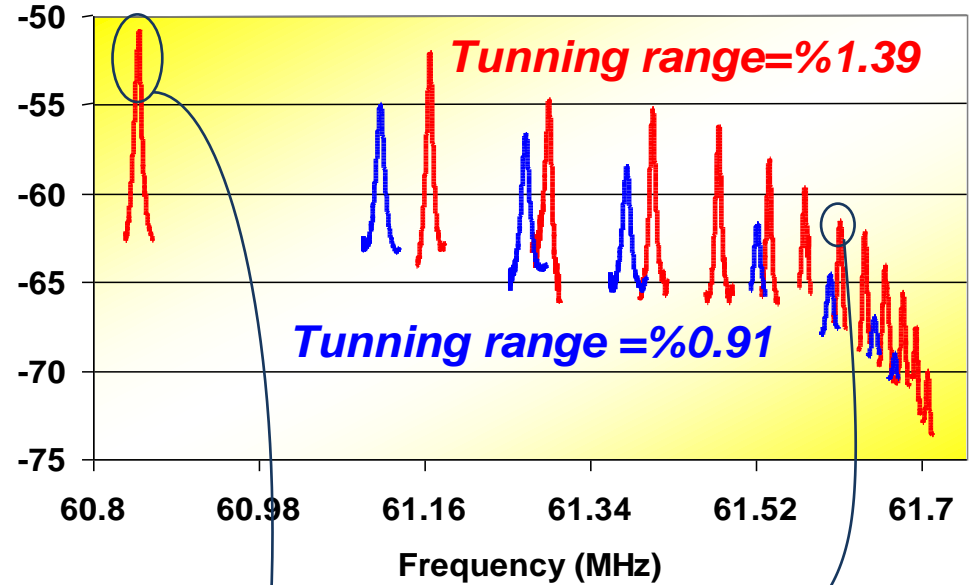
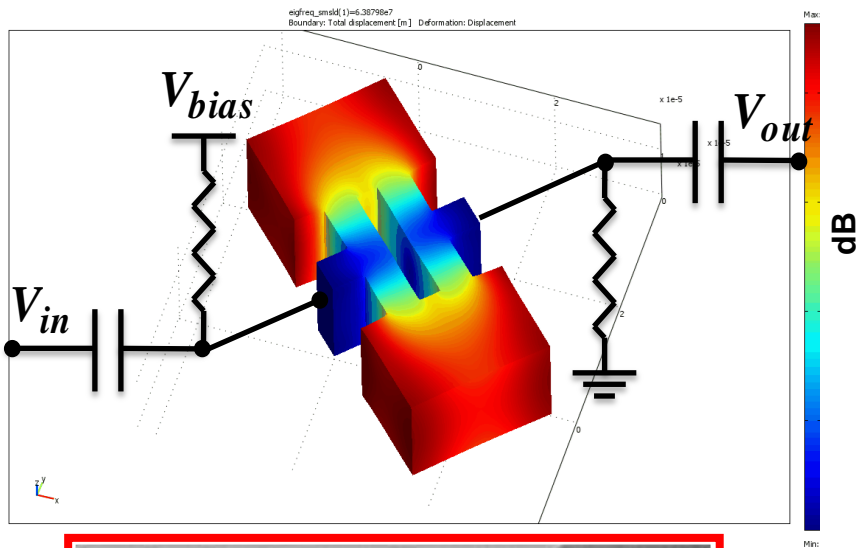
Fabrication Process



~~Spin coating photoresist on SiO₂ layer~~



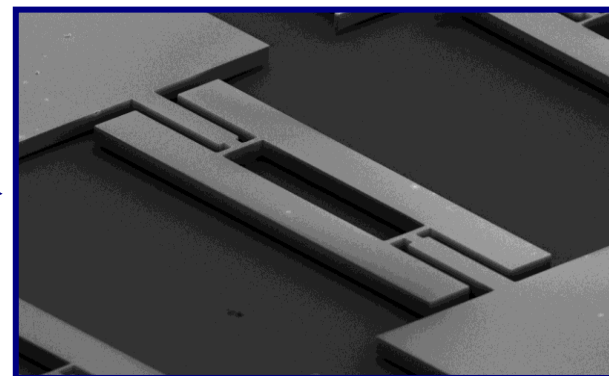
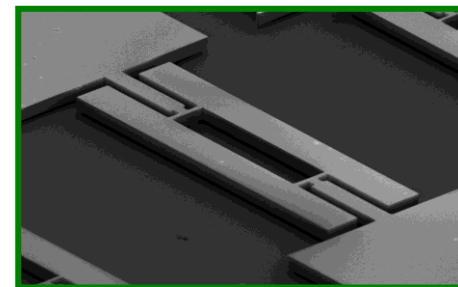
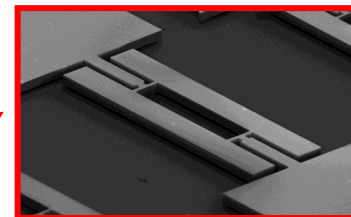
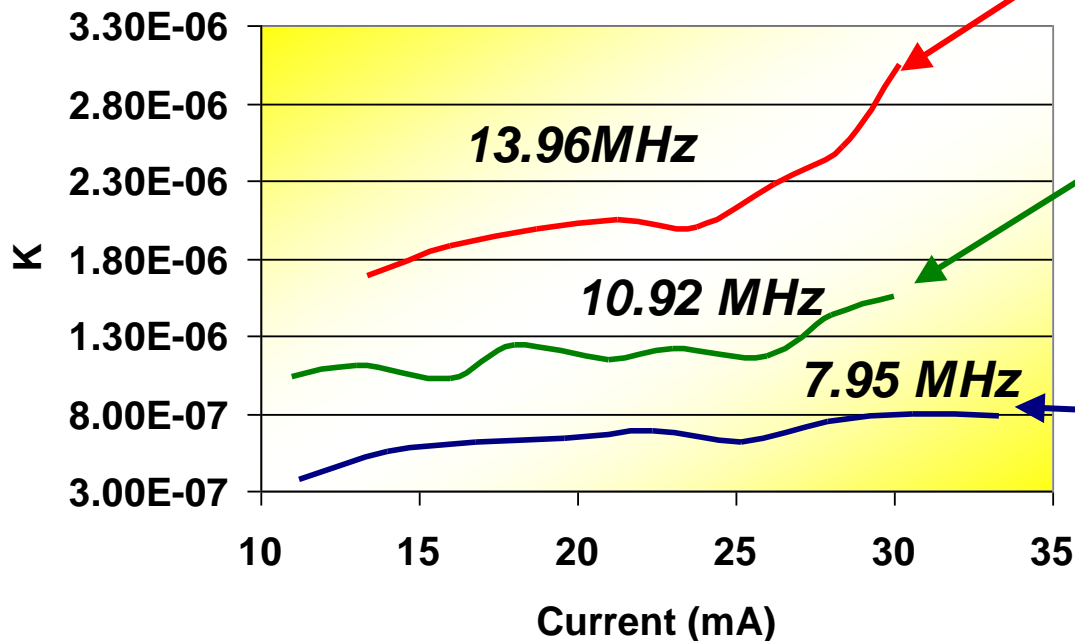
Measurement Results: 61MHz I²-BAR



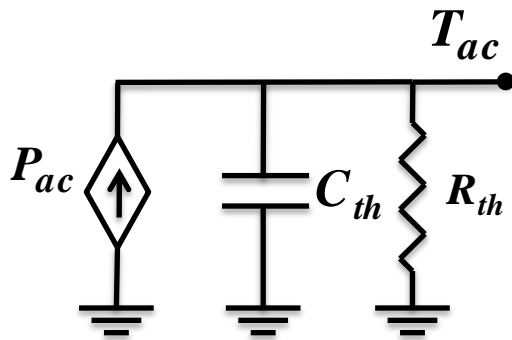
Measurement Results

□ Thermal-Piezoresistive Transduction Coefficient:

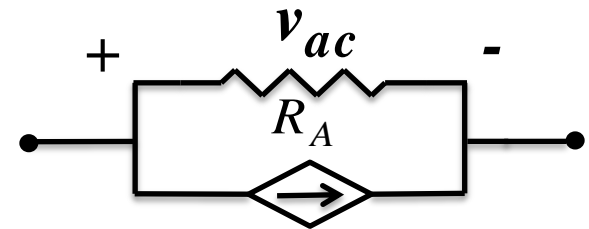
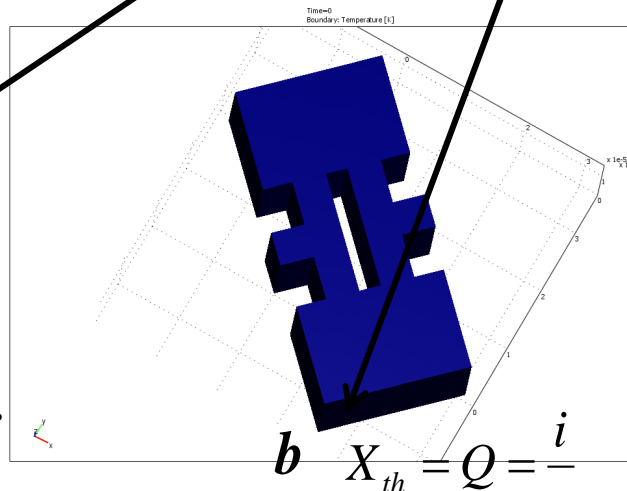
$$K = \frac{g_m}{Q \cdot I_{bias}^2}$$



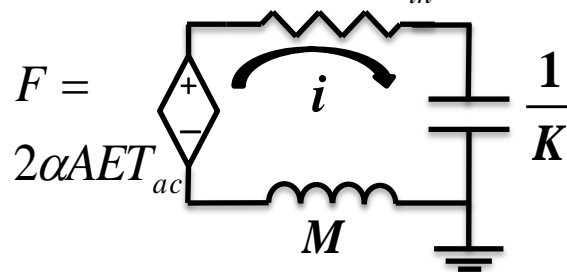
Resonator Operation



Current = Thermal Power
Voltage = Temperature



$$i_{ac} = \frac{X_{th} \pi_l EI_{dc}}{L}$$



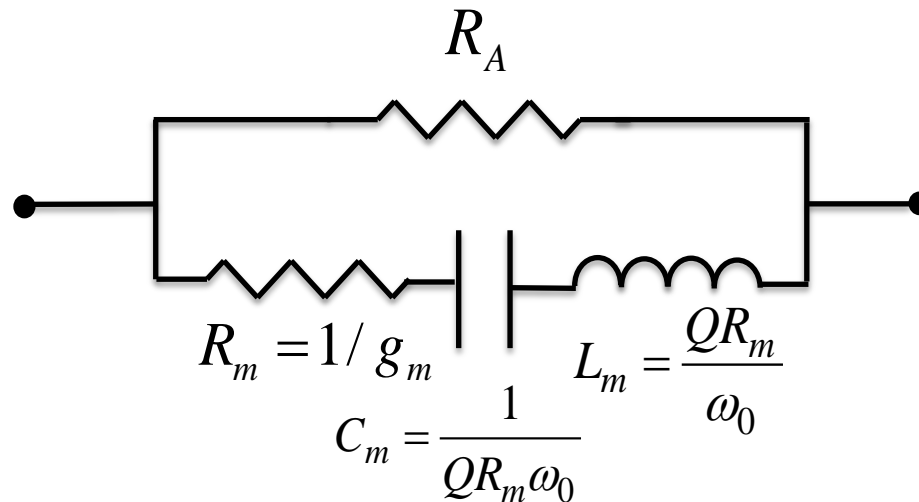
Voltage = Force *Current = Velocity*
Charge = Displacement

Resonator Electrical Model

Overall
Equivalent
Electrical Circuit



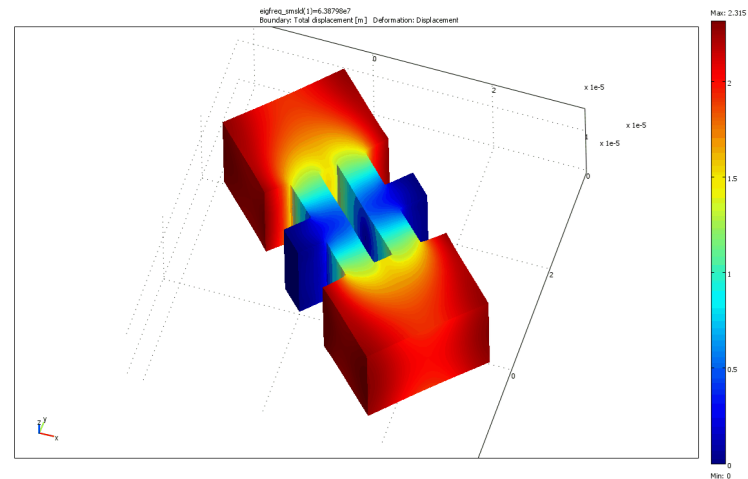
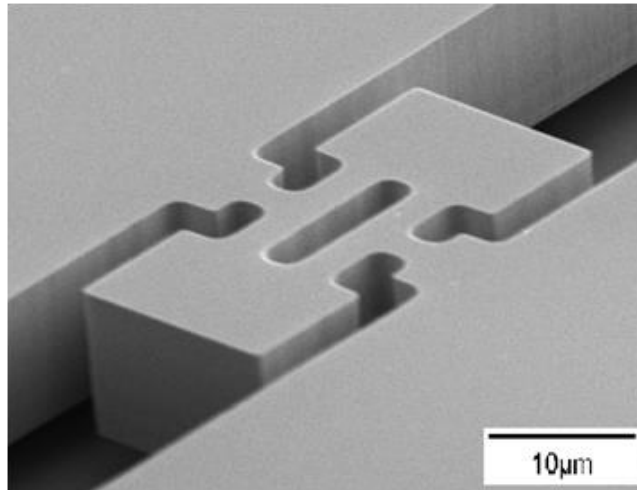
$$H_T \Big|_{s=j\omega_0} = g_m = 4\alpha E^2 \pi_l Q \frac{AI_{dc}^2}{KLC_{th}\omega_m}$$



Measurement and Simulation Results

Scale Factor	Measured/Assumed Parameters				Calculated Parameters			
	Current (mA)	Q. Factor	Freq. (MHz)	g_m (mS)	Power (mW)	R_A (Ω)	g_m (mS)	Power (μ W) @ $g_m=1$ (mS)
1X	60	14000	61.64	16.5	18.0	2.34	17.3	1041
	100	12000	60.85	62.3	50.0	2.34	42.8	1169
	60	7500	61.65	9.76	18.0	2.34	9.26	1945
	100	7700	61.11	37.5	50.0	2.34	27.1	1845

= data obtained under atmospheric pressure



Resonator Optimization

Scaling a Resonator:

$$F.M. = \frac{g_m}{P_{DC}} = 4\alpha E^2 \pi_l Q \frac{A}{\rho K L^2 C_{tl} \omega_m} \propto \frac{M^2}{L^2 A^2} \propto \frac{1}{S}$$

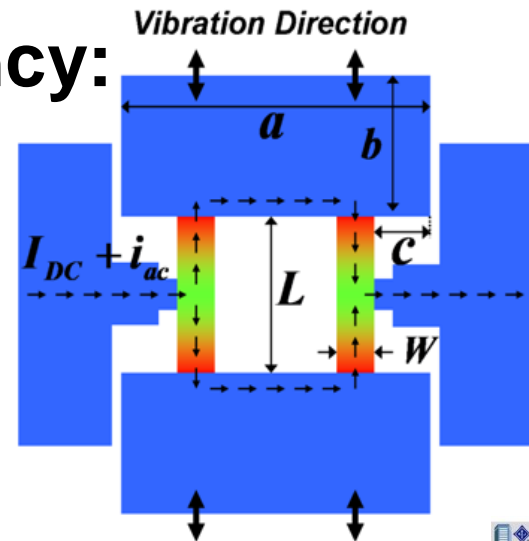
$\frac{A}{L}$ LA $\sqrt{\frac{A}{LM}}$

$S^{\frac{3}{2}}$ $\uparrow \frac{1}{2}$ $S^{\frac{3}{2}}$ S

S: scaling ratio

Optimizing at constant frequency:

$$F.M. \propto \frac{1}{L^2 W^2} \propto \frac{1}{S^2}$$



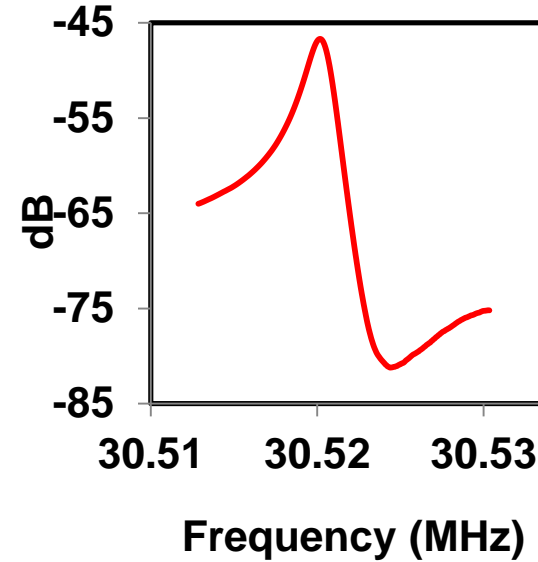
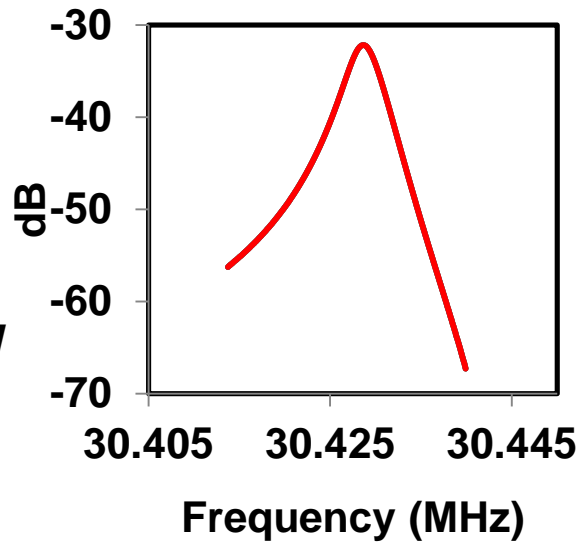
Low Power Devices

Q = 9,200 (Air)

$I_{DC} = 2.69 \text{ mA}$

$g_m = 233 \mu\text{S}$

$P_{DC} = 14.72 \text{ mW}$

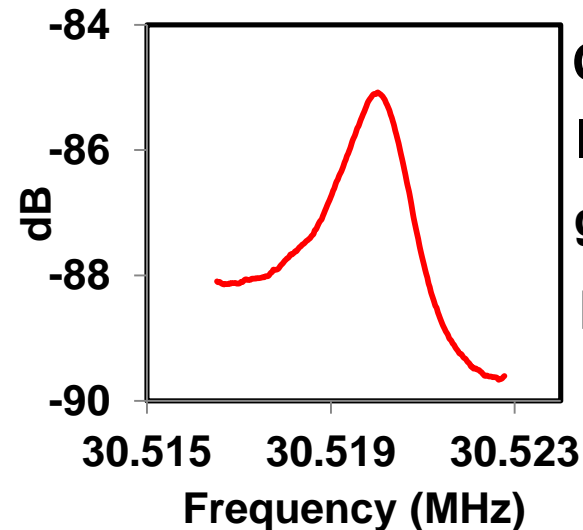
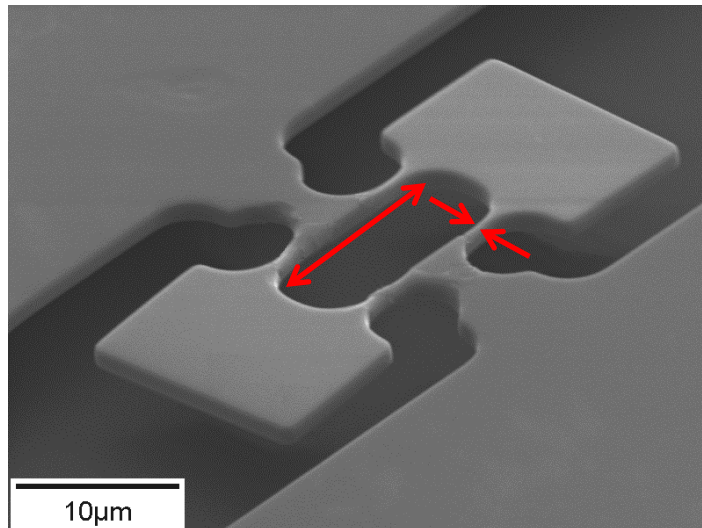


Q = 24,400 (Vac.)

$I_{DC} = 720 \mu\text{A}$

$g_m = 43.6 \mu\text{S}$

$P_{DC} = 1.01 \text{ mW}$



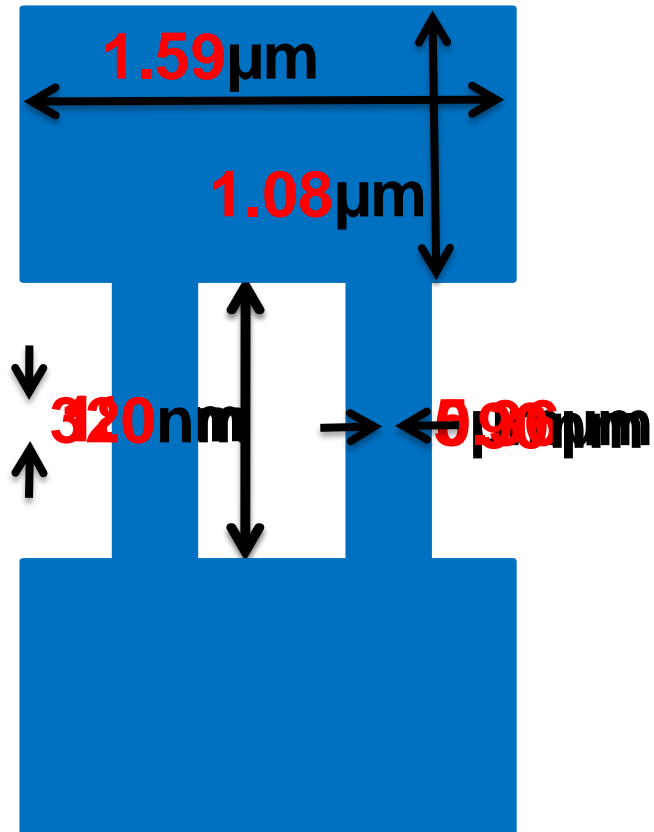
Q = 35,900 (Vac.)

$I_{DC} = 43 \mu\text{A}$

$g_m = 0.207 \mu\text{S}$

$P_{DC} = 3.63 \mu\text{W}$

Measurement and Simulation Results



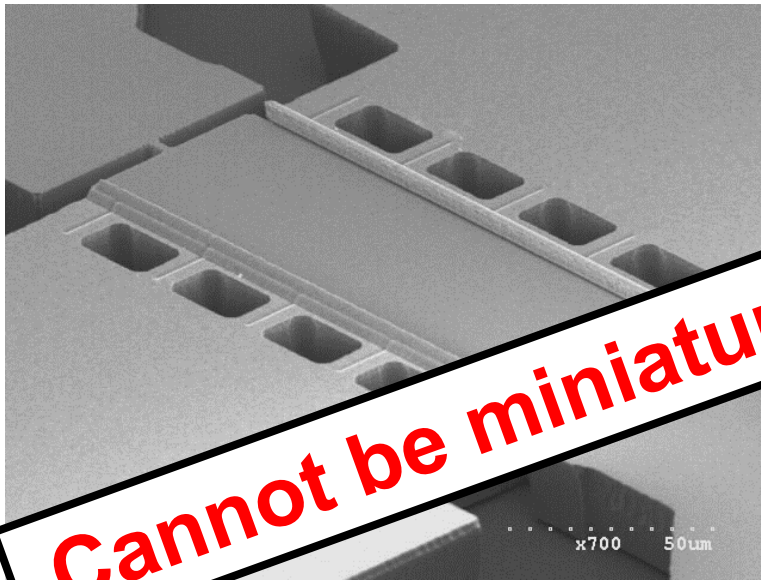
$$g_m = 1\ \text{mA/V}$$

Freq. (MHz)	F.M	P (μW)
61.6	0.686	1041
900	7.87	90.7
905.7	136	5.25
2100	18.5	38.6
2113	306	2.33

For all the calculations the **bulk** piezoresistive coefficient of silicon was used!

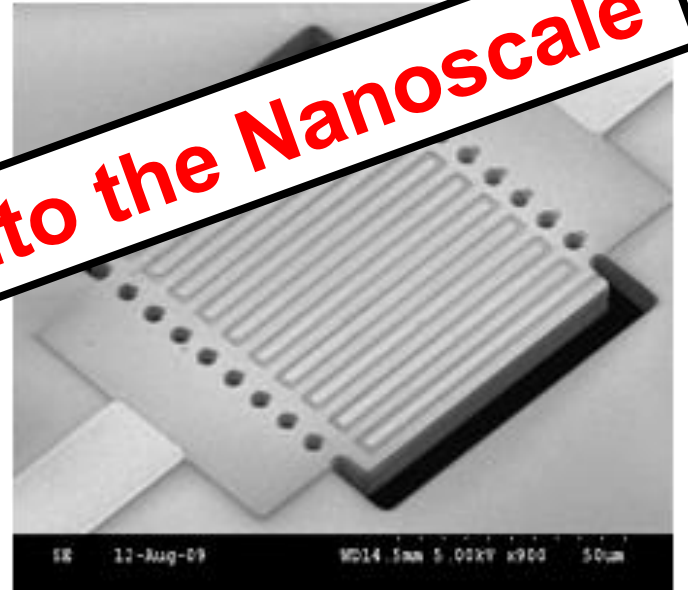
Micro-Resonator Transduction

□ Common Micro-Resonator Transduction Mechanisms:



Capacitive

Piezoelectric



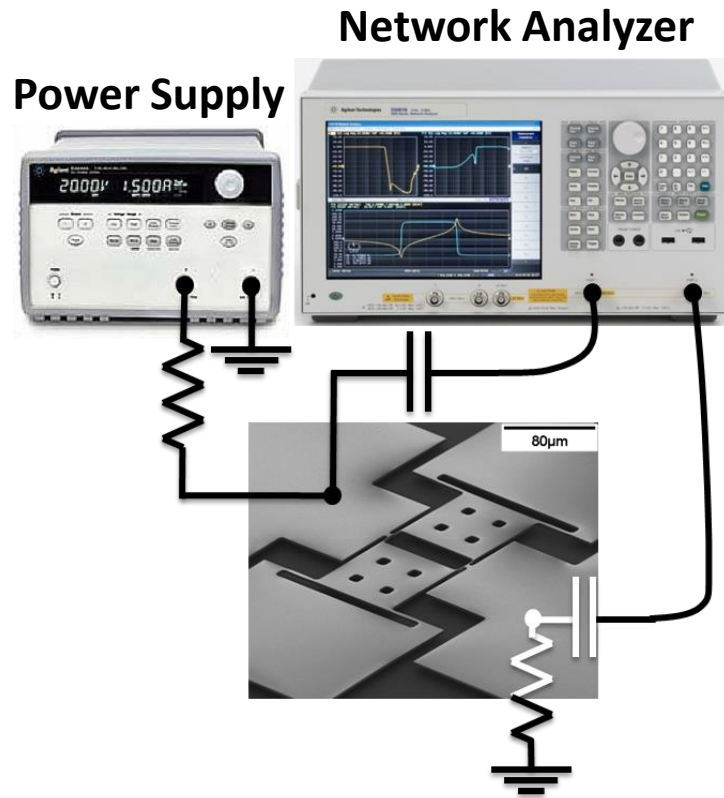
Cannot be miniaturized into the Nanoscale

Capacitive Silicon Bulk Acoustic Wave Resonator¹

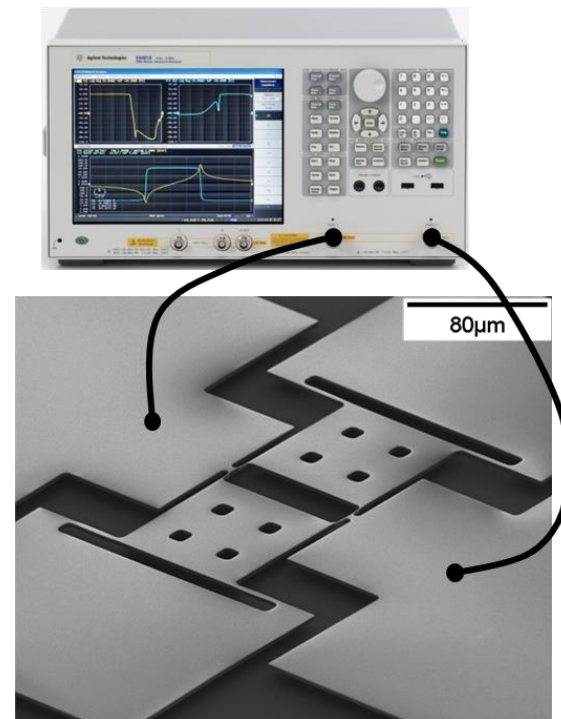
1GHz AlN on Silicon Piezoelectric Resonator²

¹S. Pourkamali, Z Hao, and F Ayazi, VHF Single Crystal Silicon Capacitive Elliptic Bulk-Mode Disk Resonators—Part I: Implementation and Characterization, JMEMS 2004.
²B. Harrington, M. Shahmohammadi, and R. Abdolvand, "Toward Ultimate Performance in GHz MEMS Resonators: Low Impedance and High Q," IEEE MEMS 2010

Zero Bias Operation Via Internal Electromechanical Mixing



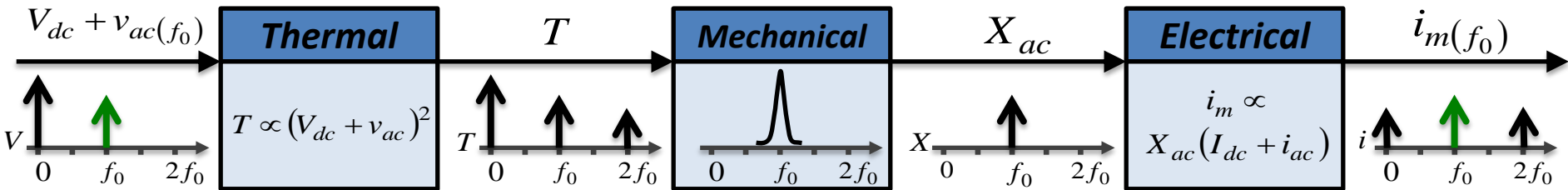
Conventional Operation (DC+AC)



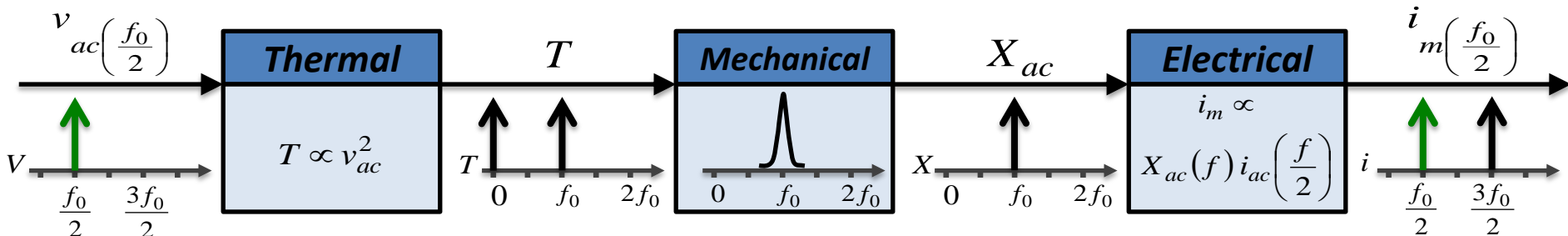
Zero Bias Operation (AC)

Zero Bias Operation Via Internal Electromechanical Mixing

Operation with DC Bias

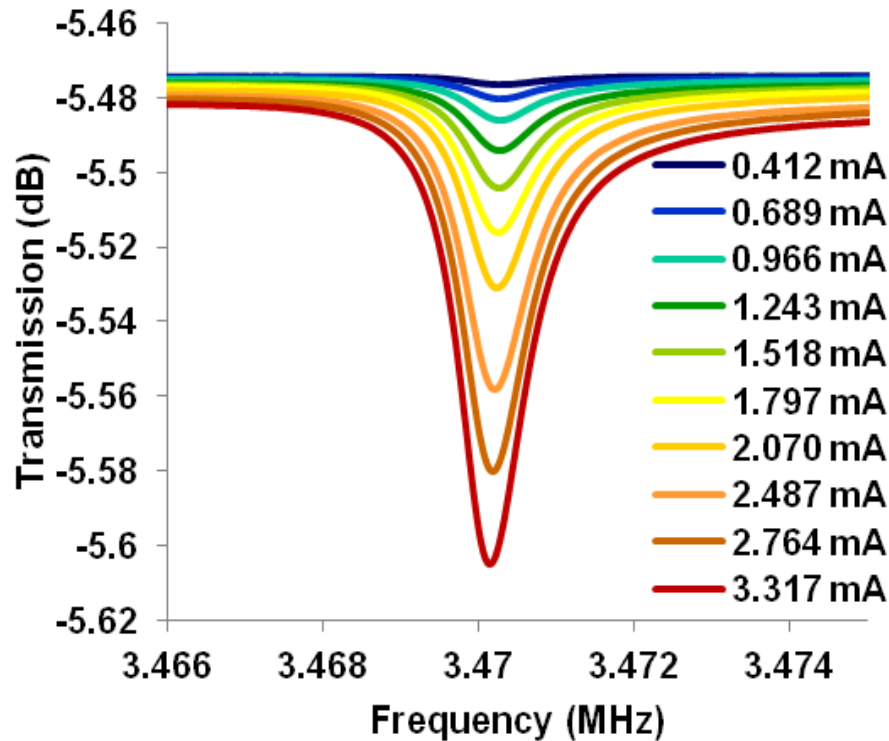


Operation without DC Bias

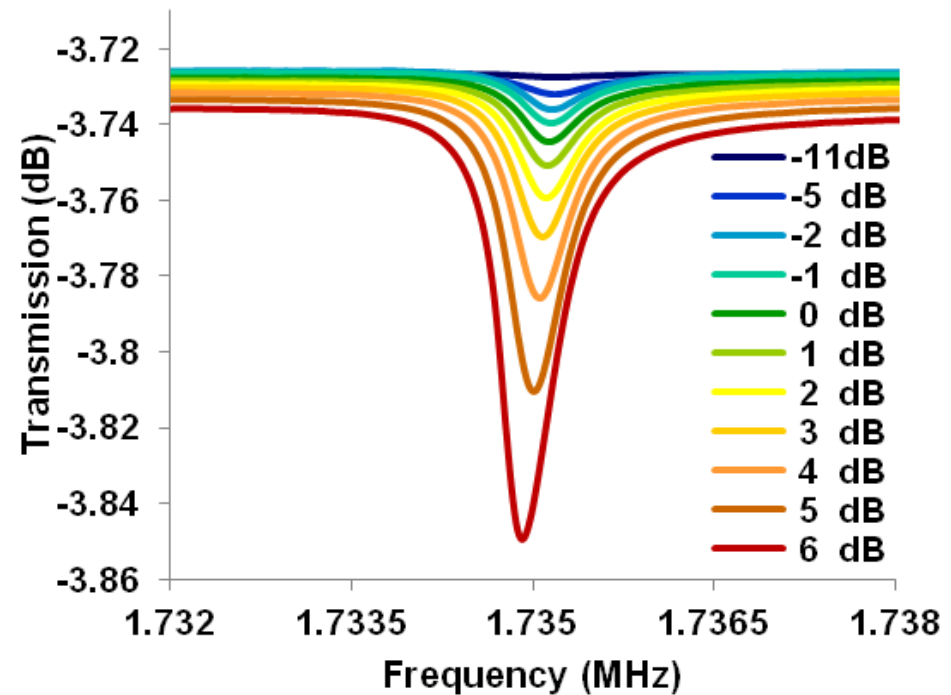


Zero Bias Operation Via Internal Electromechanical Mixing

Operation with DC Bias

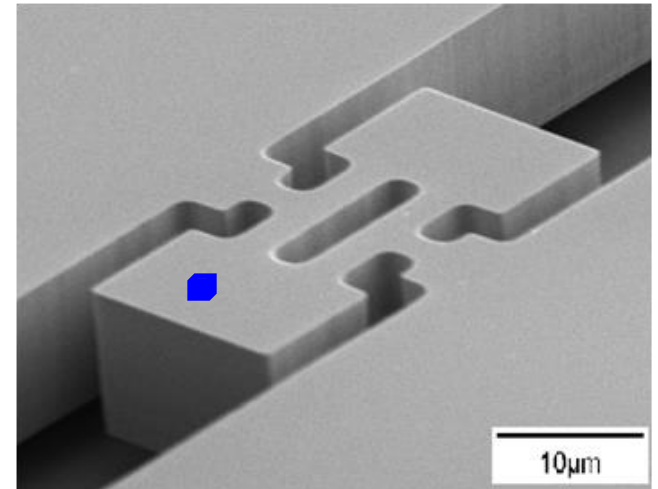
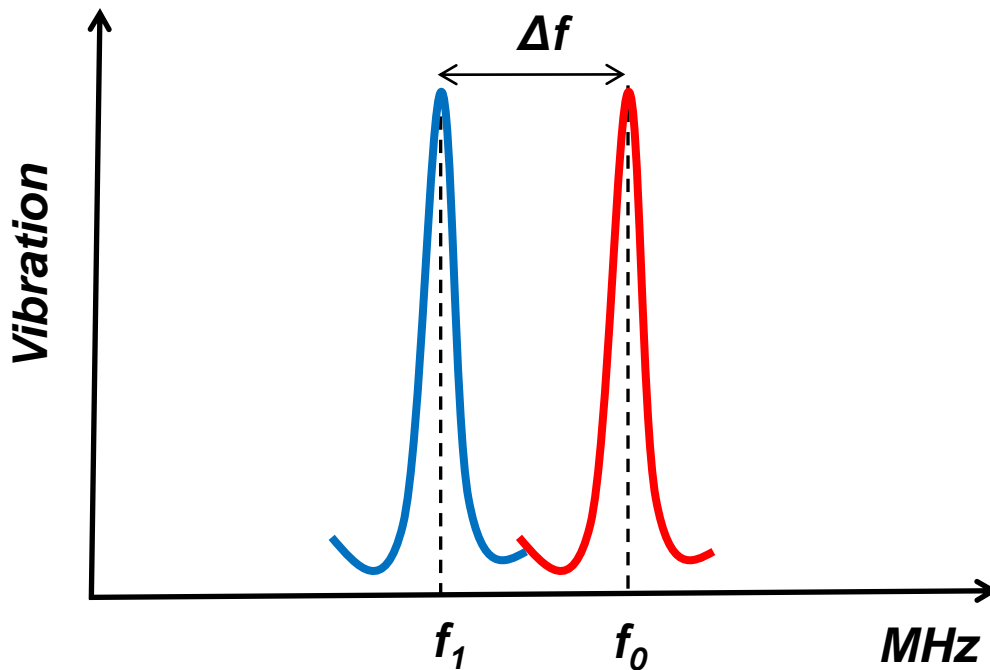


Operation without DC Bias



Applications (Mass Sensing)

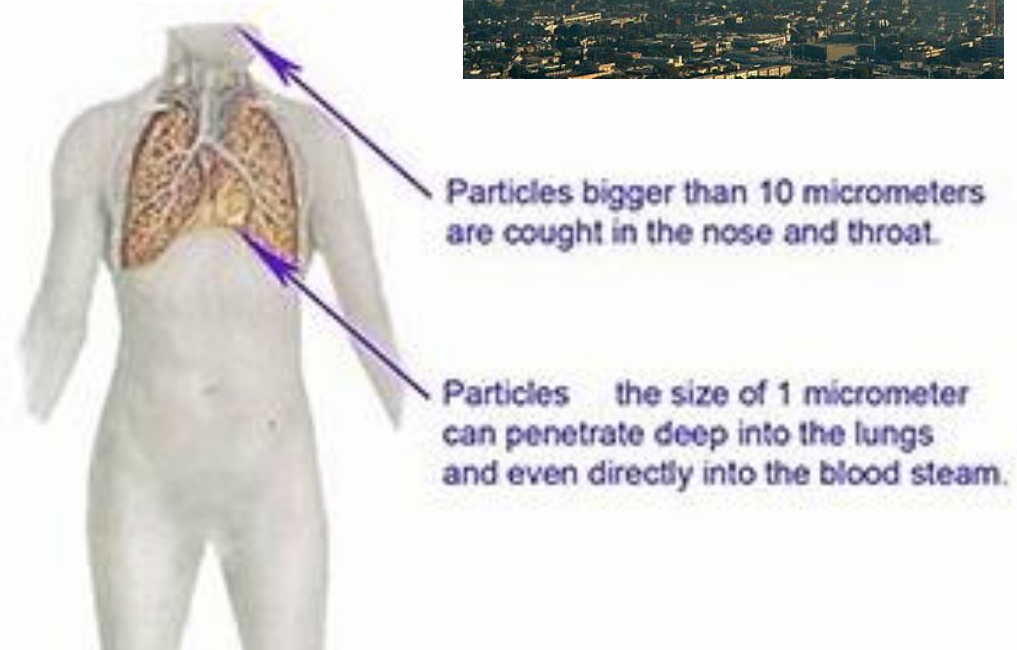
$$f = \frac{1}{2\pi} \sqrt{\frac{k}{m}} \quad \longrightarrow \quad \frac{\Delta f}{f} = -\frac{\Delta m}{2m}$$



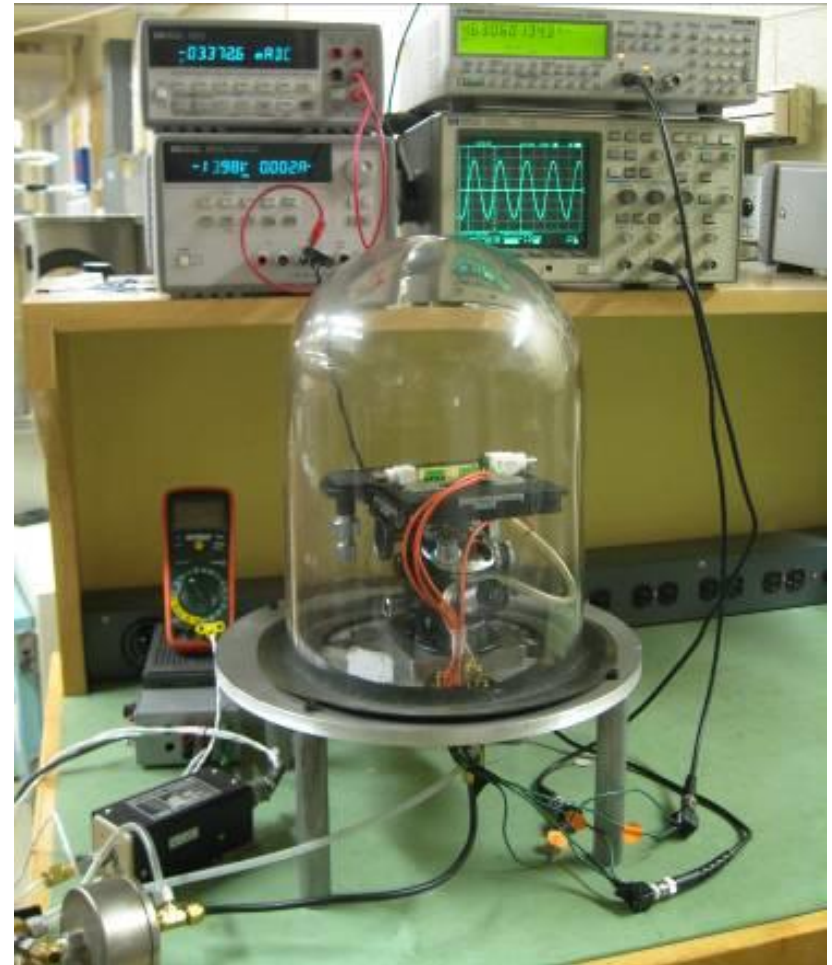
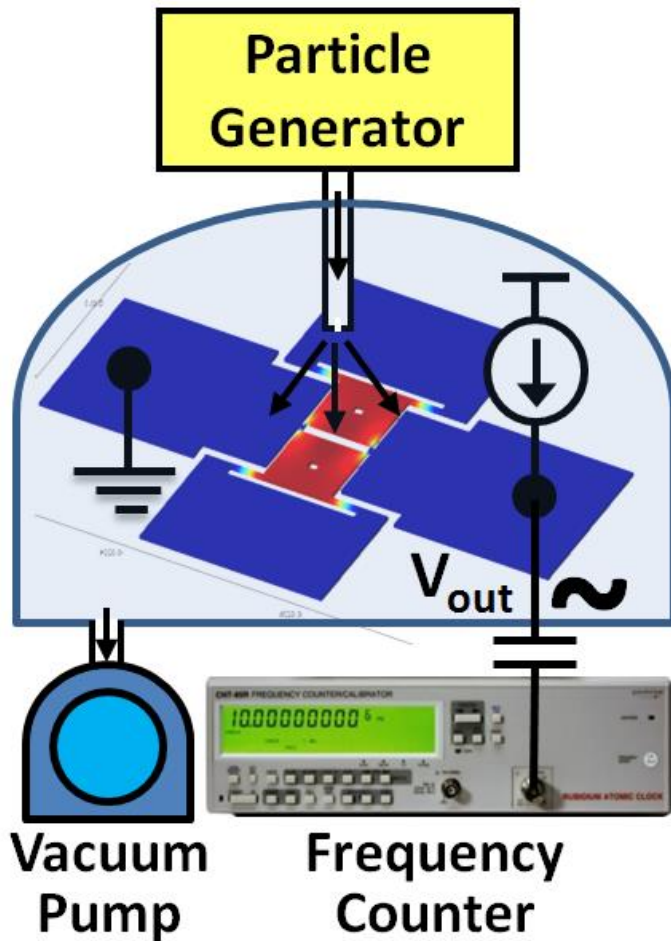
- ❑ Mechanical resonators vibrate more slowly (at lower frequencies) if they become heavier

Airborne Micro/Nanoscale Particles

- ❑ Air-borne particle concentration and Size distribution measurement and monitoring
- ❑ Importance
 - Human health
 - Climate change
 - Controlled Environments

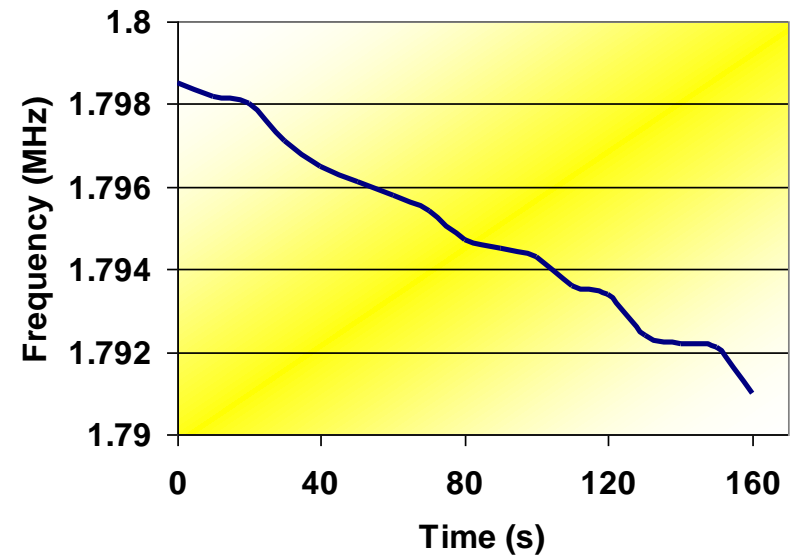
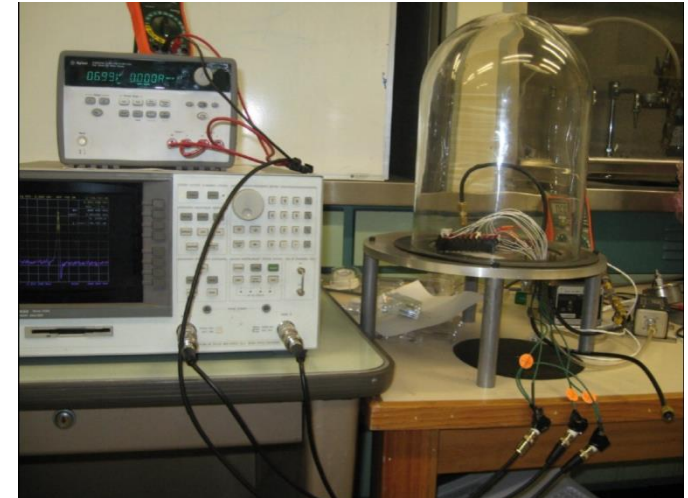
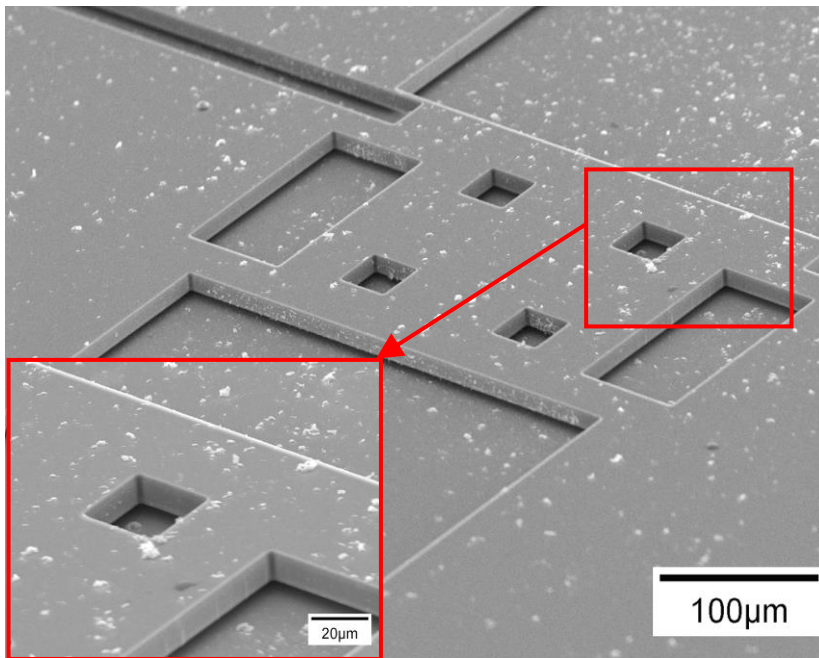


Measurement Setup



Weighing Air-Borne Particle

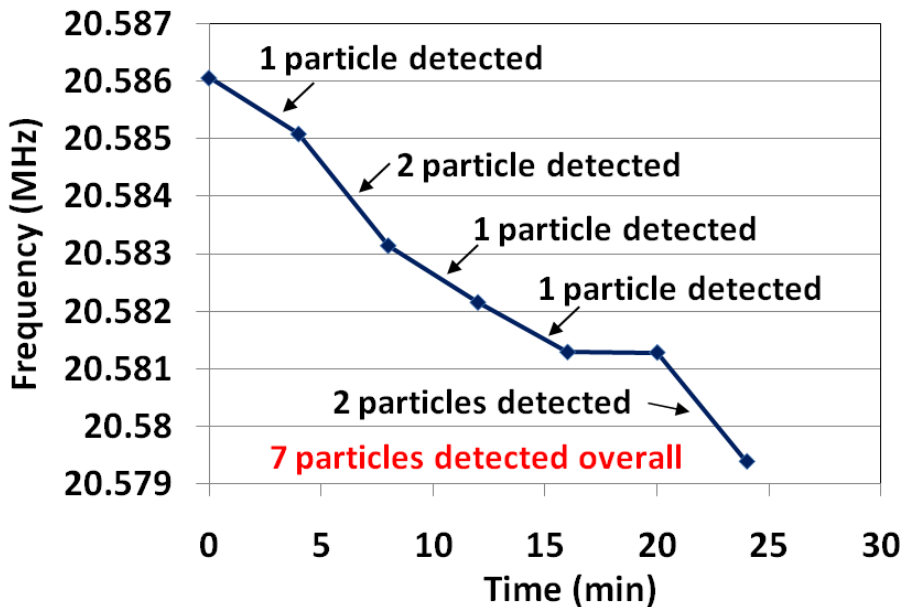
- Deposited mass in 10s intervals = 1-5 ng
- Particle mass density in lab air = $14.2 \mu\text{g}/\text{m}^3$



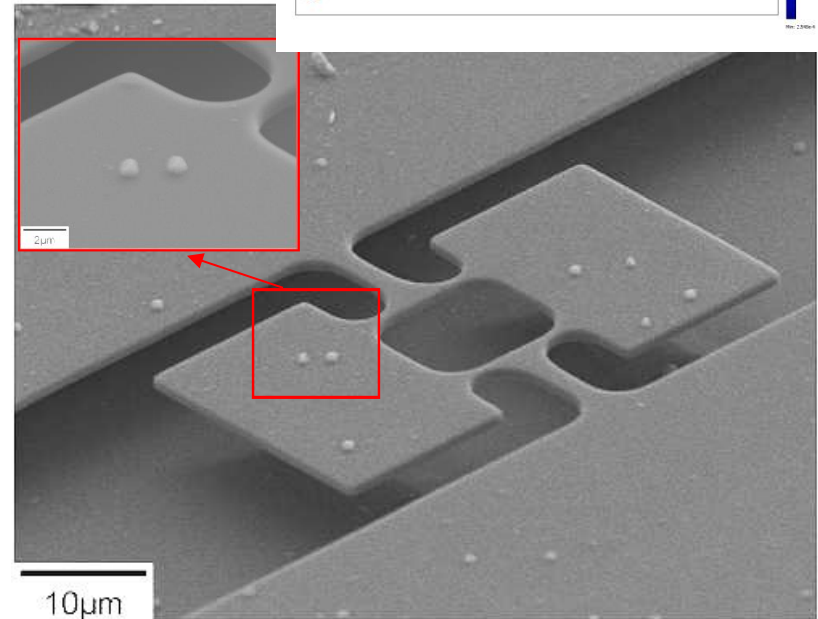
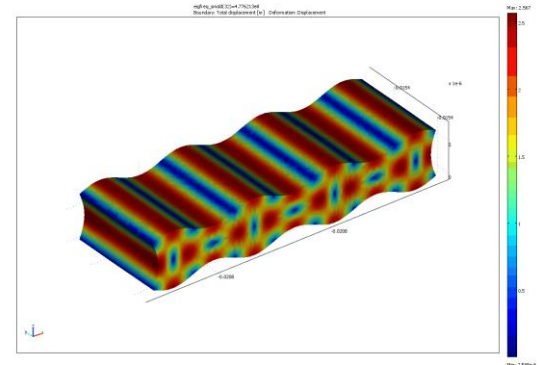
Single Particle Detection

- ❑ Shift in frequency quantized, multiples of
- ❑ Some intervals shift is double
- ❑ One interval no shift

~900Hz shift per particle

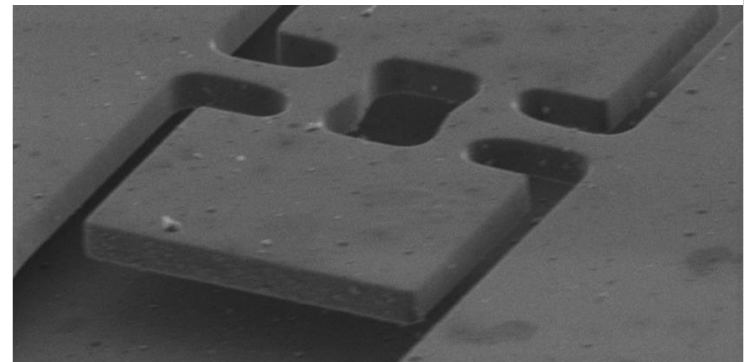
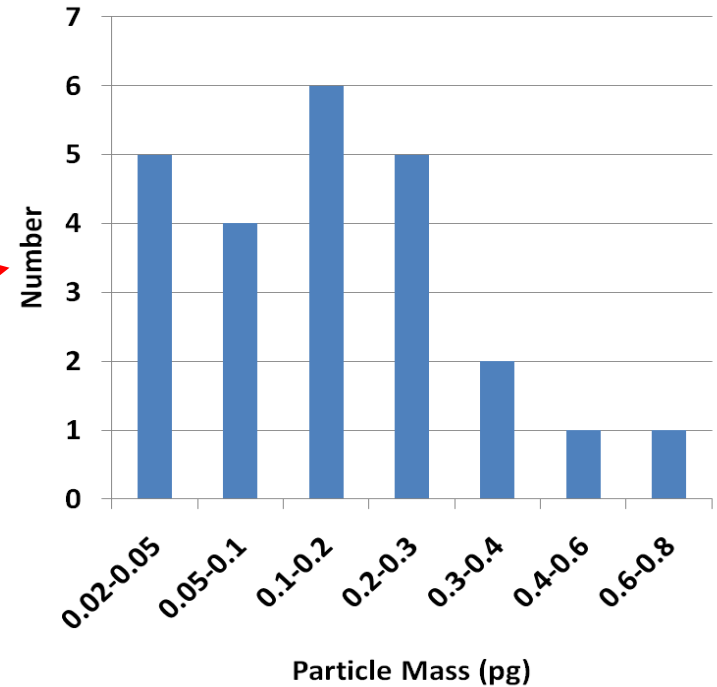
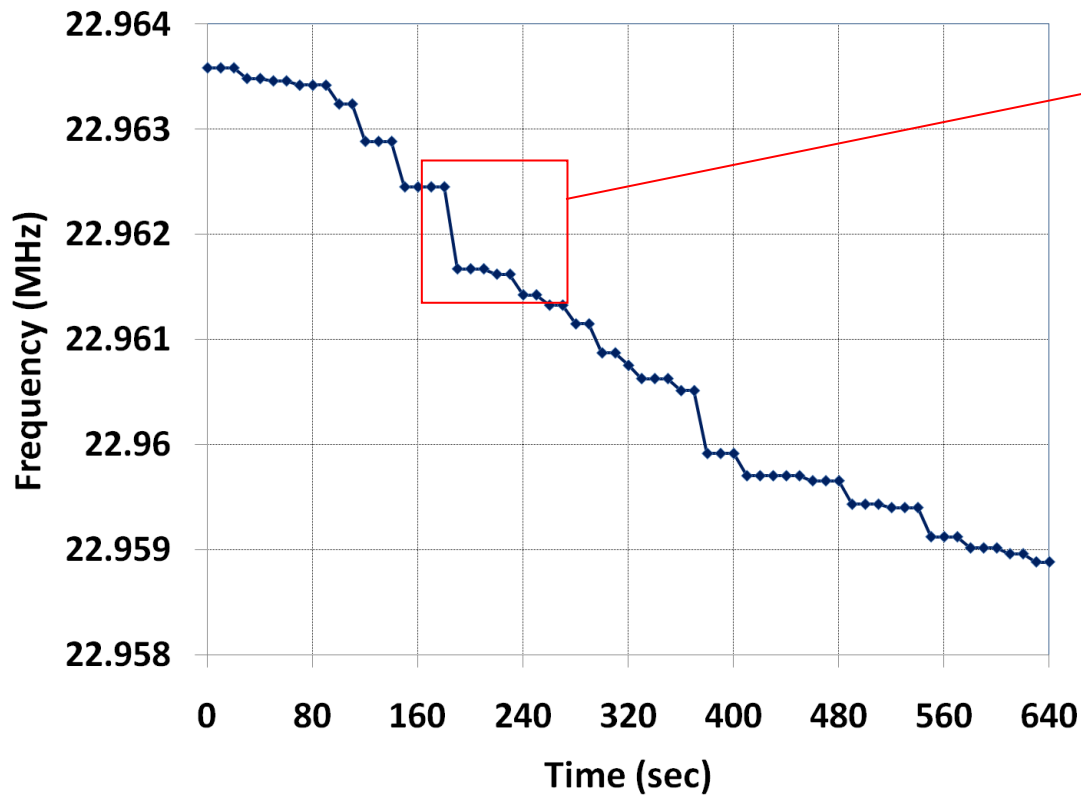


7 partic

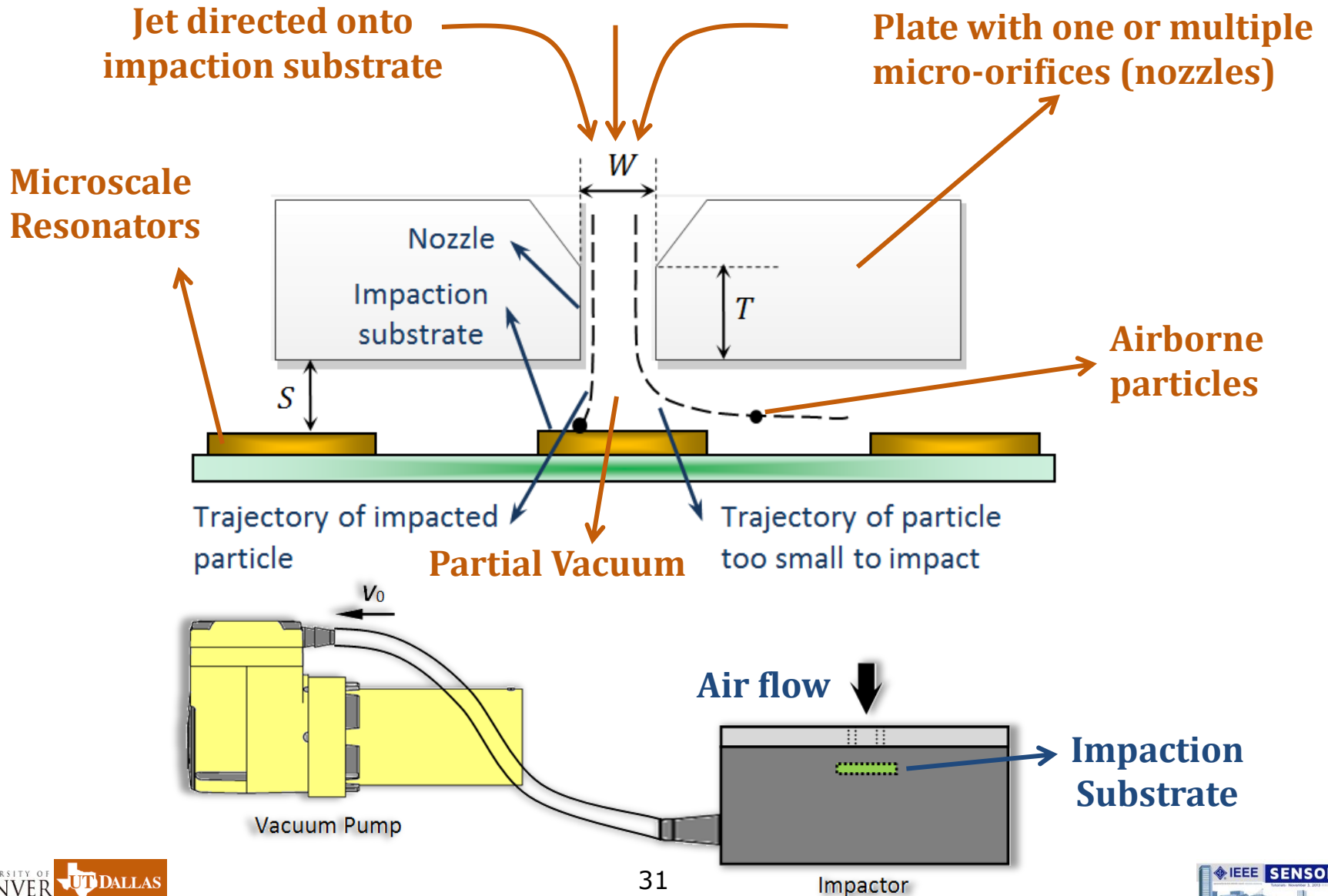


SEM of the resonator after deposition

Particle Mass Distribution Analysis



Inertial Aerosol Impactor

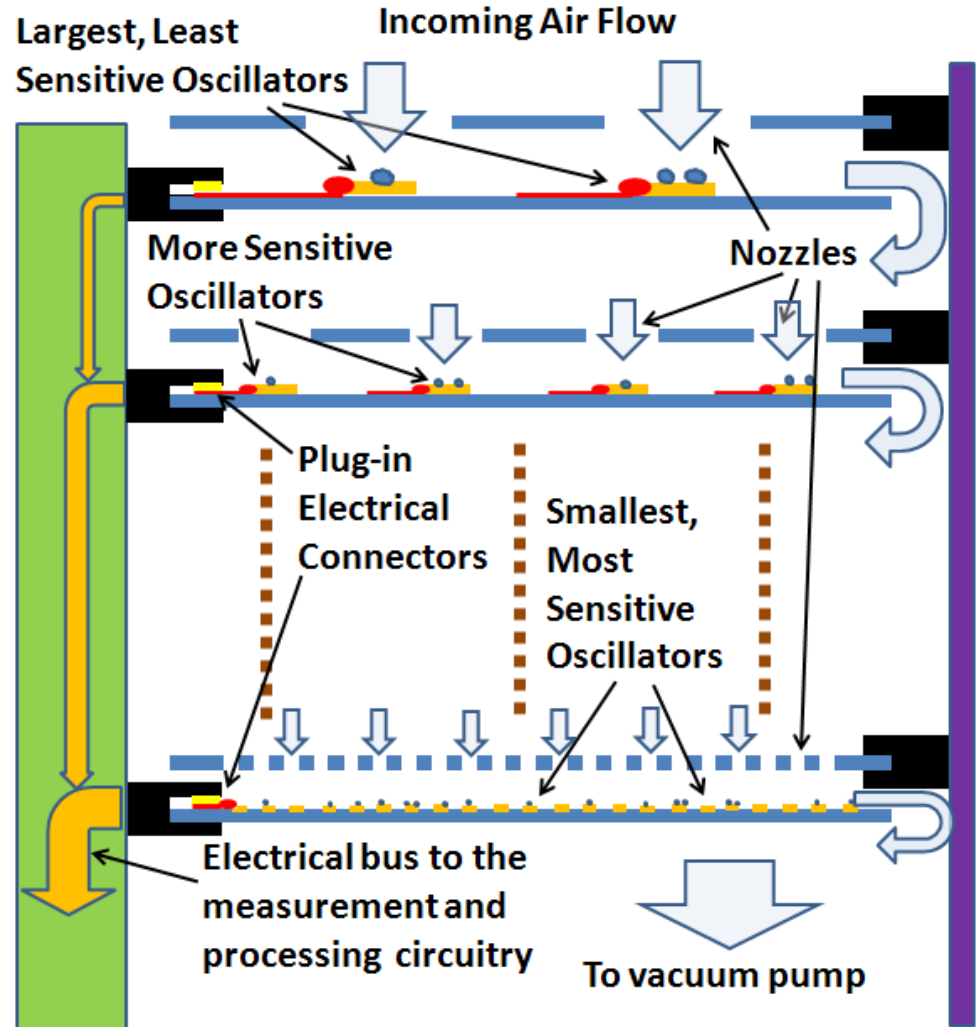


Fully MEMS Cascade Impactor

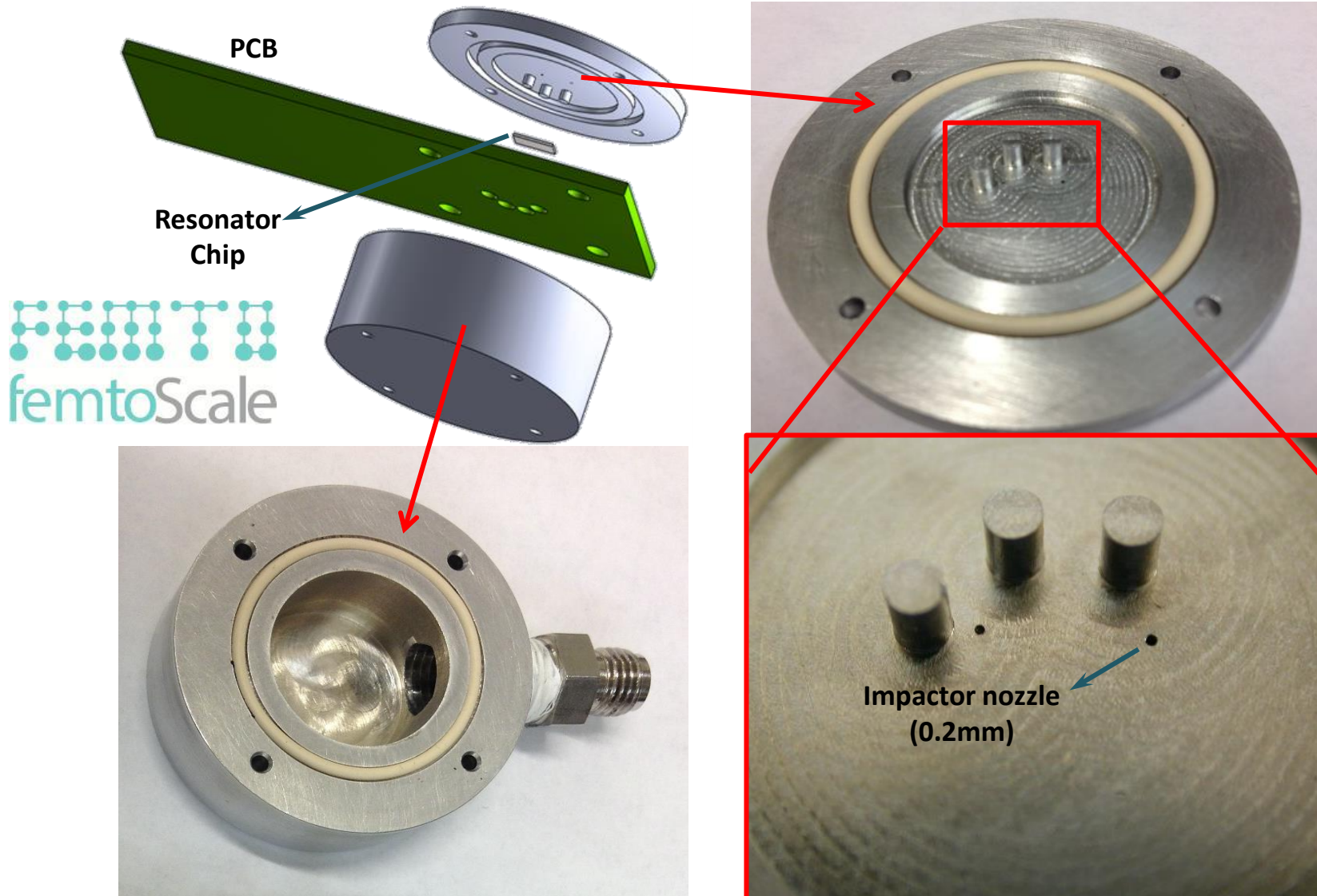
Weight: 12kg (26lb)
Diameter: 220mm
Height: 560mm
Power: 1.5kW
Stages: 13
Flow Rate: 30L/min
Real time Monitoring: NO



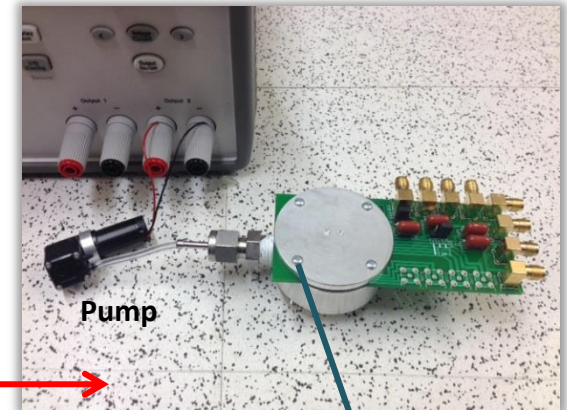
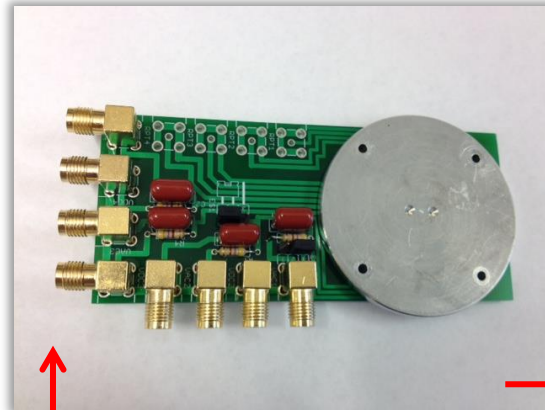
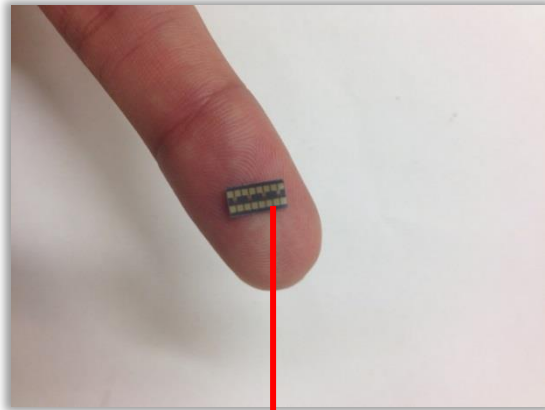
Model 122
30 L/min 13 Stage MOUDI-II



Impactor Fabrication

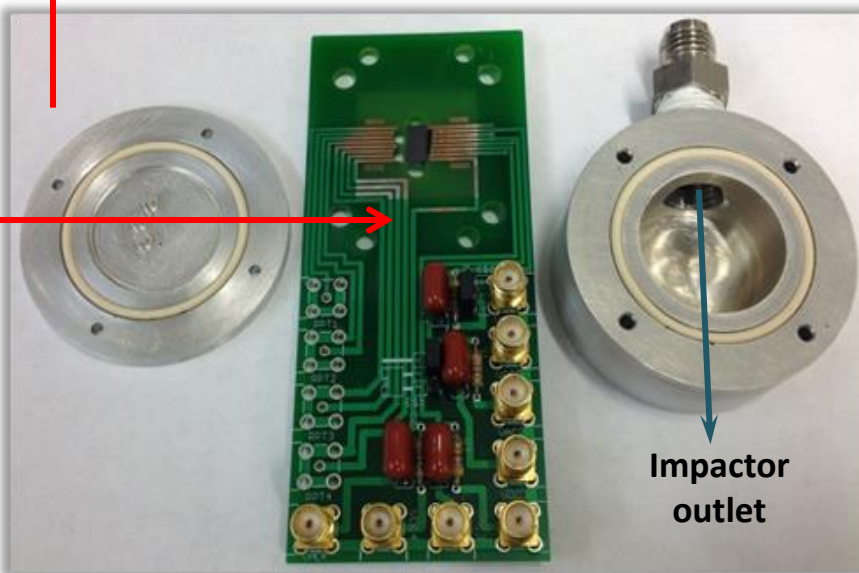
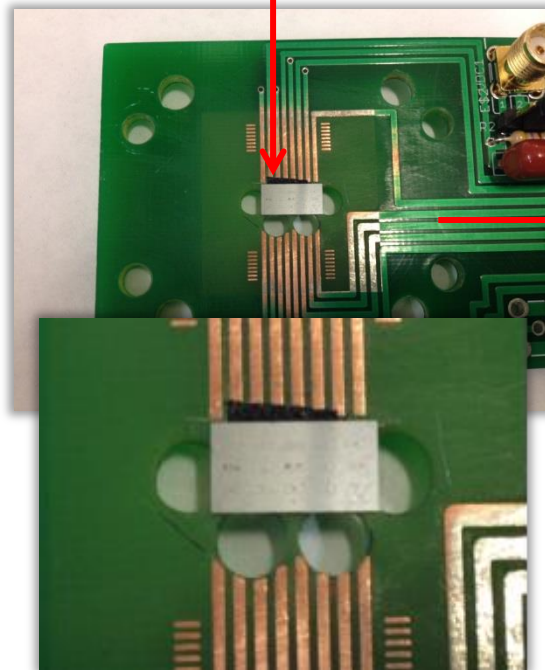


Assembly Procedure



Pump

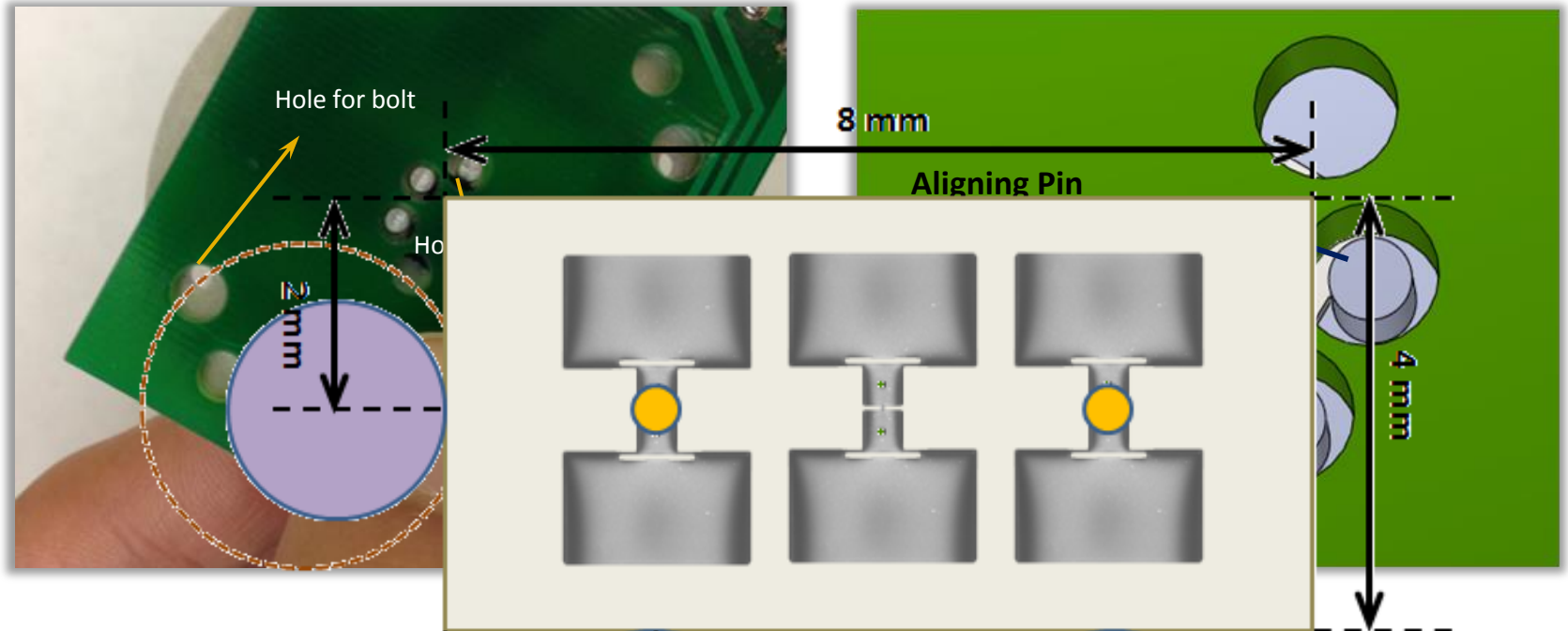
Bolts for holding pieces



Impactor outlet

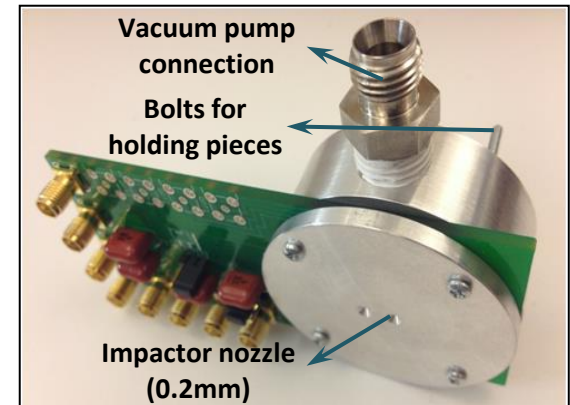
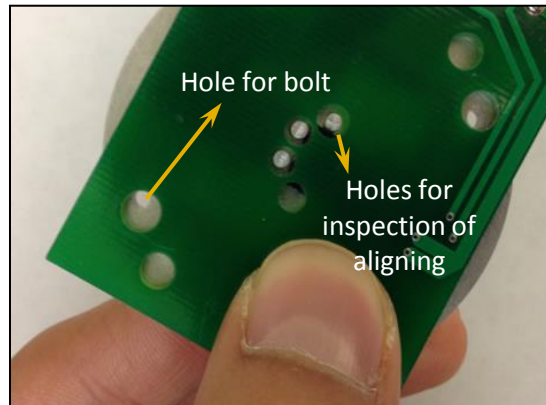
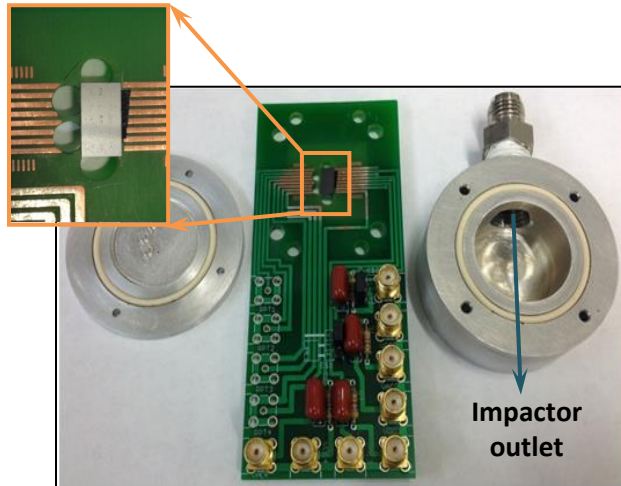
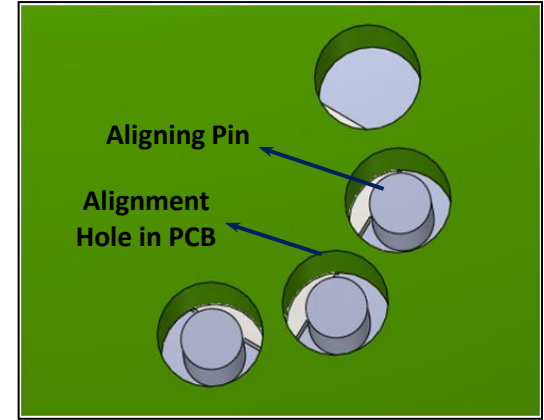
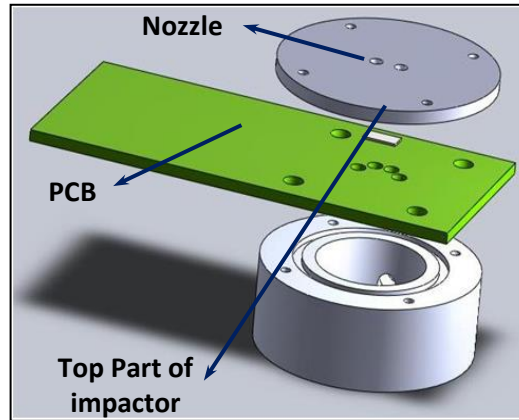
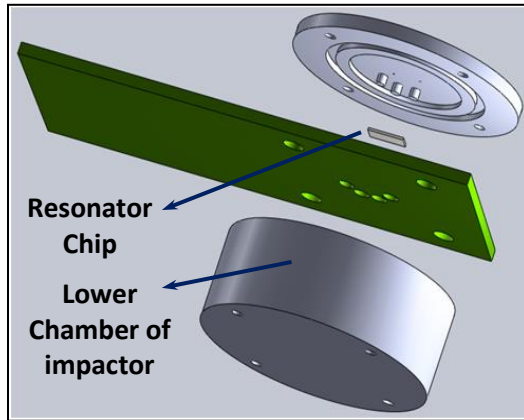
femtoScale

Alignment Technique

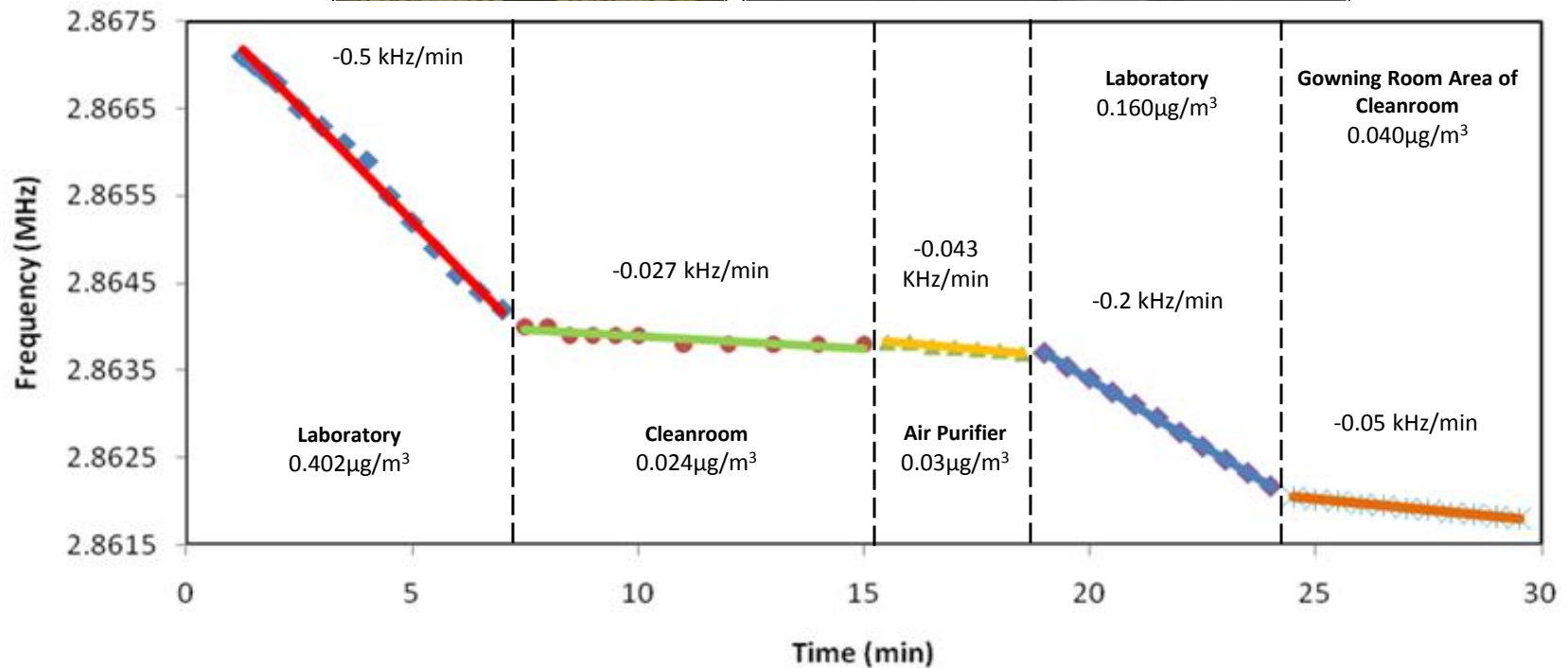
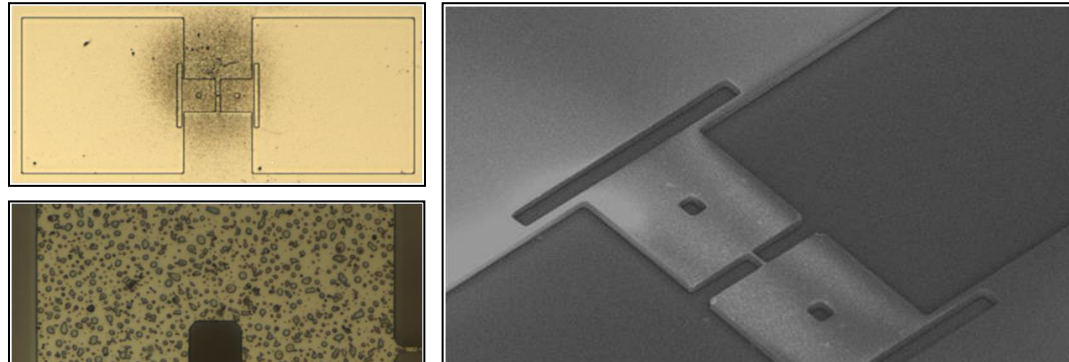


- ❑ Three precisely machined alignment pins are used for aligning the resonator chip with the Impactor nozzle.
- ❑ Alignment is performed by pushing the pins against the edges of the resonator chip.

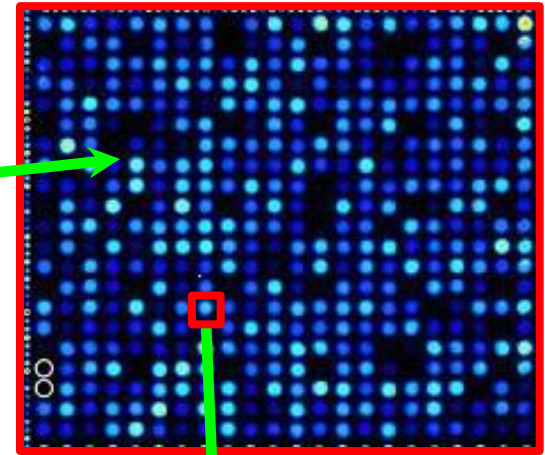
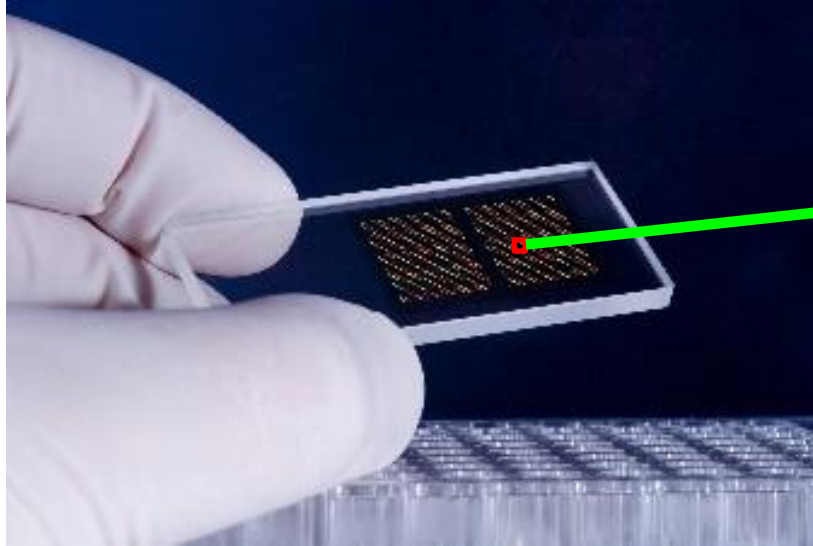
Combined Resonator/Impactor System Assembly



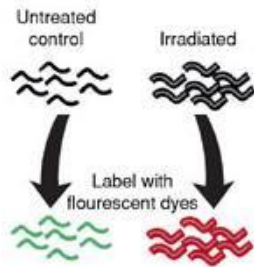
Test Results



Biosensing: Microarray Technology



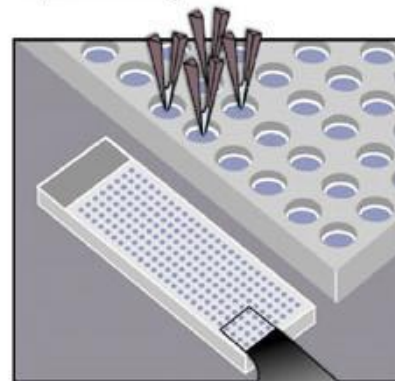
Prepare DNA probe



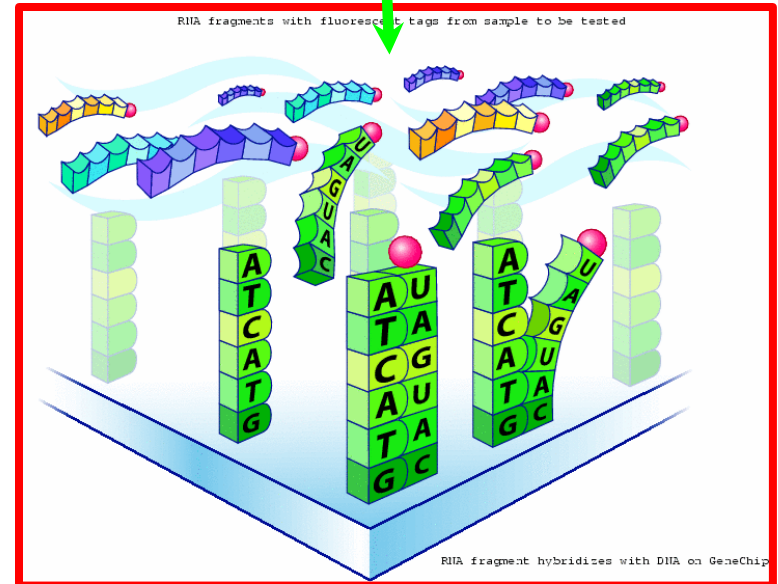
Combine equal amounts

Hybridize probe to microarray

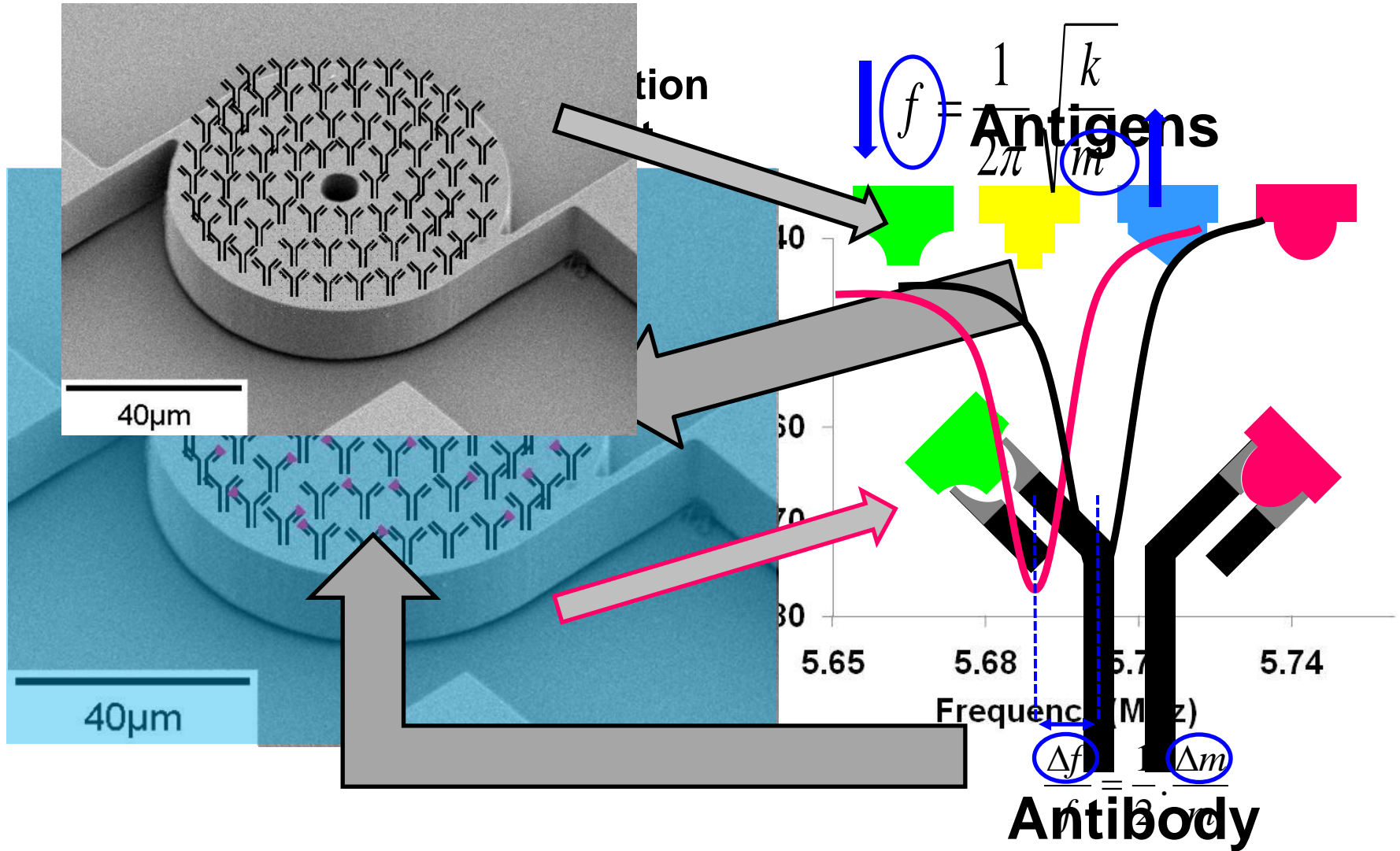
Prepare microarray



Scan

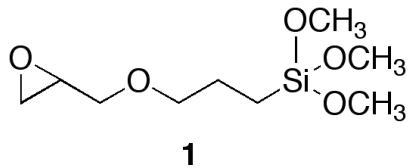


Biomolecular Mass Sensing

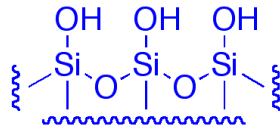


Surface Linking Synthetic Scheme

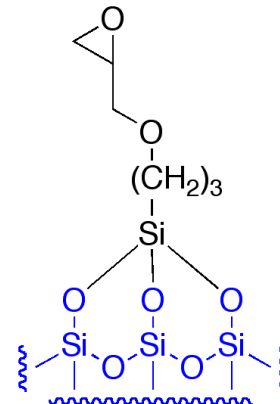
3-Glycidoxypropyltrimethoxysilane



silicon oxide surface
activated with HNO_3

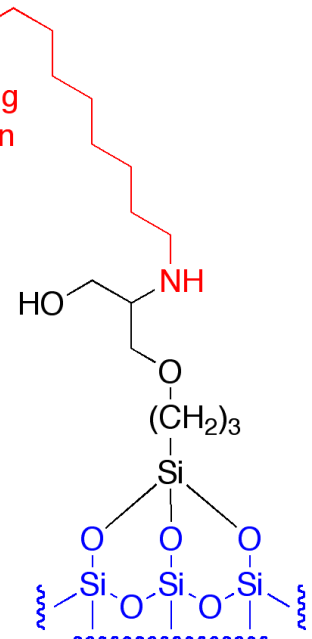


$i\text{-Pr}_2\text{NEt}$, xylene
 80°C



addition of 4.5×10^{-22} g
mass for each reaction
with octadecylamine

octadecylamine
 R-NH_2
Ethanol
room temperature
18 h



Biosensor Design:

R-NH_2 = amino-terminated ssDNA,
protein or antibody lysine residue, or
artificial receptor / sensor molecule

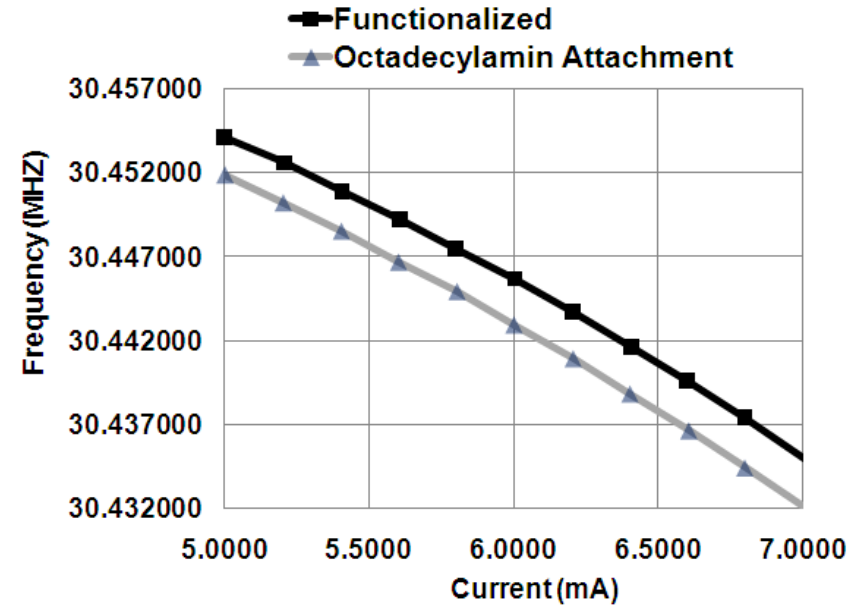
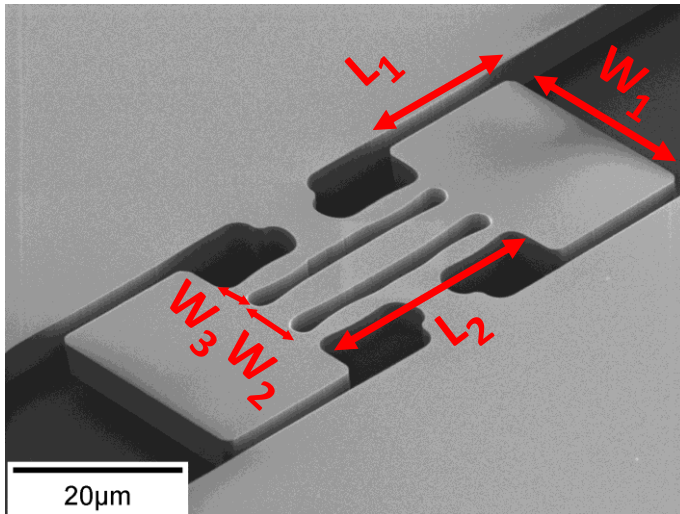


Frequency
Measurement 1



Frequency
Measurement 2

Single Molecular Layer Detection



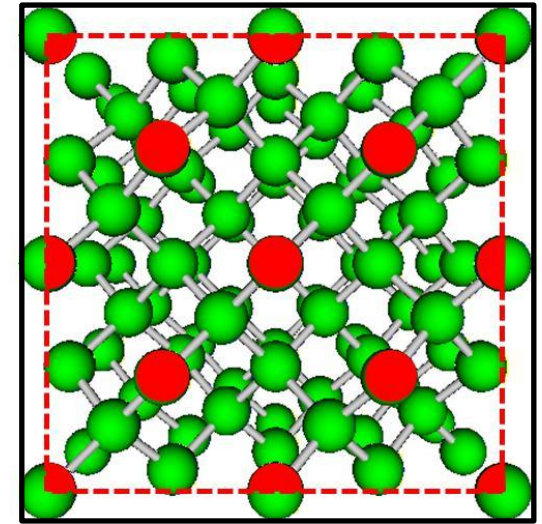
L_1, L_2, W_1, W_2, W_3 (μm)	f_1 (MHz) Functionalized	f_2 (MHz) Octadecylamine	Δf (Hz)	Δf (ppm)
23,36,33,4,2	30.437427	30.434413	3014	99
23,36,33,4,2	29.891373	29.888322	3051	100
23,36,33,--, 2	23.809419	23.805919	3400	140
23,36,33,--, 2	27.001593	26.998914	2679	99

Resonator Surface Coverage

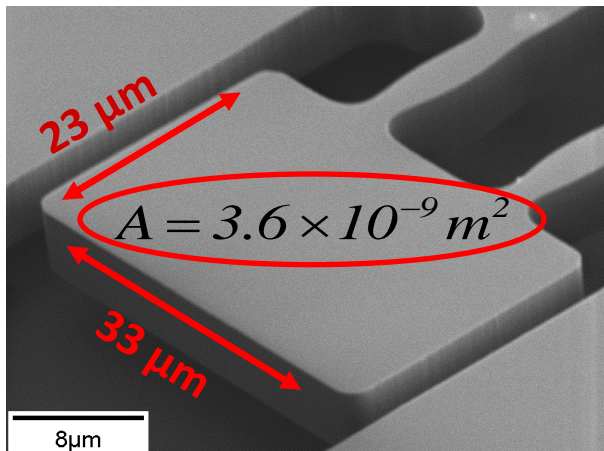
- Based on the frequency shift, device mass and frequency

$$\frac{\Delta f}{f} = -\frac{\Delta m}{2m} \Rightarrow \Delta m = 1 \text{ pg}$$

- Considering the theoretical maximum possible added mass in $1 \text{ nm}^2 = 4 \times 10^{-9} \text{ pg}$



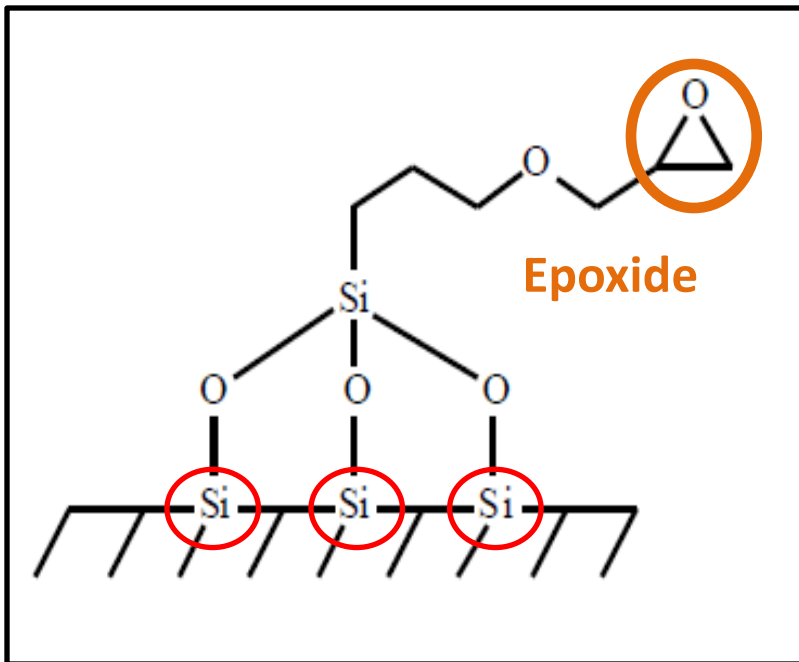
8 Dangling Bonds in every silicon crystal for Surface Linking



\Rightarrow Surface Coverage = 6.9%

Resonator Surface Coverage

Dangling Bonds/3 = Epoxides

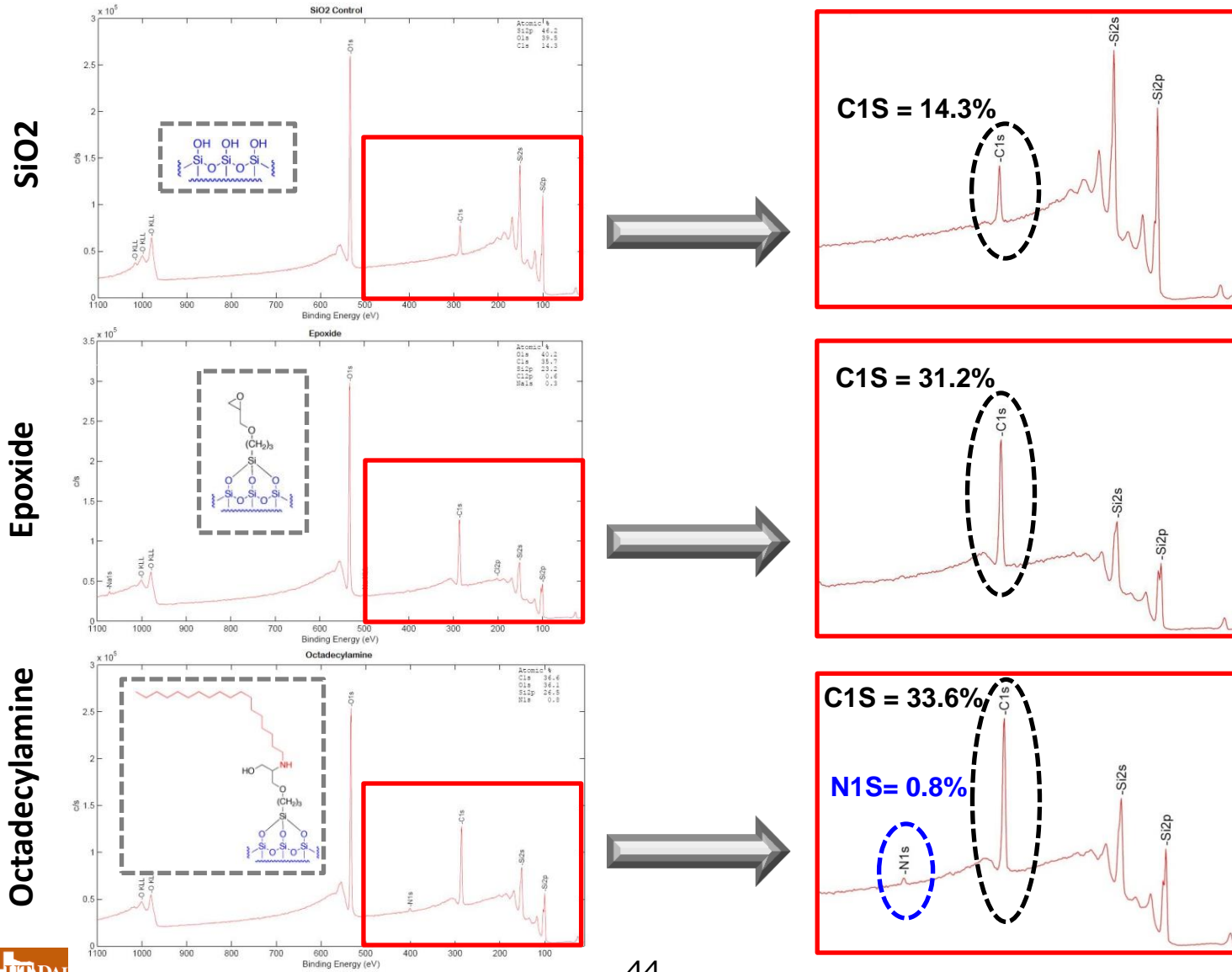


The Maximum Possible
Number of
Octadecylamine in
 $1 \text{ nm}^2 = 8.8 \text{ Molecules}$



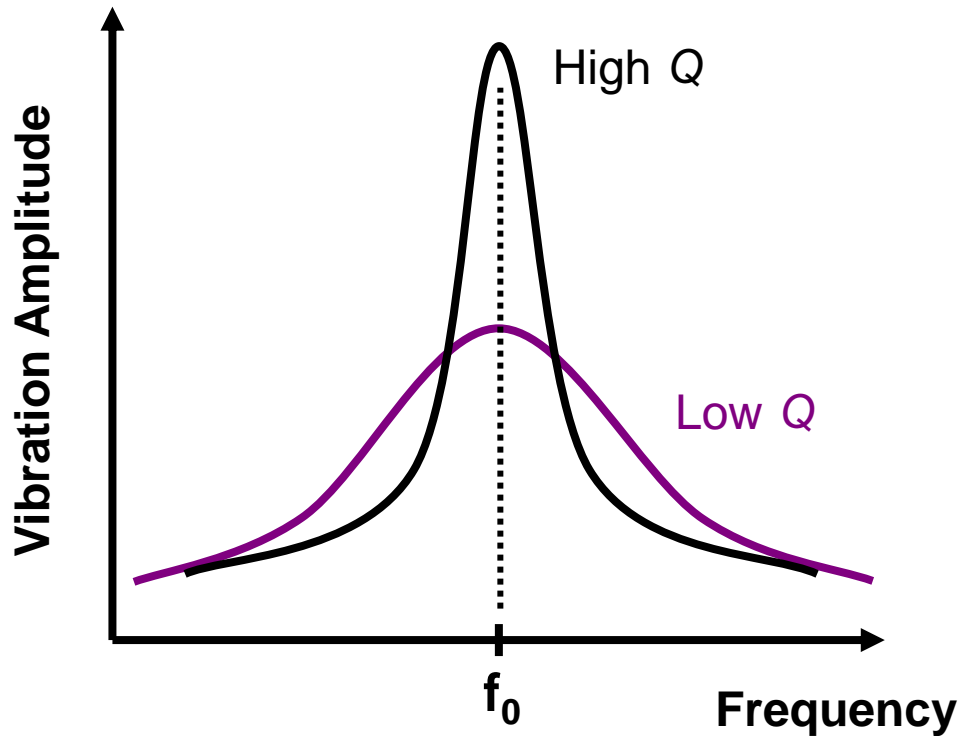
The Theoretical Added Mass in
 $1 \text{ nm}^2 = 4 \times 10^{-9} \text{ pg}$

Surface X-ray Photoelectron Spectroscopy (XPS) Analysis

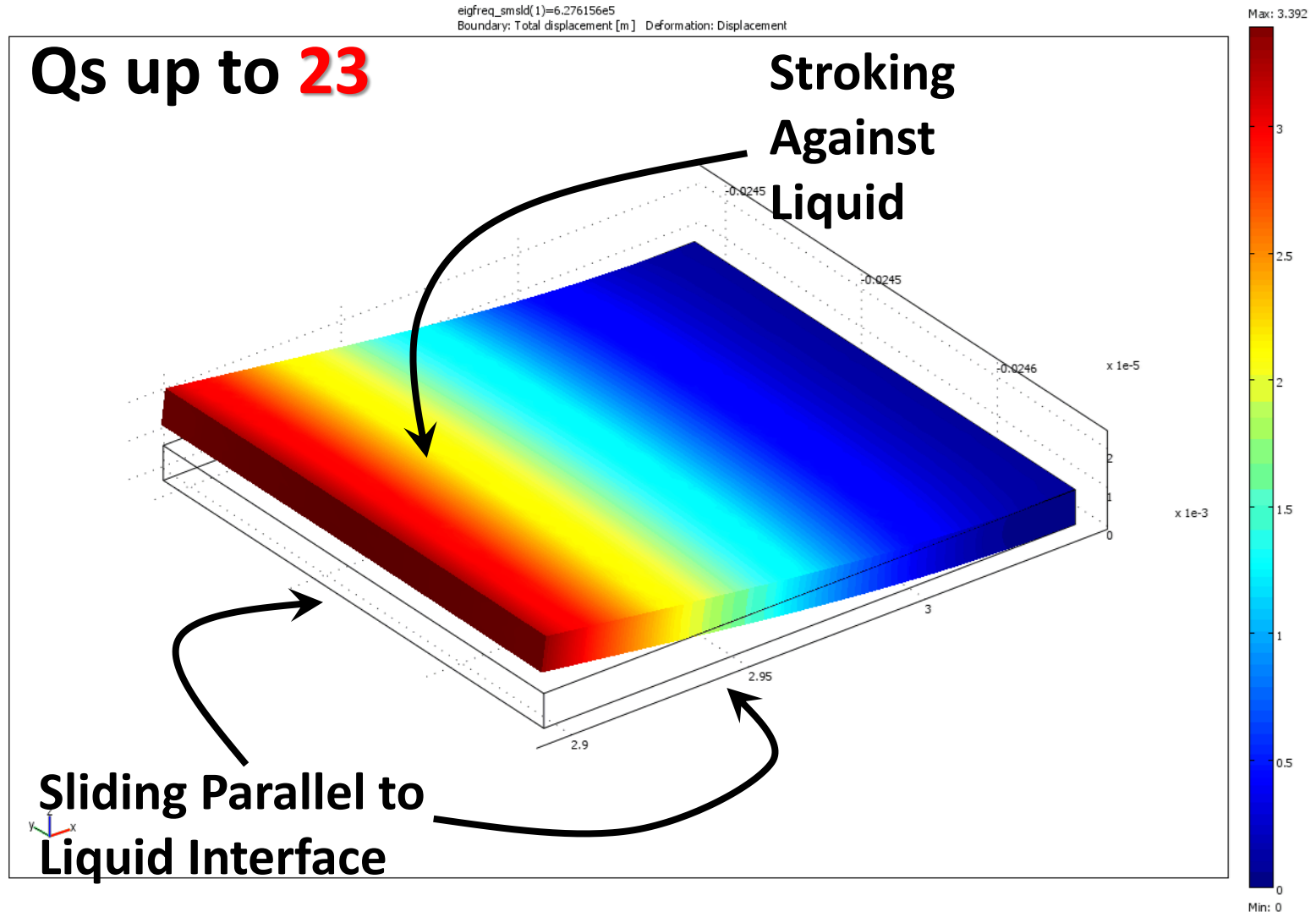


Direct in-Liquid Measurement

- ❑ Viscous damping from surrounding liquid significantly suppresses mechanical resonance and lowers quality factor (Q)
- ❑ High Q is needed for accurate frequency measurement and effective resonator transduction



Direct in Liquid Measurement: Out-of-Plane Microcantilever



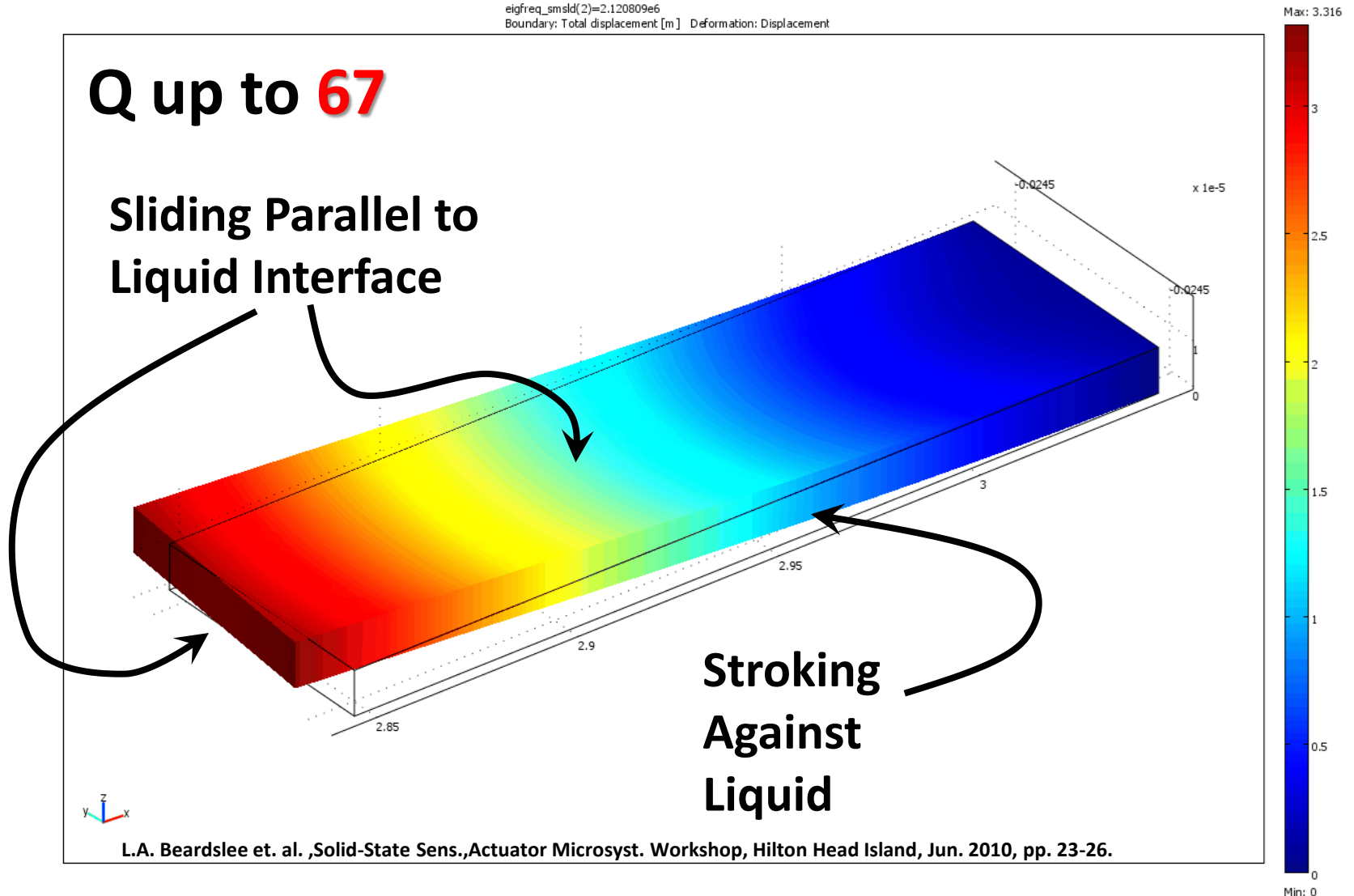
Direct in Liquid Measurement: In-Plane Microcantilever

eigfreq_smsld(2)=2.120809e6
Boundary: Total displacement [m] Deformation: Displacement

Q up to **67**

Sliding Parallel to
Liquid Interface

Stroking
Against
Liquid

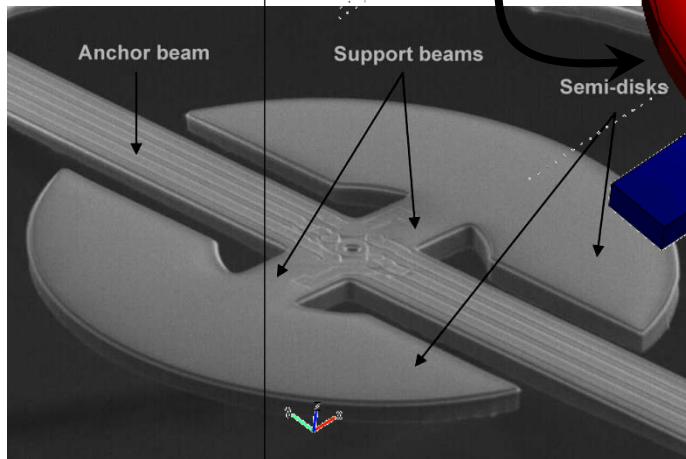


Quasi-Rotational Dual-Half-Disk

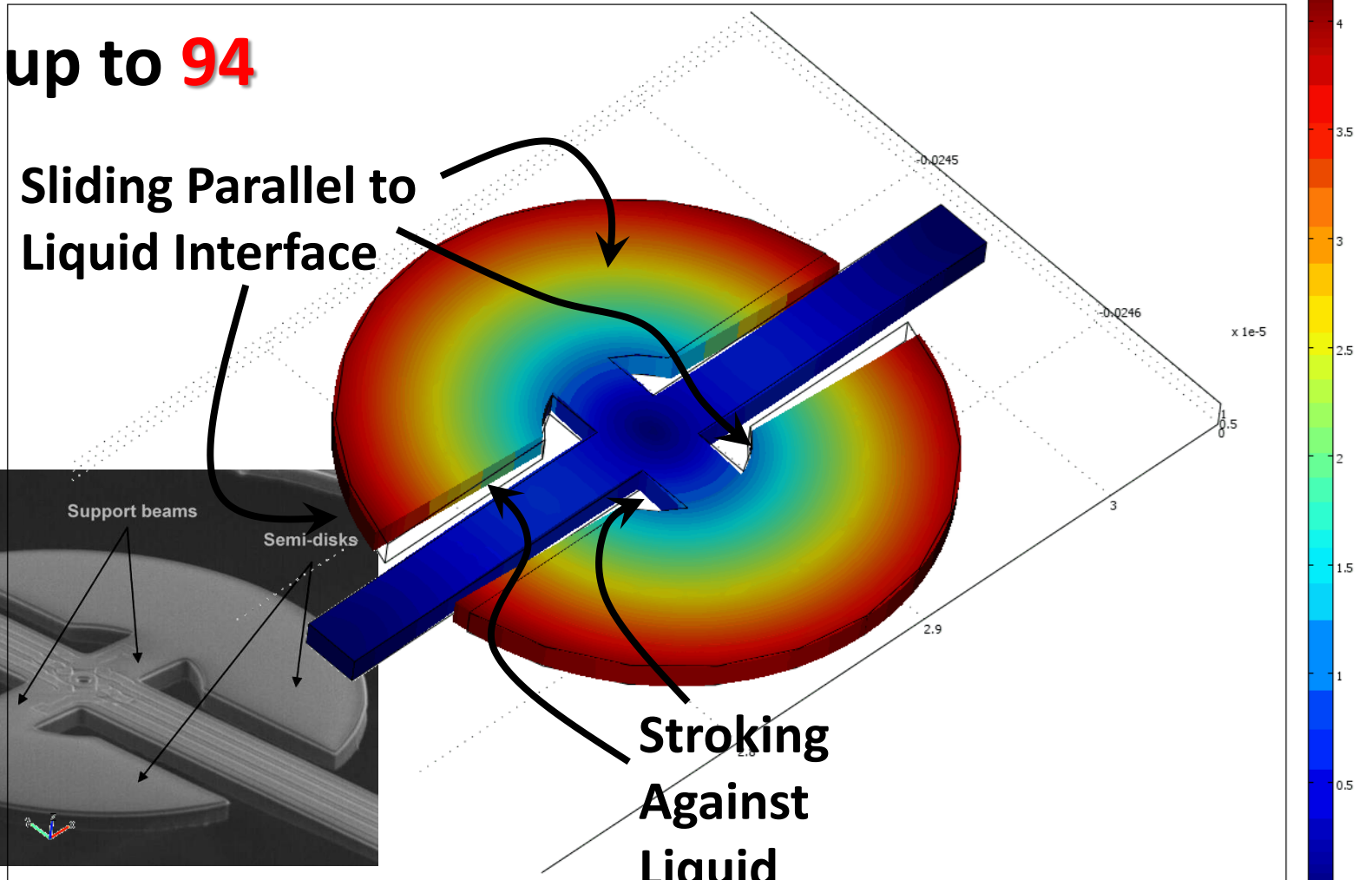
Q up to **94**

Sliding Parallel to
Liquid Interface

Stroking
Against
Liquid

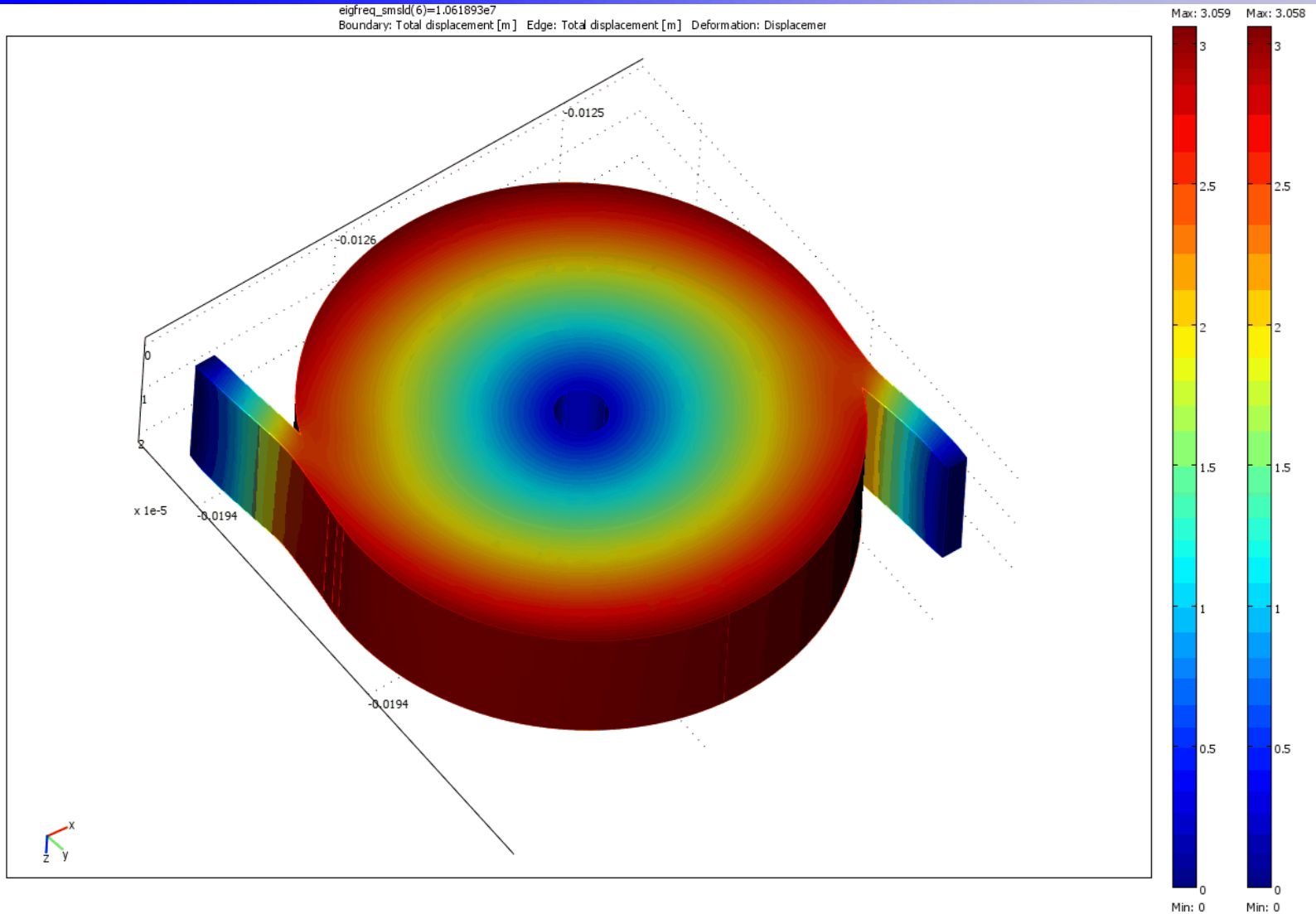


eigfreq_smsld(5)=6.240789e5
Boundary: Total displacement [m] Deformation: Displacement



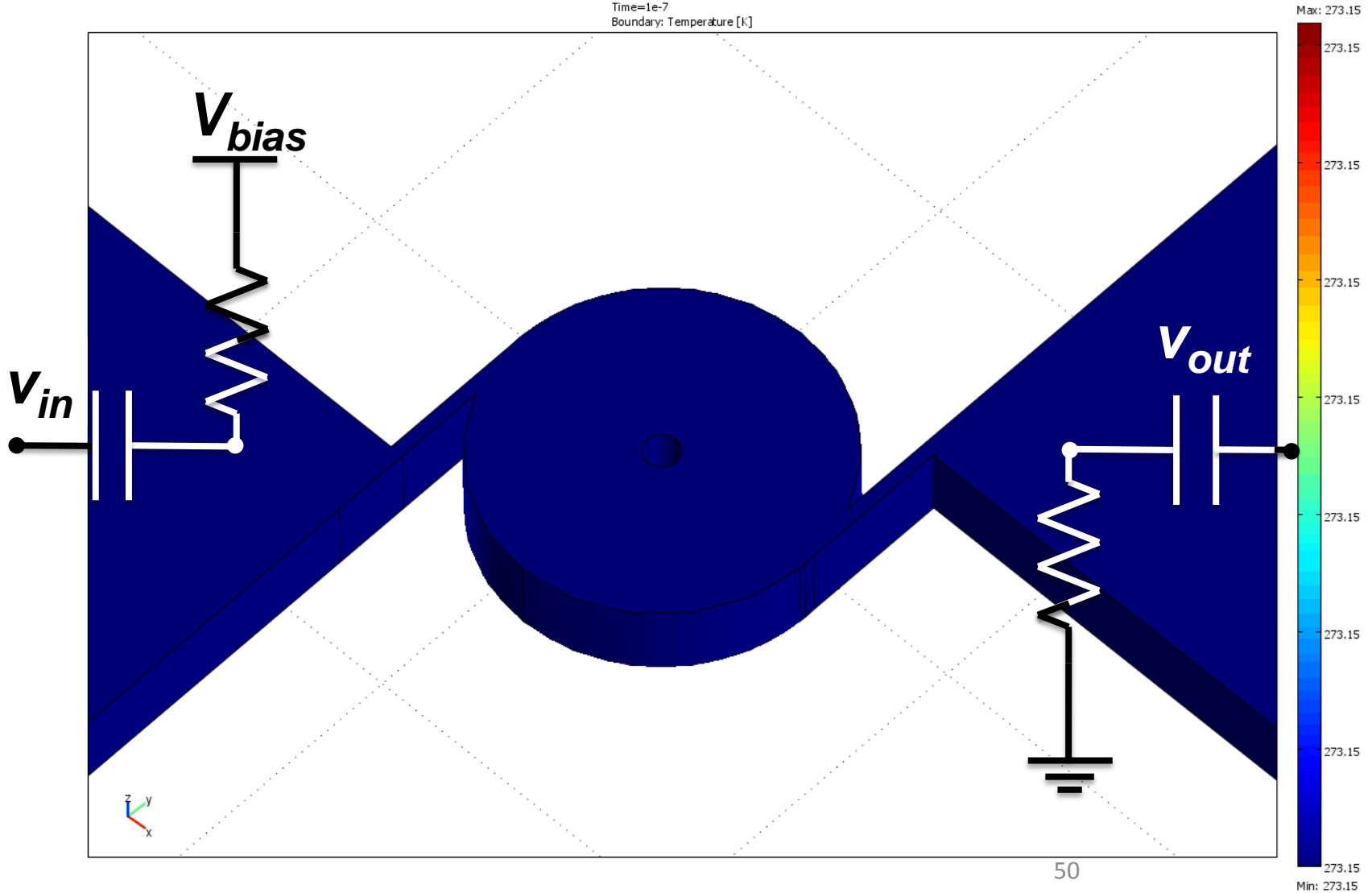
J. H. Seo and O. Brand, JMEMS 2008, Vol. 17, issue 2, pp. 483-493.

Our Approach: Rotational Mode Disk



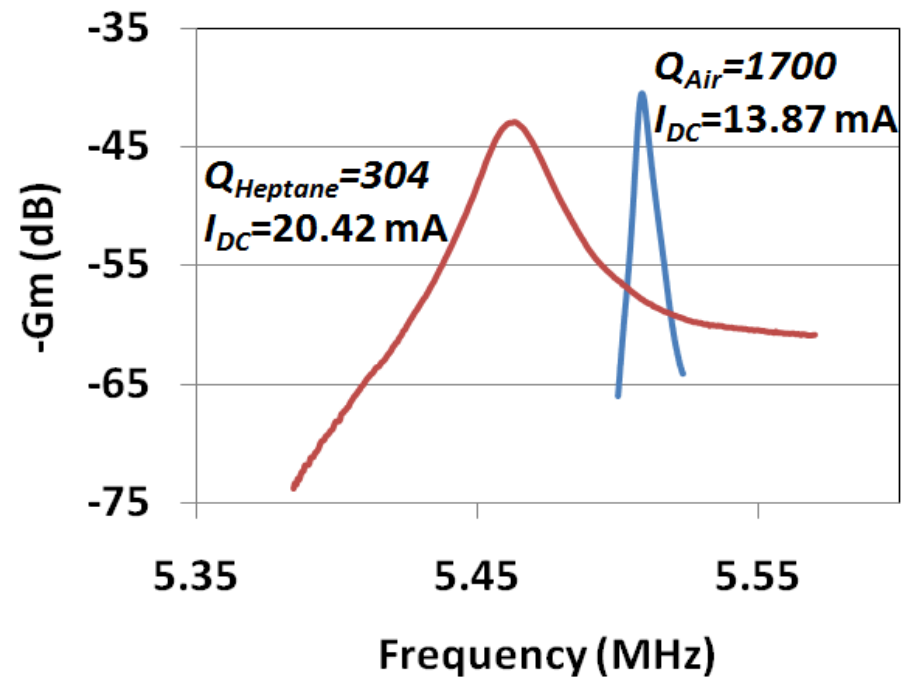
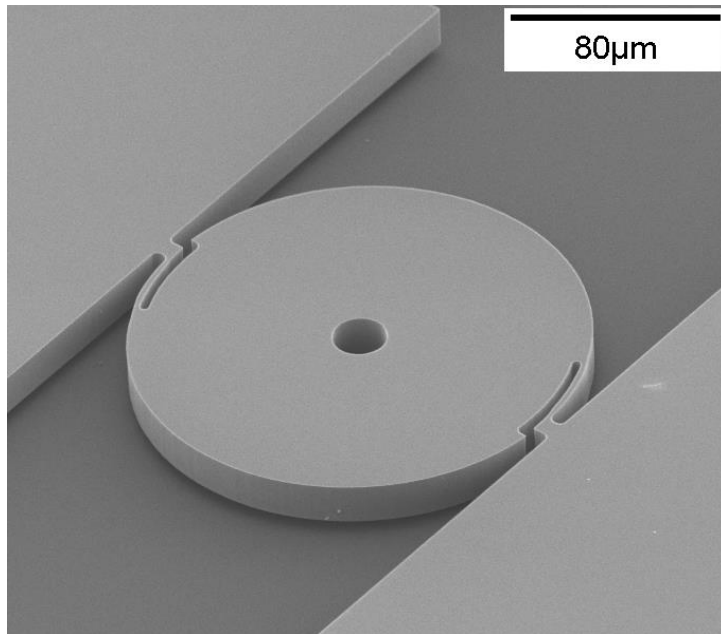
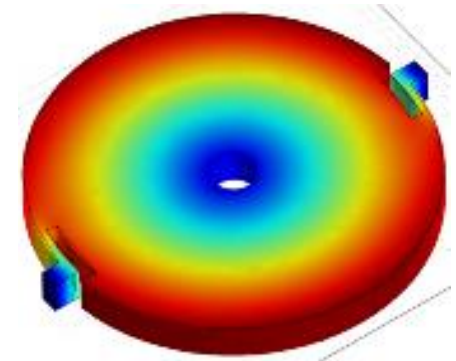
Resonator Operation

Time=1e-7
Boundary: Temperature [K]

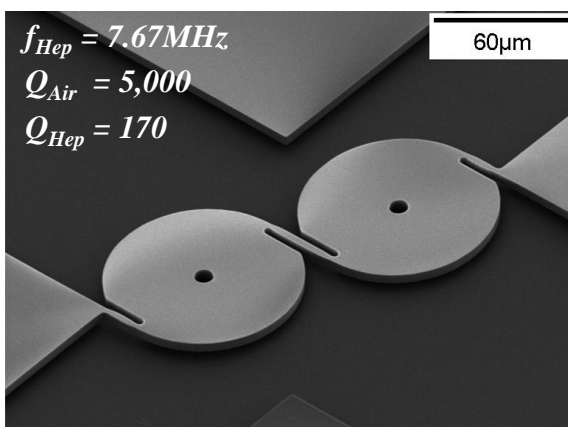
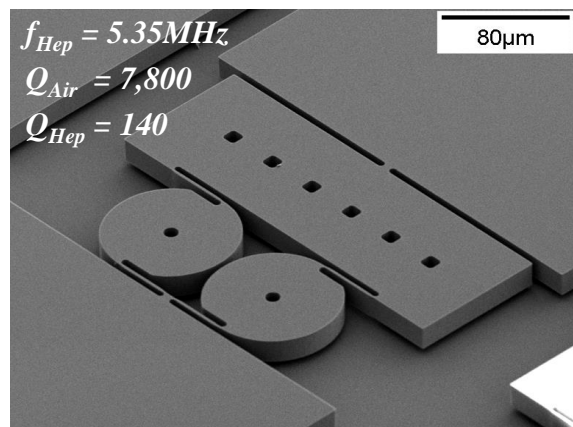
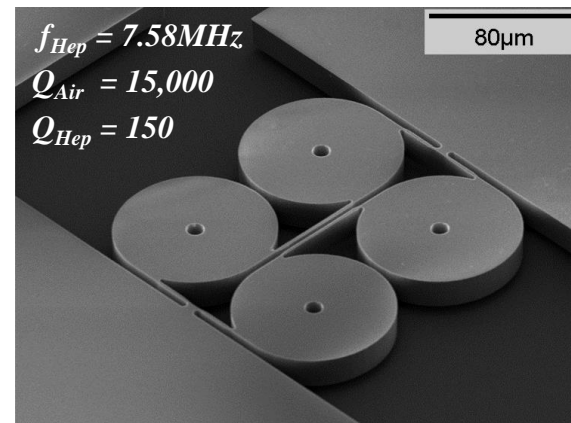
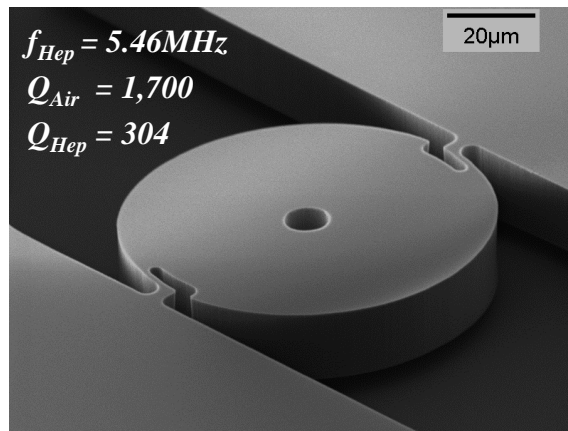
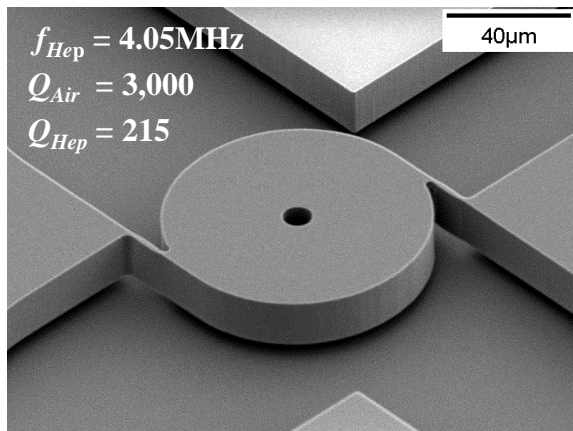


Measurement Results

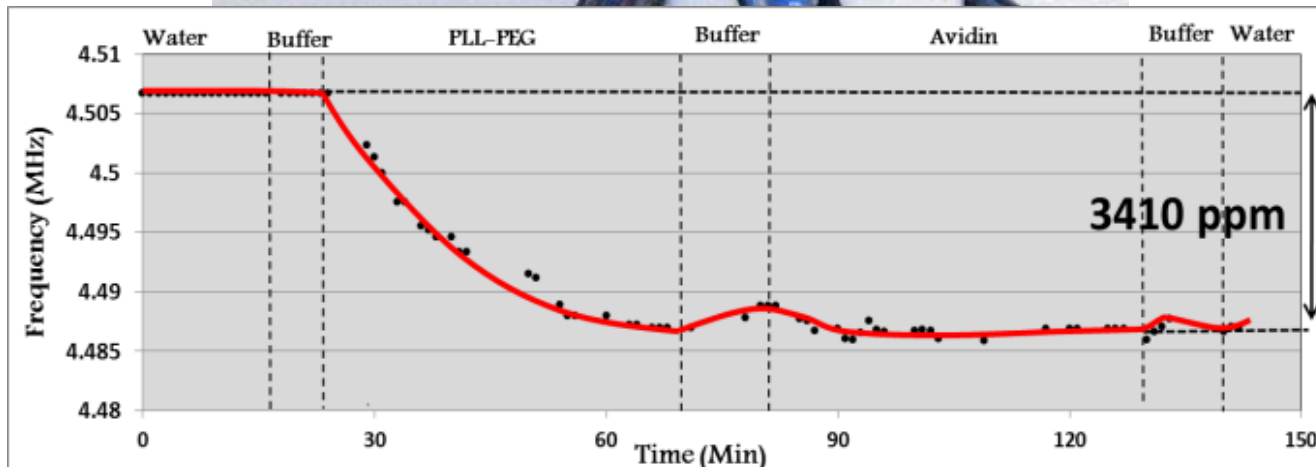
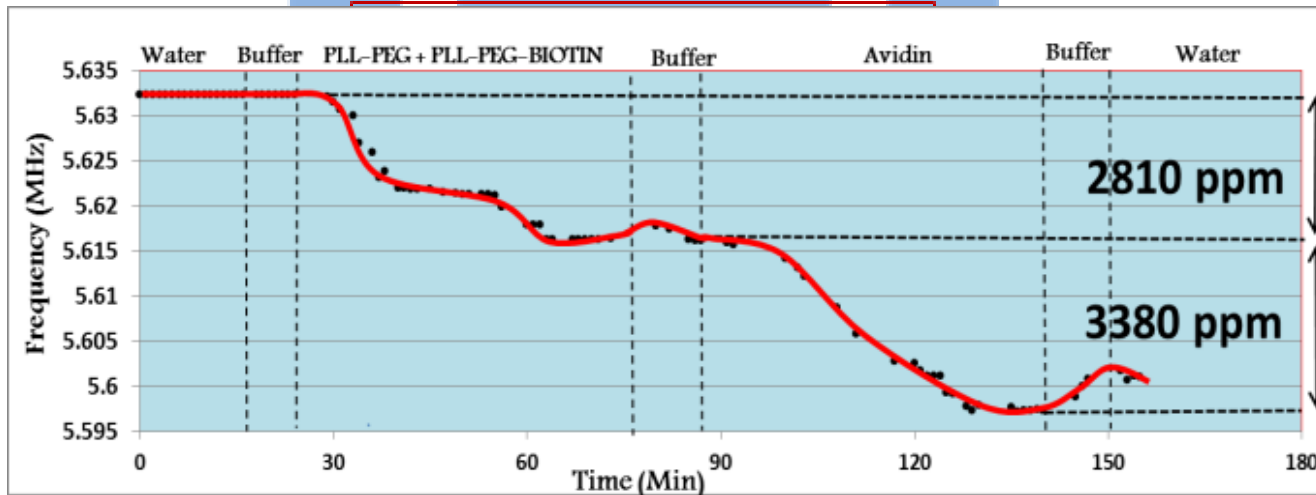
- ❑ Record high quality factor of **304** measured in liquid
- ❑ Potential for direct sensing of biomolecules in biological samples



Different Disk Resonator Topologies

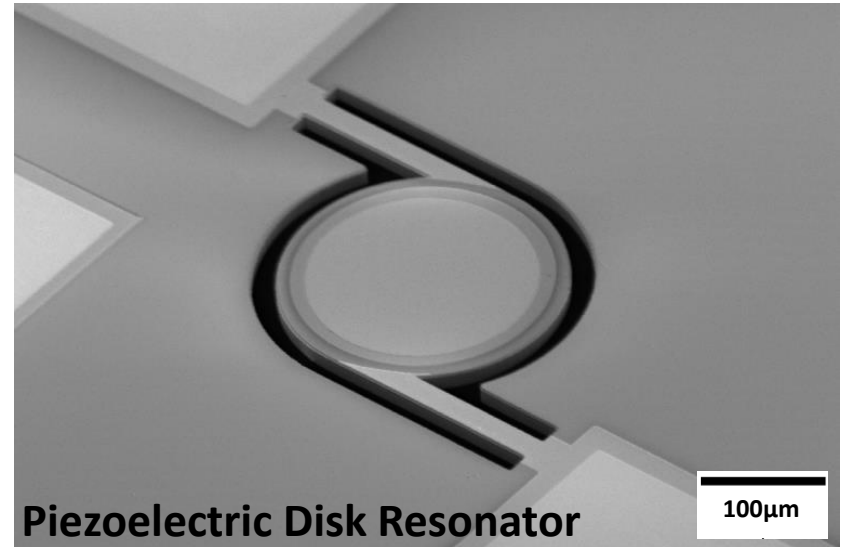
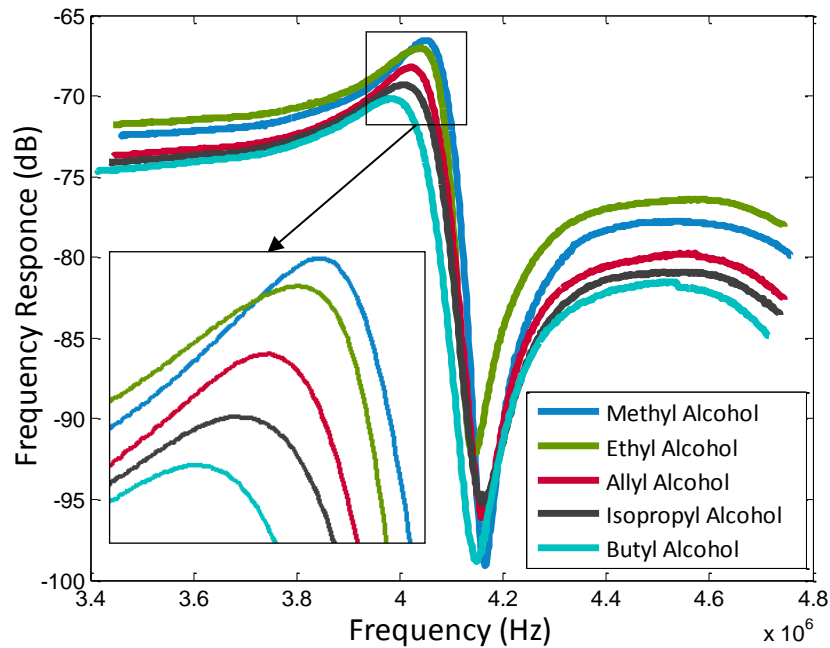


Resonators Encapsulated in Micro-Fluidic Channels



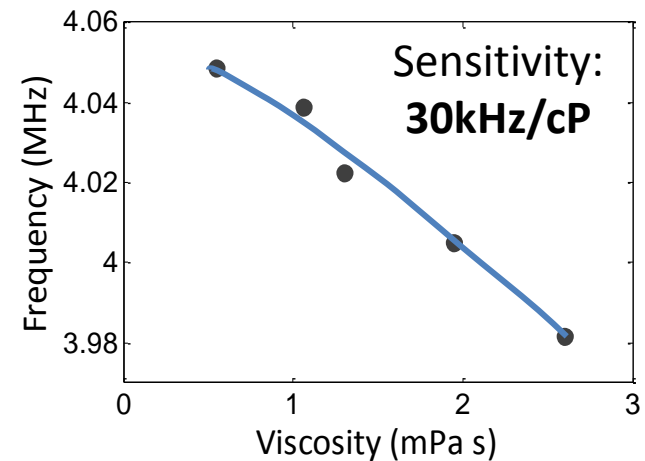
Liquid Viscosity Monitoring

□ Piezoelectric Rotational Mode Disk Resonators as viscosity monitors



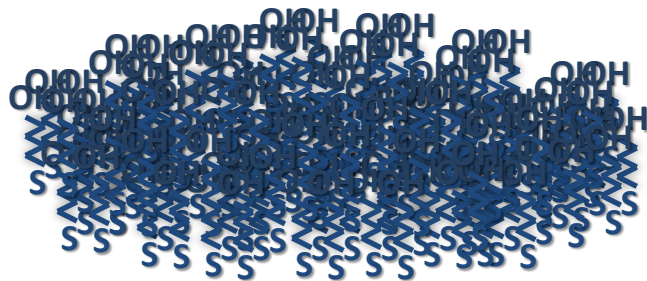
Piezoelectric Disk Resonator

Prof. Abdolvand Group, Oklahoma State University

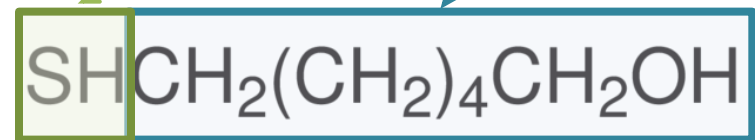


Experiments and Results

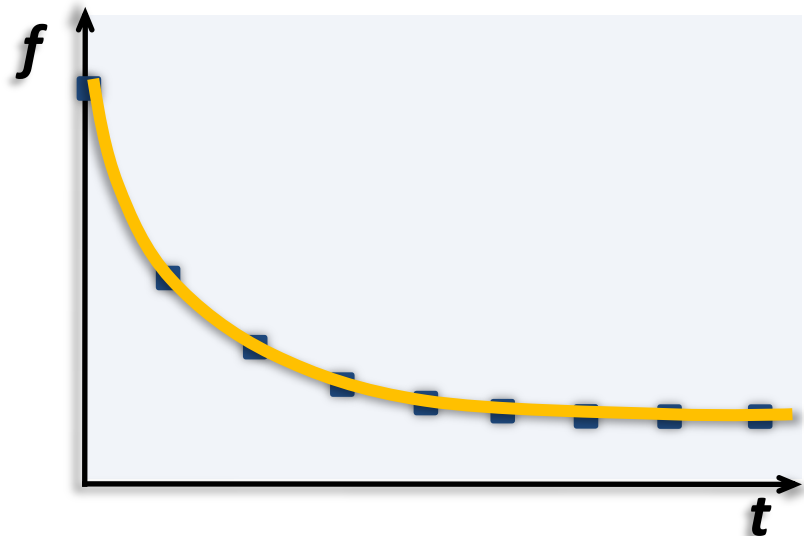
- ❑ Direct detection of MCH molecules in liquid media
- ❑ MCH interact easily with Au through the sulfur atom



Mercapto-Hexanol (MCH)

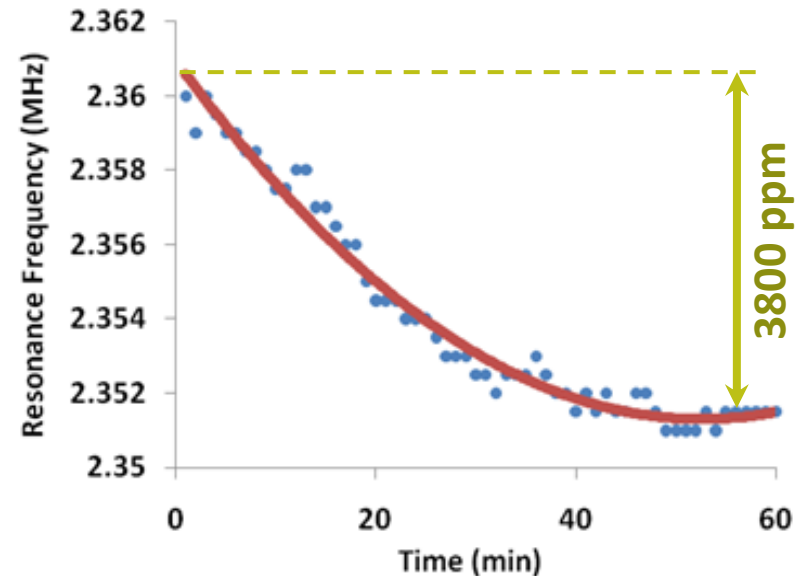
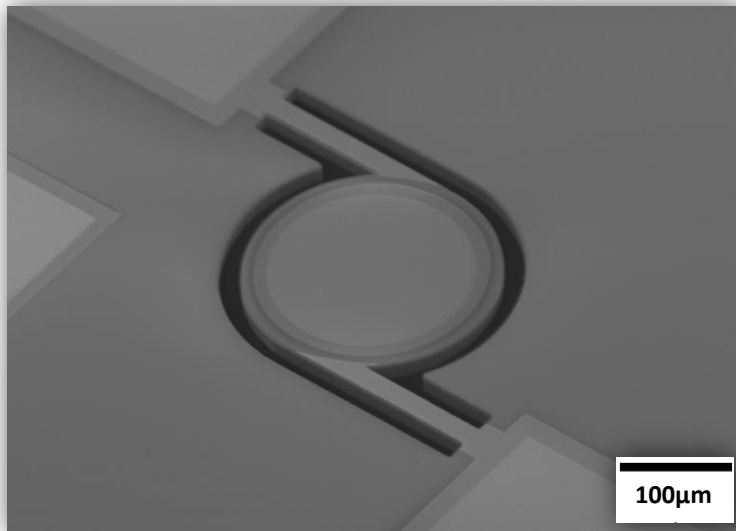
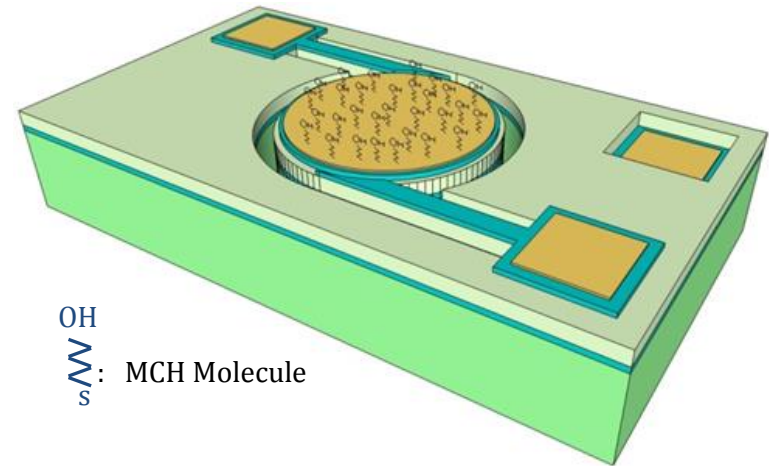


Blank Gold surface



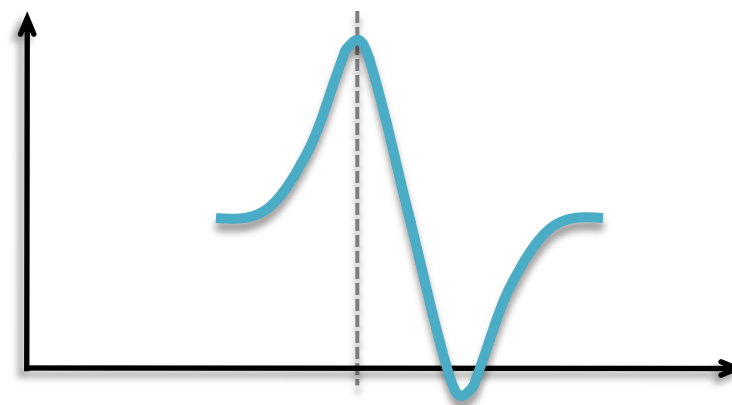
Piezoelectric Disk Resonators for Direct Molecular Sensing

- ❑ Rotational mode disk resonators are demonstrated as direct real-time bio-molecule monitors
- ❑ Exposure to 1.0 mM MCH in aqueous solution
- ❑ Saturation is reached after 1hr



Experiments and Results

DNA Detection Mechanism



Blank gold surface

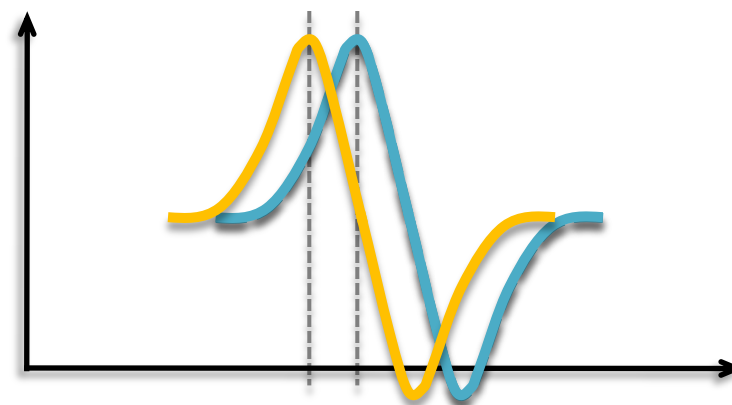
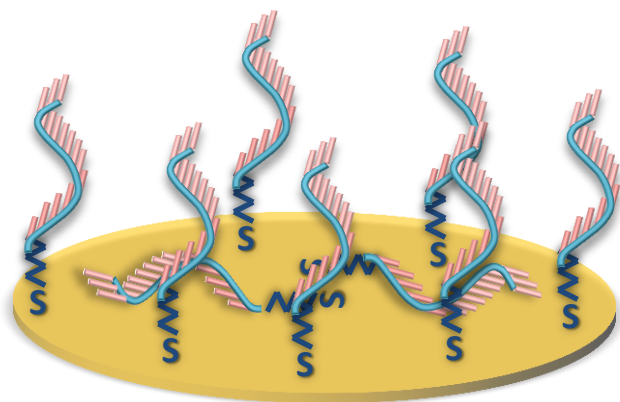
(I) Treatment with HS-ssDNA (2.0 μM /1.0 M KH_2PO_4 , PH 4.2)

(II) Exposure to 1.0 mM Mercapto-Hexanol in aqueous solution

**(III) Hybridization with Complementary DNA Solution (1.0 μM /1.0 M NaCl Tris-HCl
1.0 mM EDTA)**

Experiments and Results

DNA Detection Mechanism



Blank gold surface

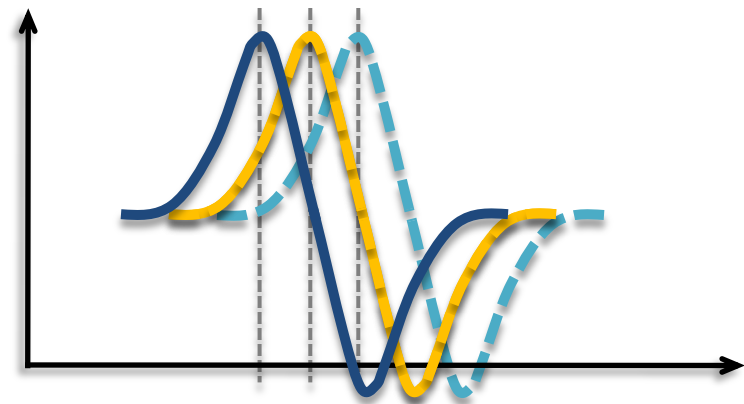
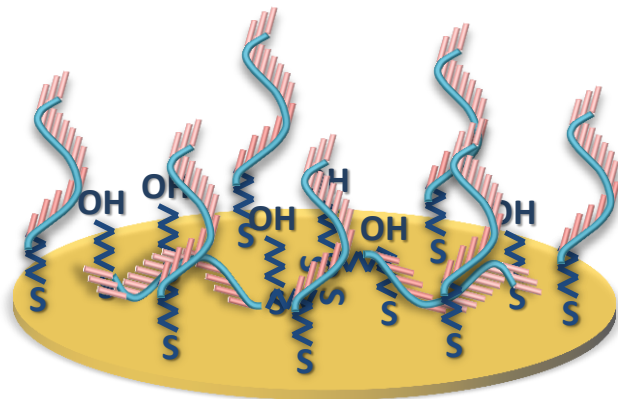
(I) Treatment with HS-ssDNA (2.0 μM /1.0 M KH_2PO_4 , PH 4.2)

(II) Exposure to 1.0 mM Mercapto-Hexanol in aqueous solution

(III) Hybridization with Complementary DNA Solution (1.0 μM /1.0 M NaCl Tris-HCl
1.0 mM EDTA)

Experiments and Results

DNA Detection Mechanism



Blank gold surface

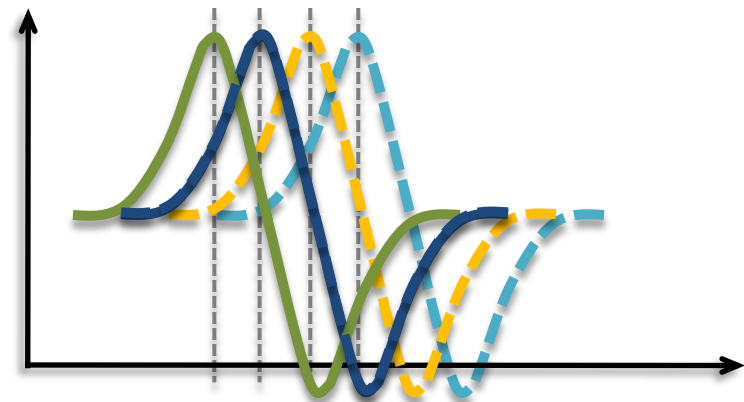
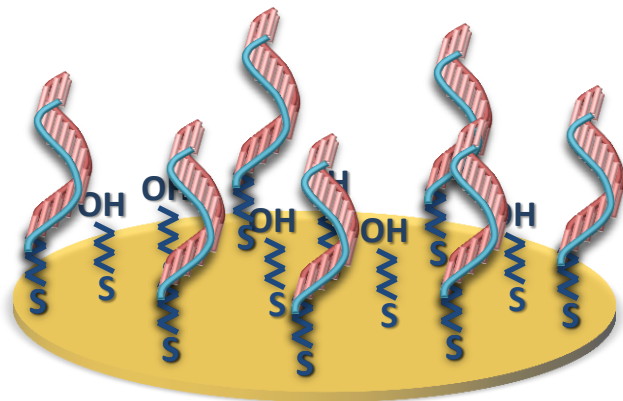
(I) Treatment with HS-ssDNA ($2.0 \mu\text{M}/1.0 \text{ M KH}_2\text{PO}_4$, PH 4.2)

(II) Exposure to 1.0 mM Mercapto-Hexanol in aqueous solution

(III) Hybridization with Complementary DNA Solution ($1.0 \mu\text{M}/1.0 \text{ M NaCl Tris-HCl}$
1.0 mM EDTA)

Experiments and Results

DNA Detection Mechanism



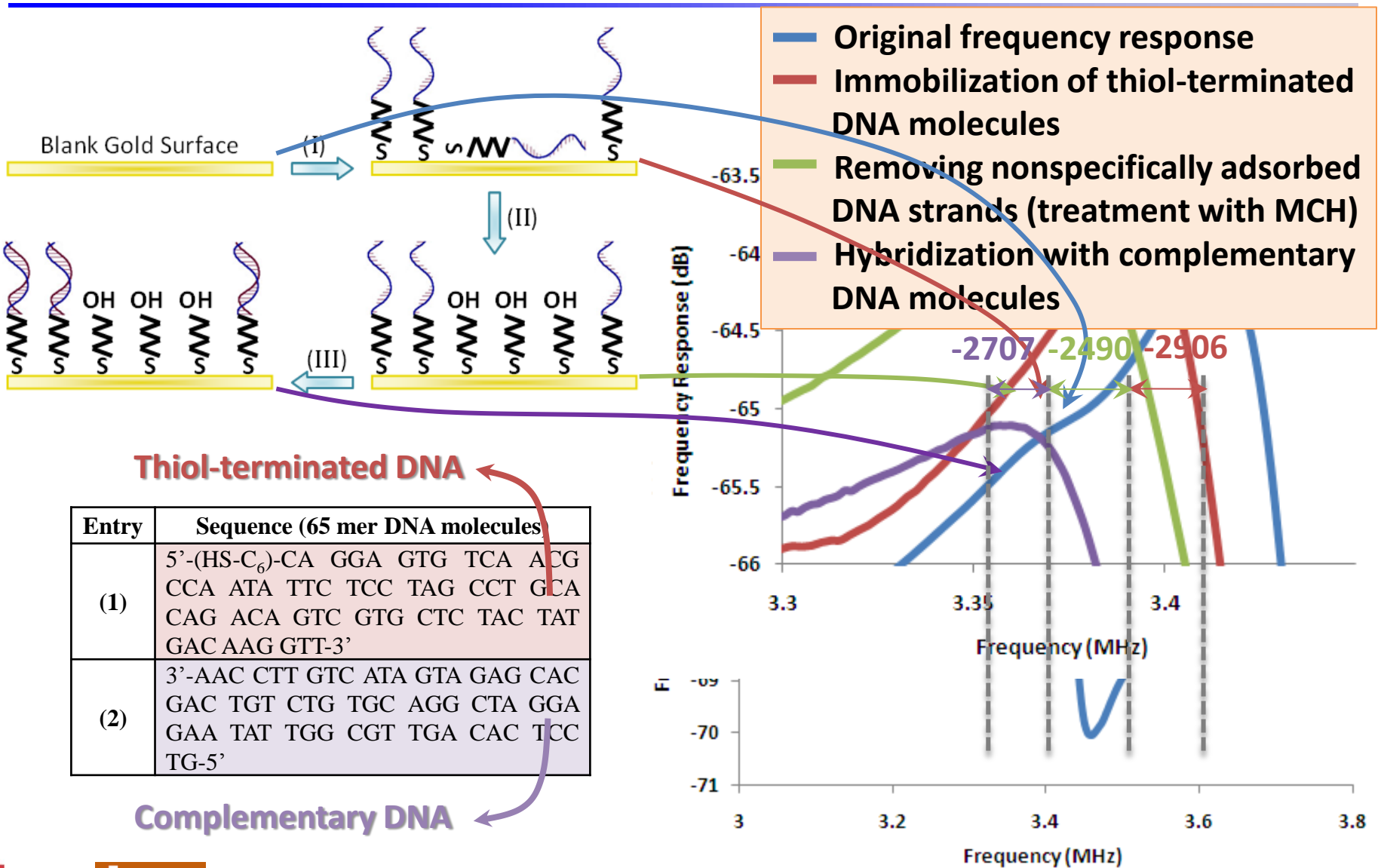
Blank gold surface

(I) Treatment with HS-ssDNA ($2.0 \mu\text{M}/1.0 \text{ M KH}_2\text{PO}_4$, PH 4.2)

(II) Exposure to 1.0 mM Mercapto-Hexanol in aqueous solution

**(III) Hybridization with Complementary DNA Solution ($1.0 \mu\text{M}/1.0 \text{ M NaCl Tris-HCl}$
 1.0 mM EDTA)**

DNA Detection Results



Gas Sensing: Detection of Volatile Organic Compounds

- ❑ Sensors capable of organic compounds detection in gas phase have numerous applications in oil and gas industry



- ❑ Rapid estimation of oil content of oil sand samples and early detection of hazardous leaks

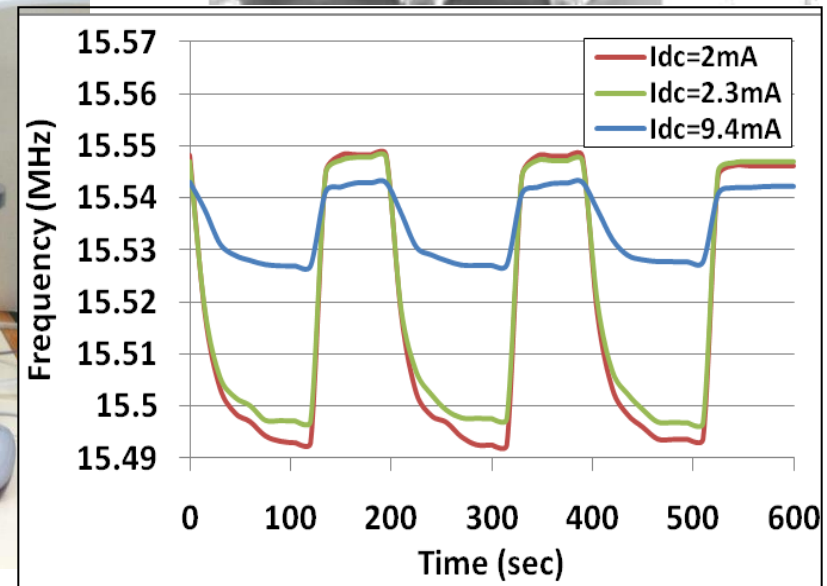
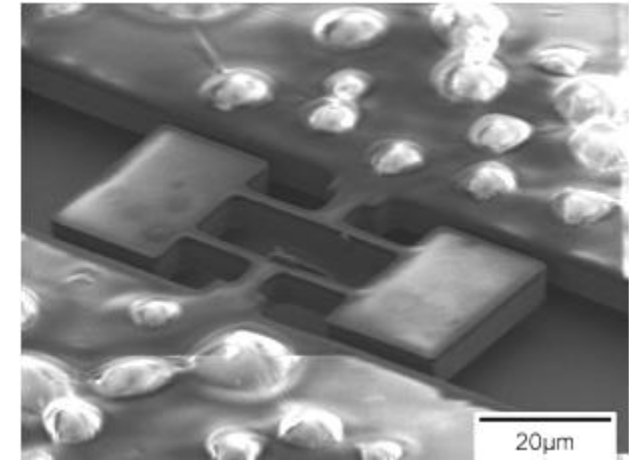
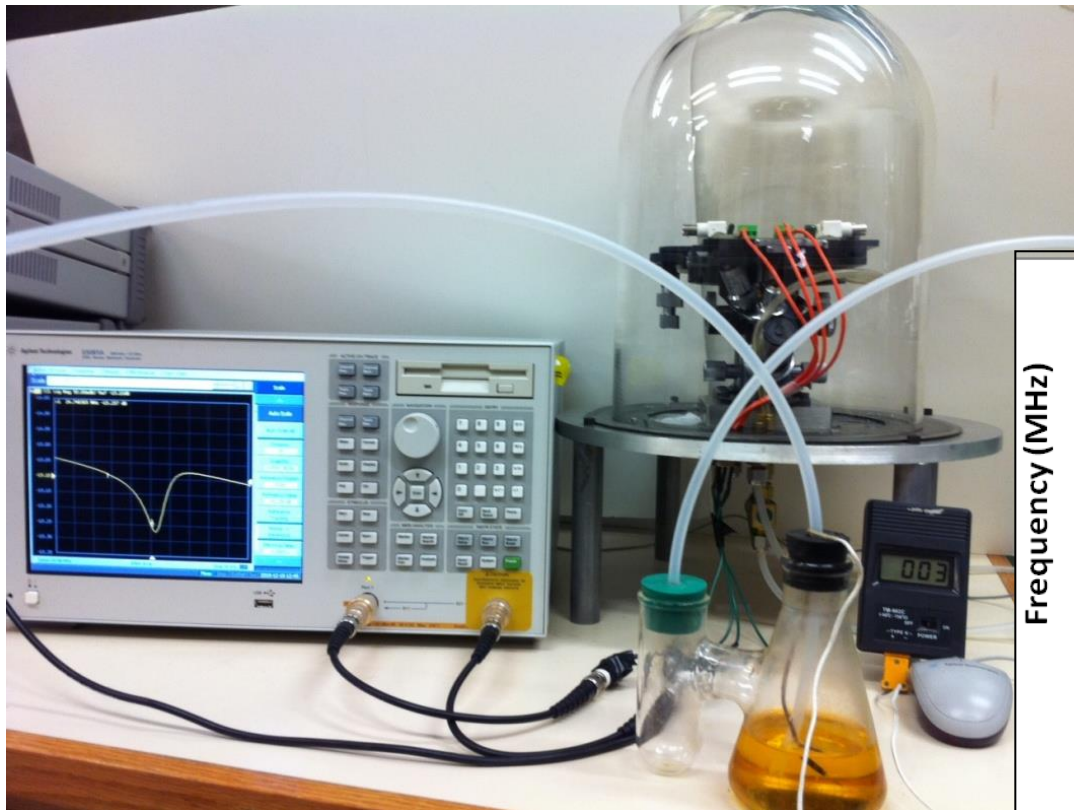


- ❑ Costly and time consuming process of using off-site laboratory analysis avoided

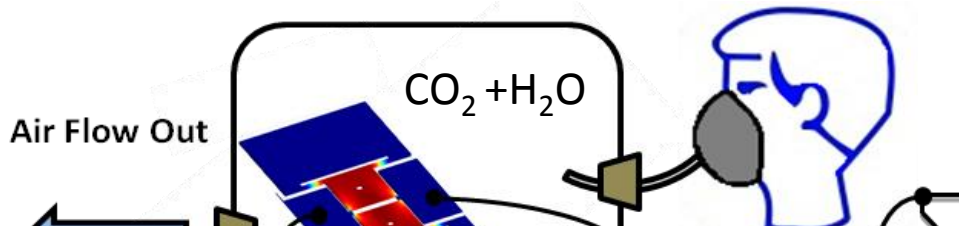


Detection of Gasoline Vapor

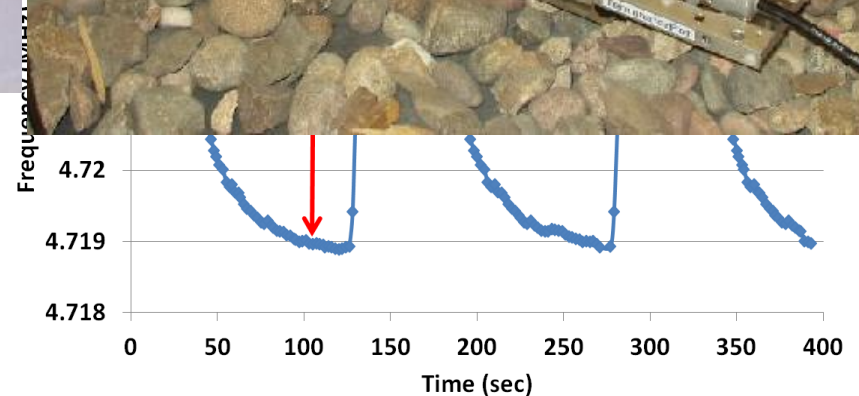
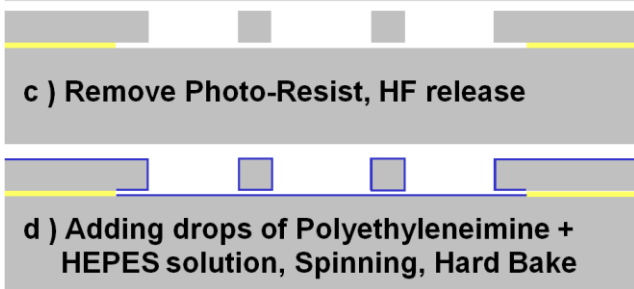
□ Thin polymer coating to absorb organic vapors



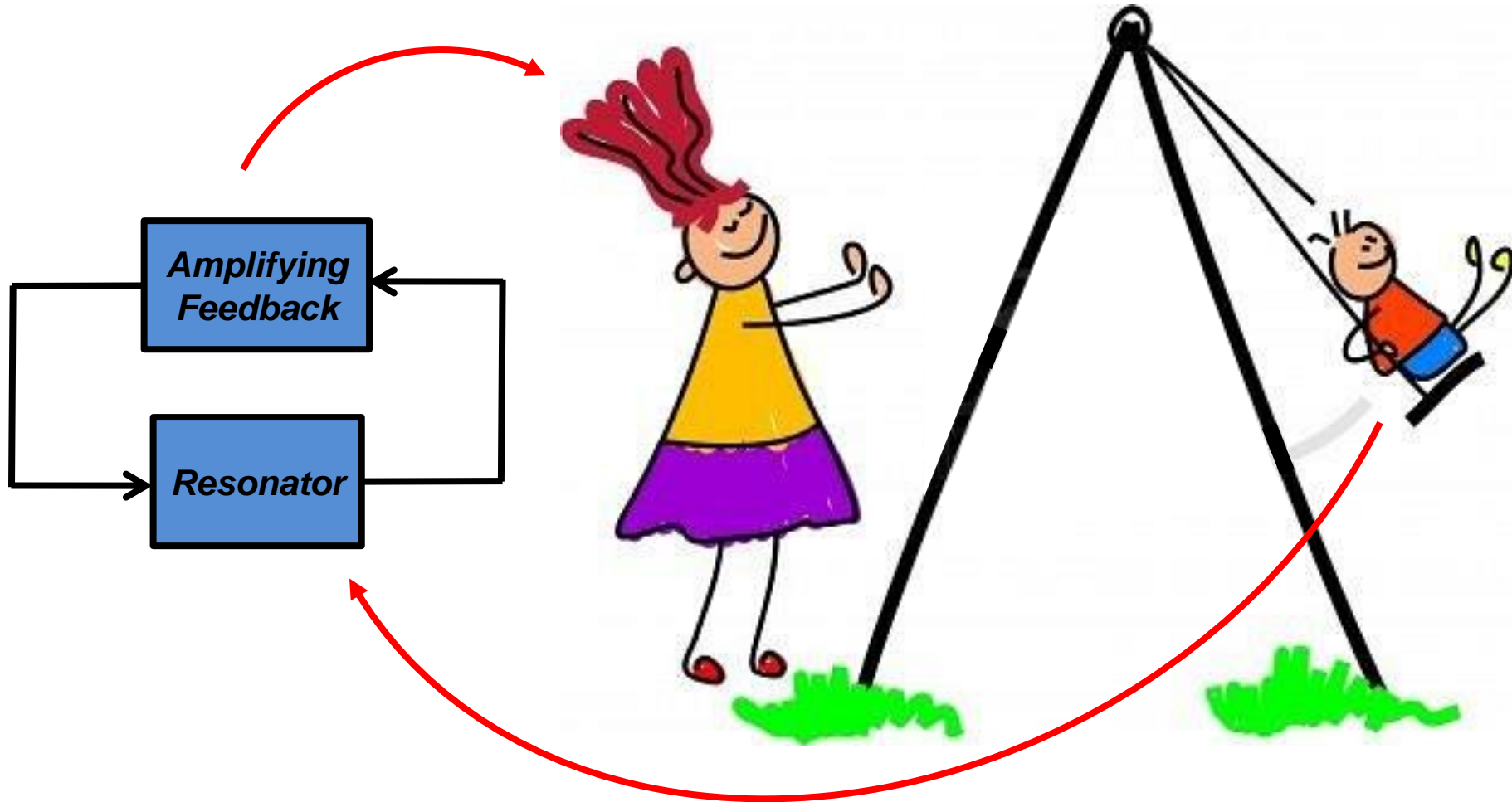
Disaster Survivor Detection!



Resonator with poly-ethyleneimine (PEI) Coating

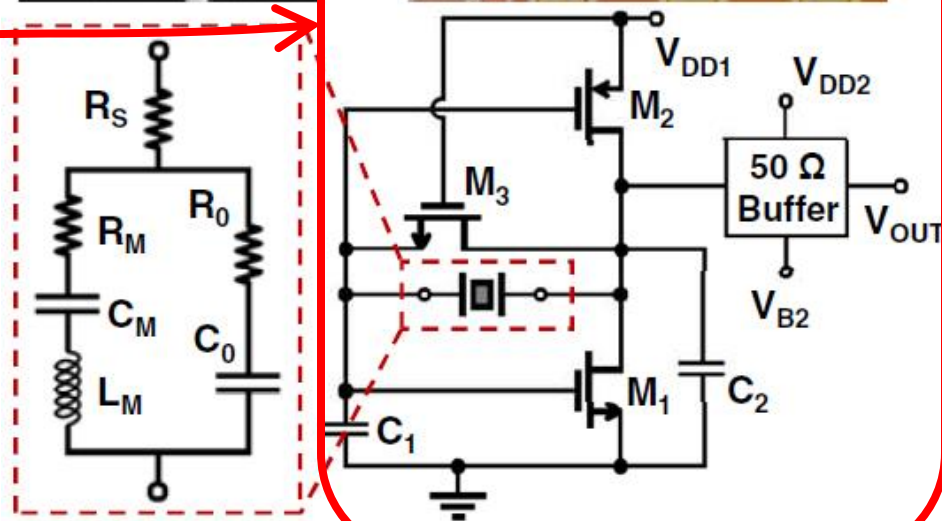
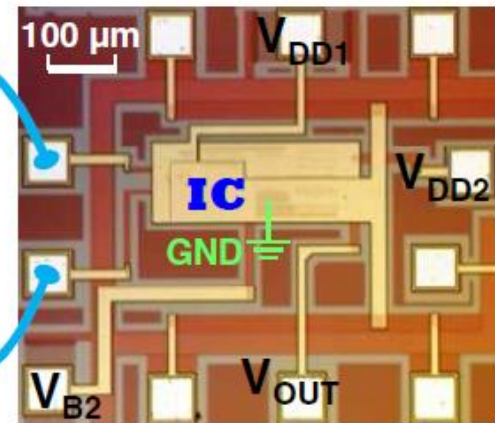
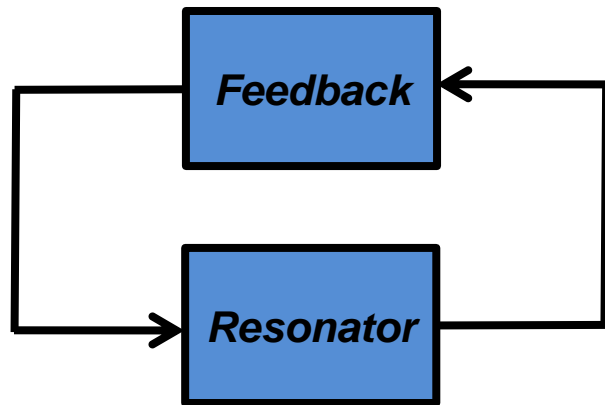


Oscillator vs. Resonator



Oscillation Requirement

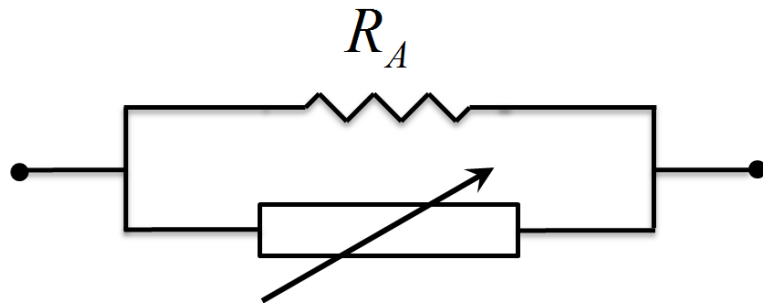
□ Piezoelectric and Electrostatic MEMS Resonators (**External Amplification**)



Chengjie Zuo; Van der Spiegel, J.; Piazza, G.; , "1.5-GHz CMOS voltage-controlled oscillator based on thickness-field-excited piezoelectric AlN contour-mode MEMS resonators," *Custom Integrated Circuits Conference (CICC), 2010 IEEE* , vol., no.,

Positive Feedback Loop for Oscillation

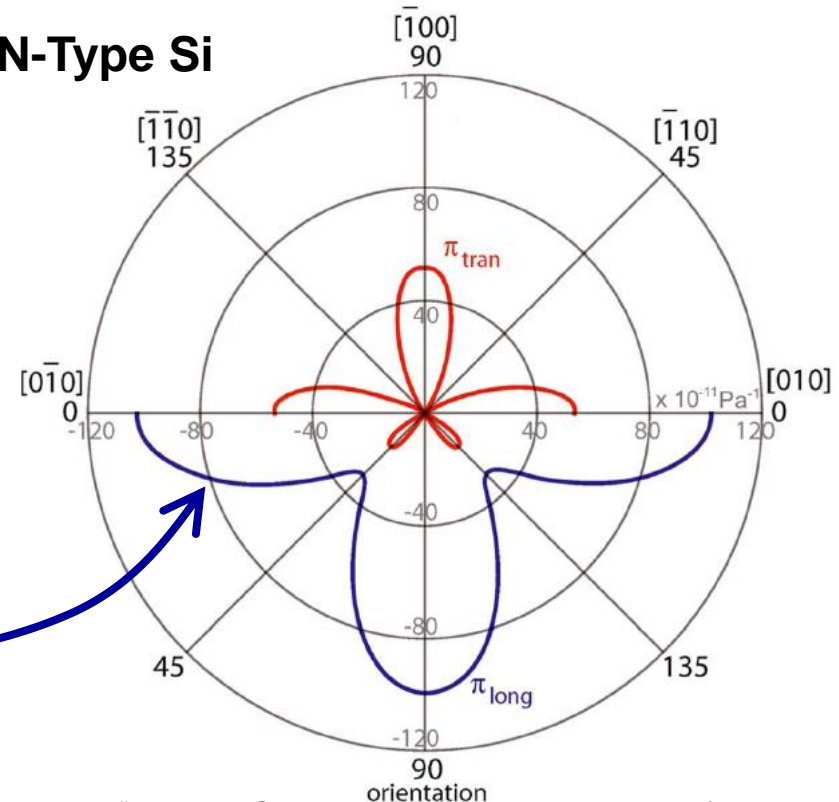
□ Thermal- Piezoresistive Resonators (**Internal Amplification**)



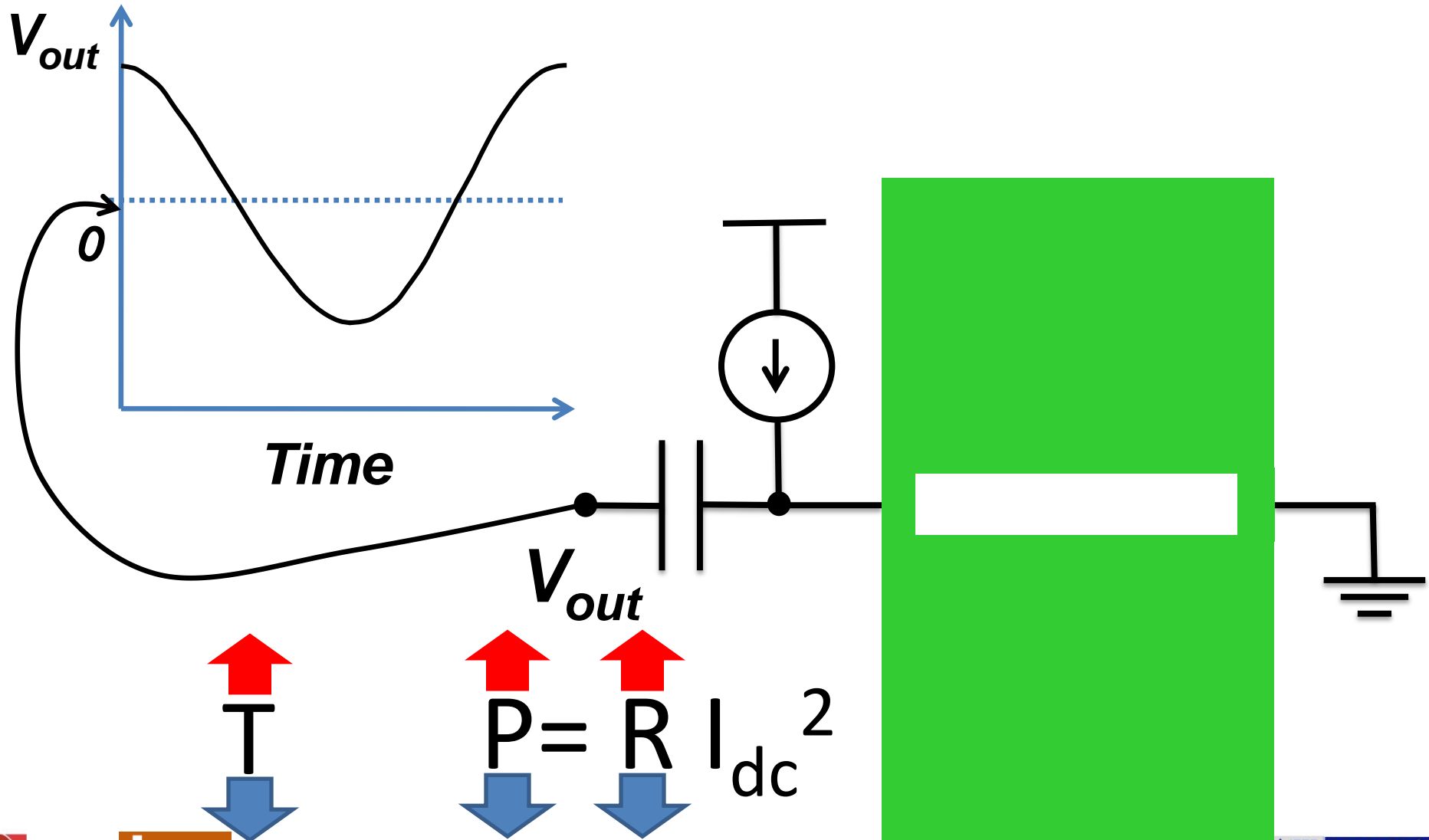
Motional Conductance (g_m)

$$g_m = 4\alpha E^2 \pi_l Q \frac{AI_{dc}^2}{KLC_{th}\omega_m}$$

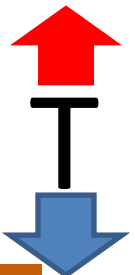
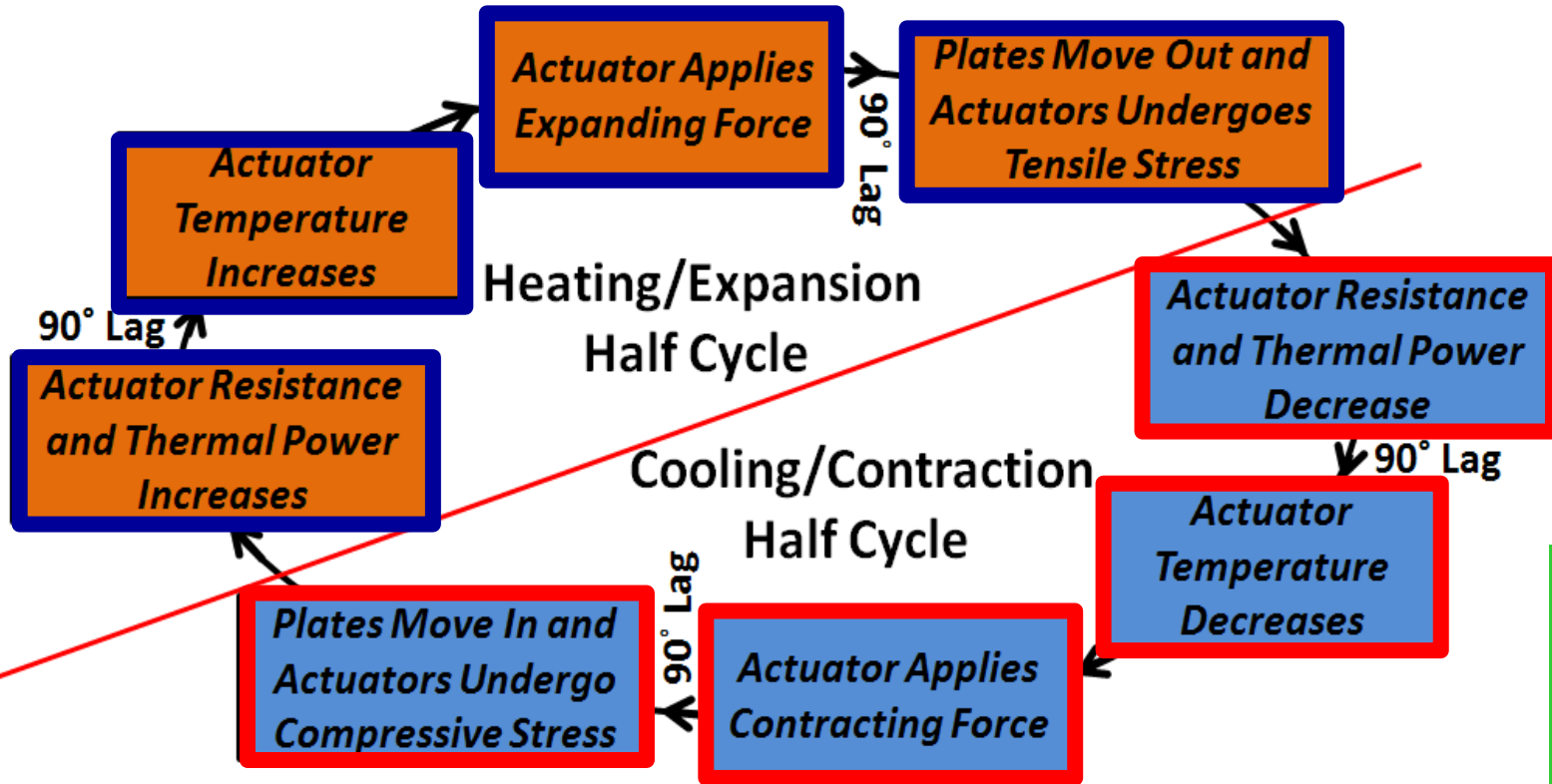
N-Type Si



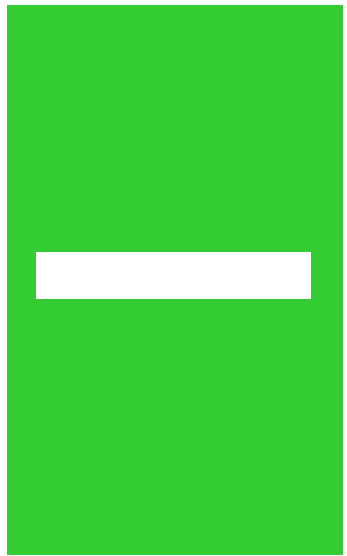
Thermal-Piezoresistive Oscillation Concept



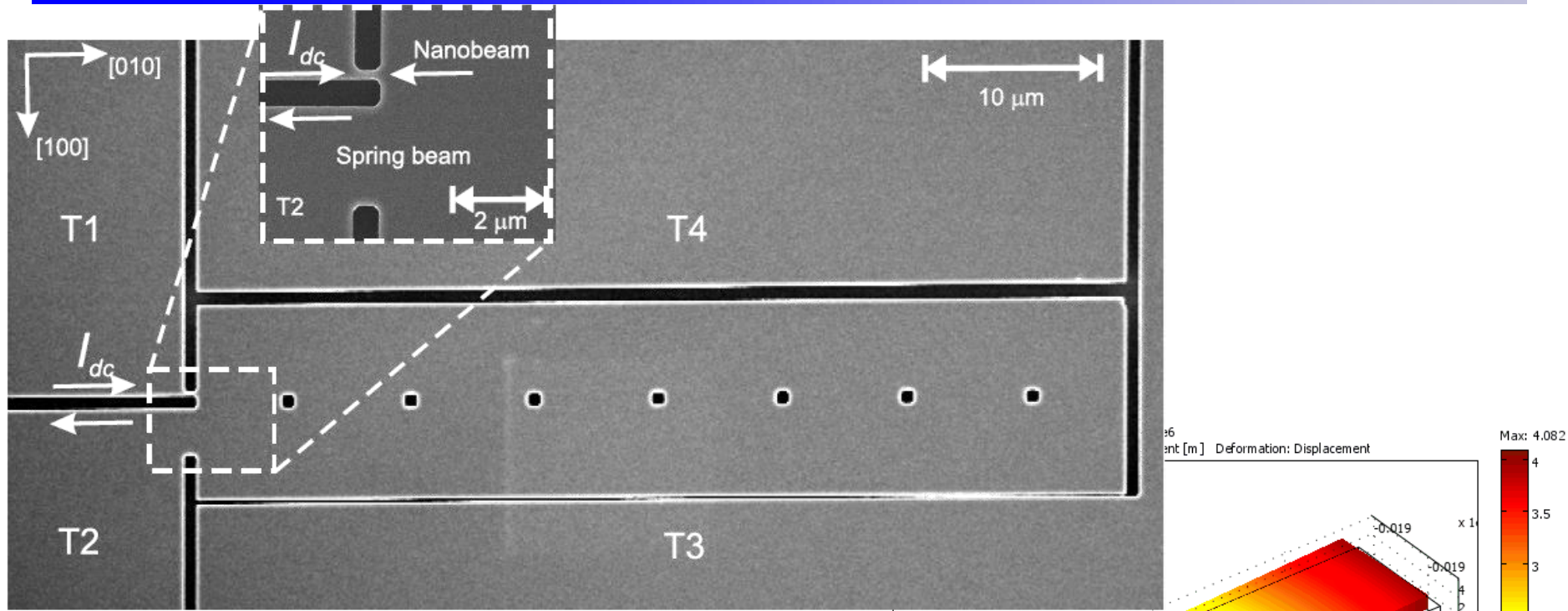
Thermal-Piezoresistive Oscillation Concept



$P = R I_{dc}^2$



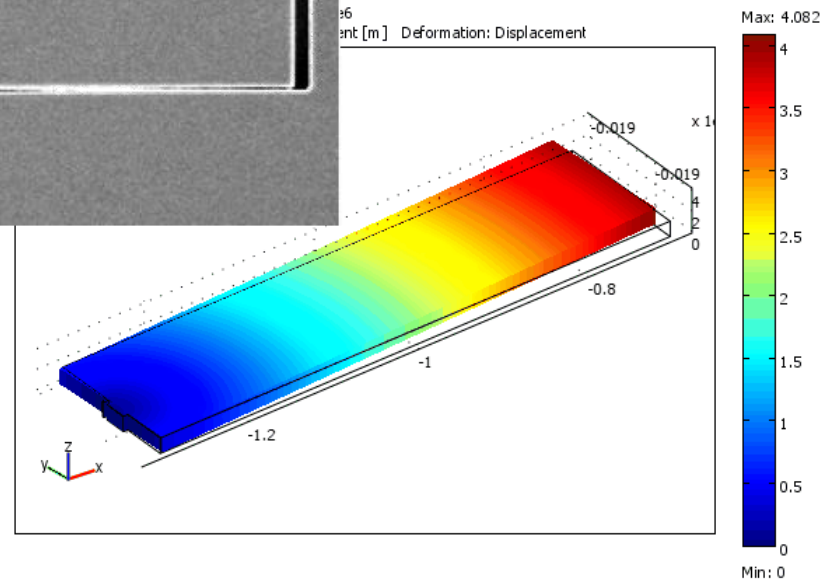
Previous Work from NXP SC



1.26MHz (Vacuum) $I_{dc} = 1.20 \text{ mA}$

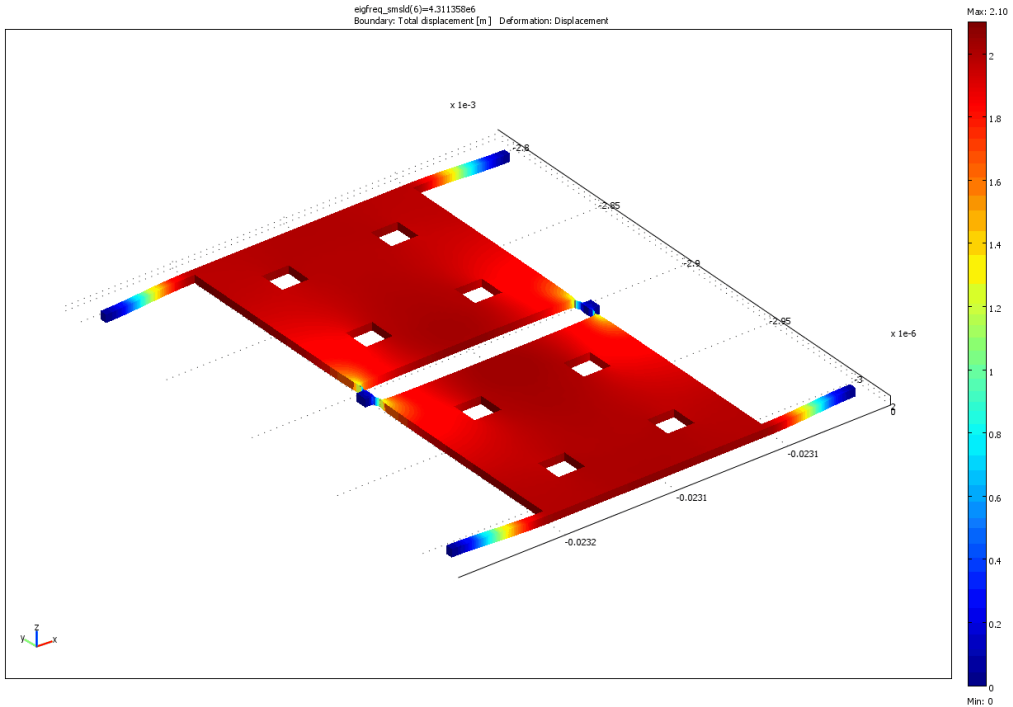
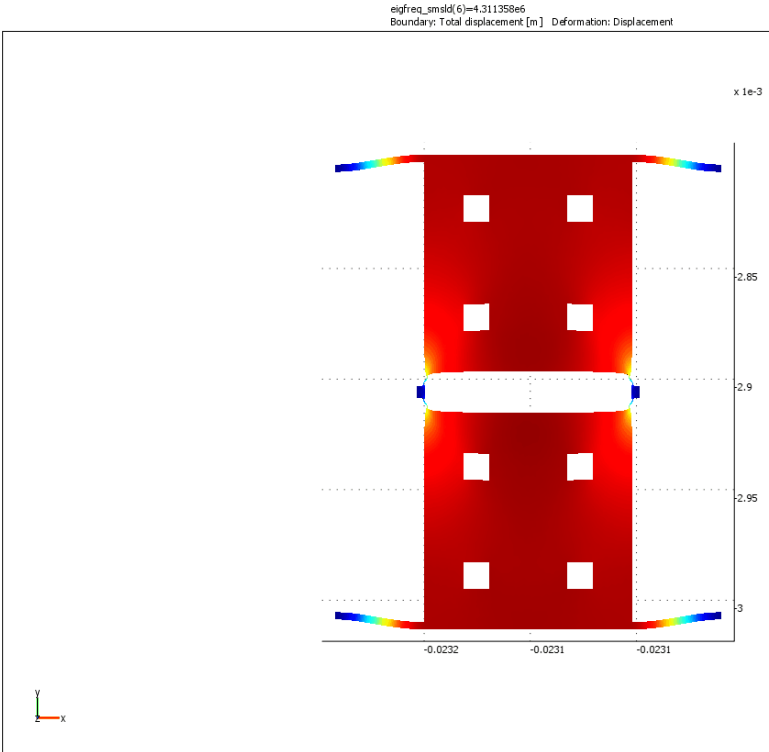
$V_{p-p} = 54 \text{ mV}$

$P_{dc} = 1.19 \text{ mW}$

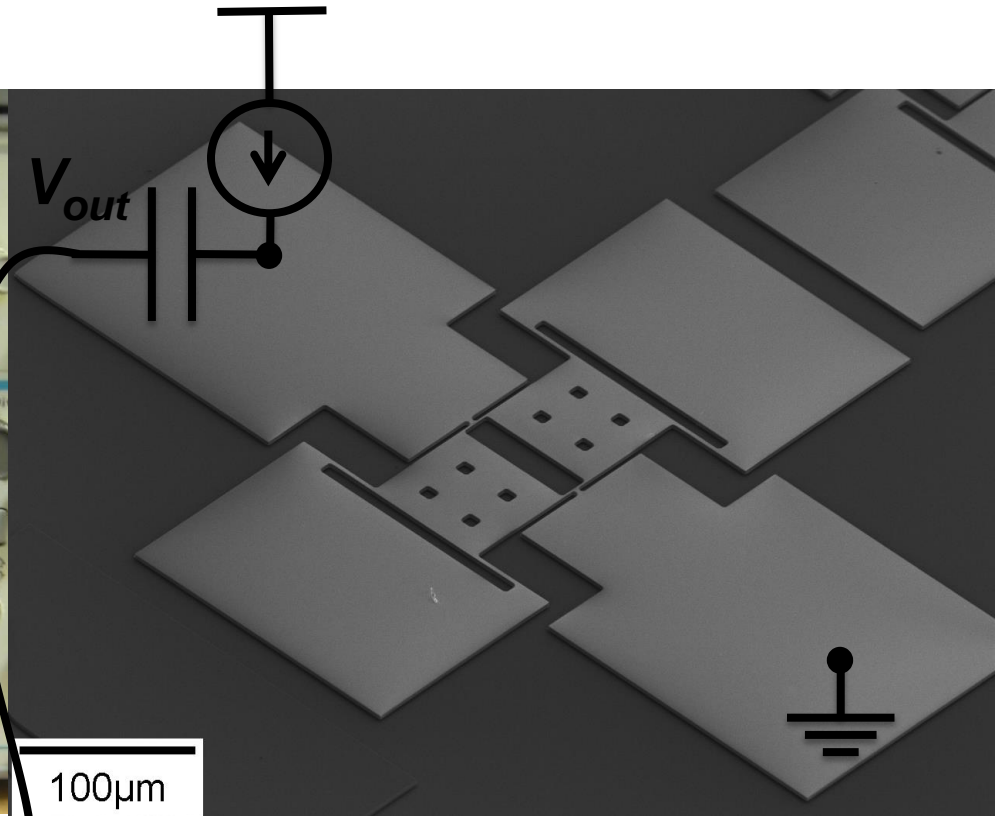
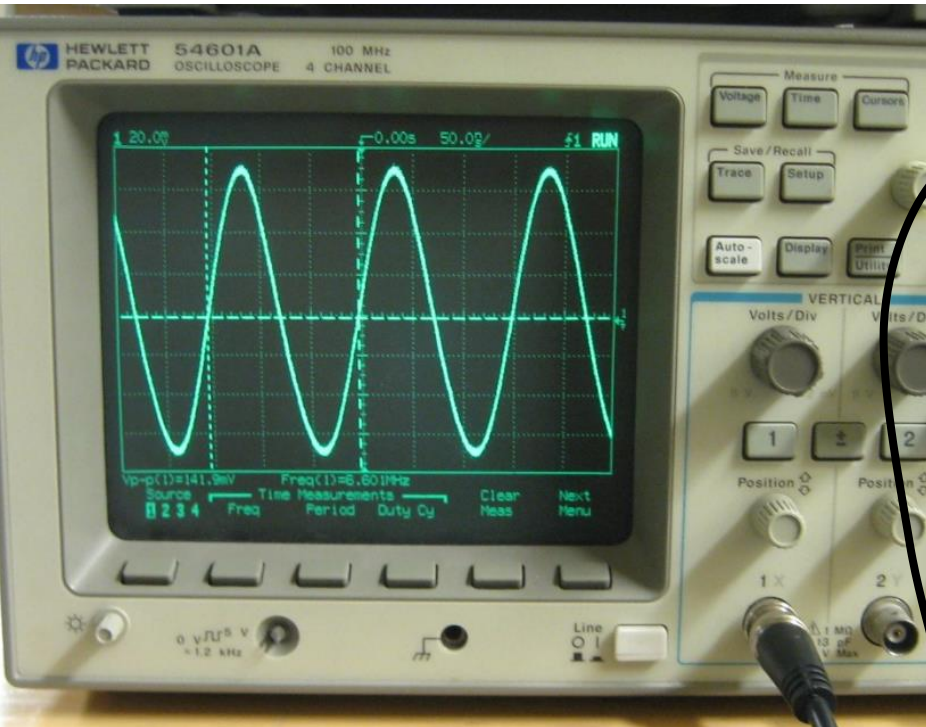


K. L. Phan, P. G. Steeneken, M. J. Goossens, G. E.J. Koops, G. J.A.M. Verheijden and J.T.M.v. Beek, "Spontaneous mechanical oscillation of a DC driven single crystal," to be published, <http://arxiv.org/abs/0904.3748> (2009).

Fabricated Thermal-Piezoresistive Resonator



Oscillation Results



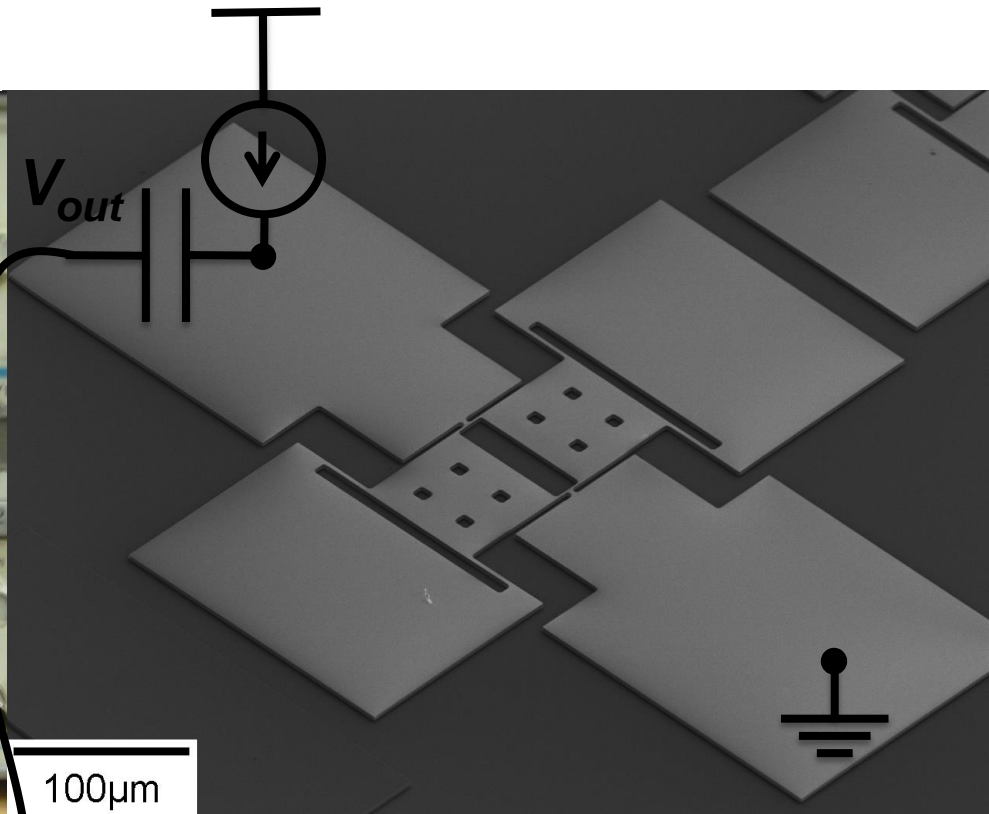
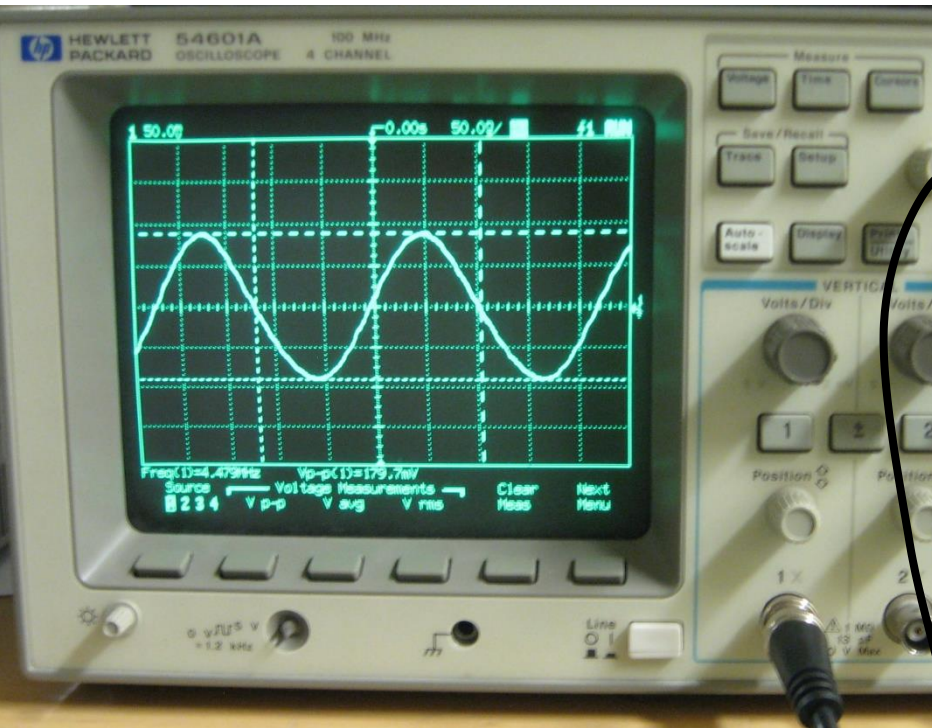
Freq. = 4.5MHz (Air)

$V_{p-p} = 400mV$

$I_{dc} = 3.5mA$

$P = 23.2mW$

Oscillation Results



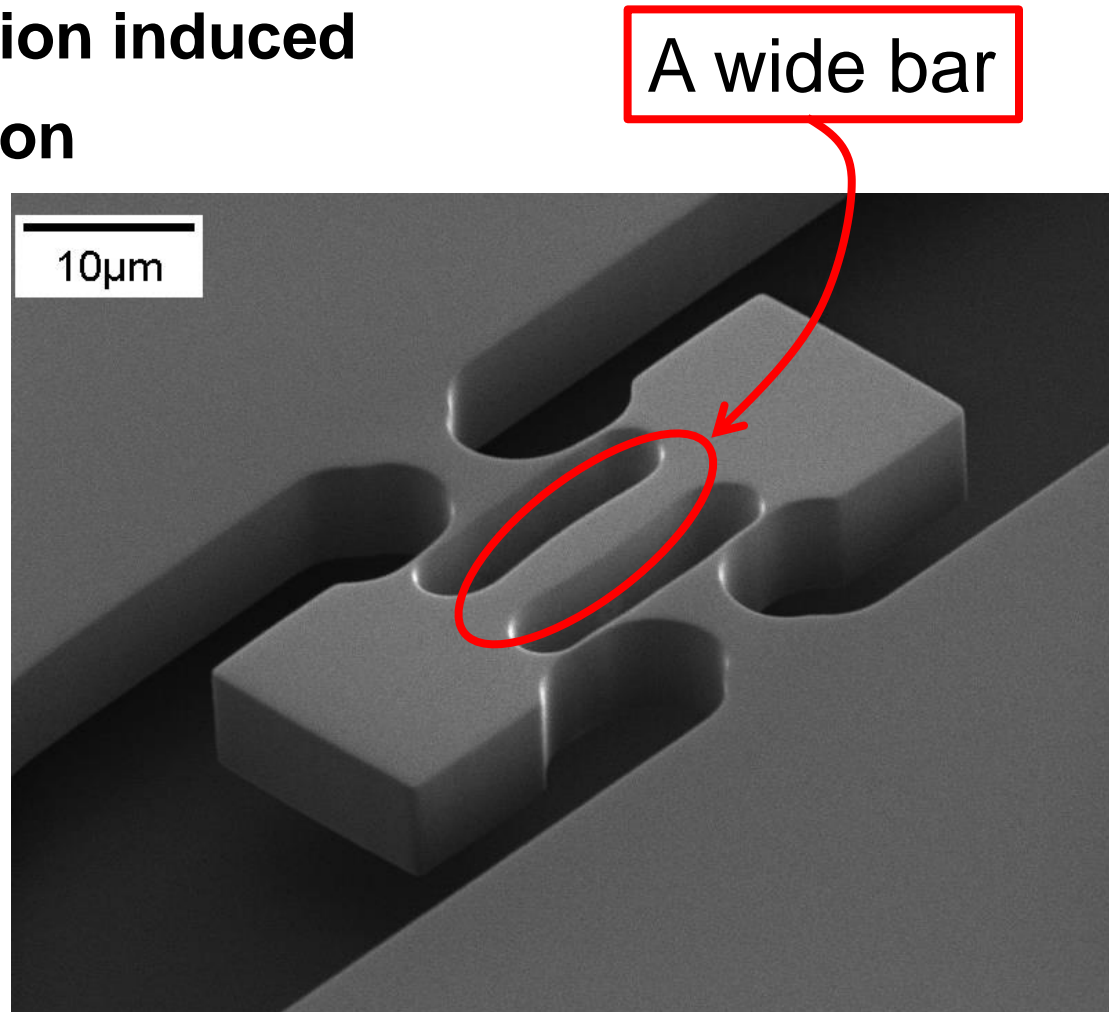
Freq. = 3.54MHz (Vacuum) $I_{dc} = 1.2mA$

$V_{p-p} = 138mV$

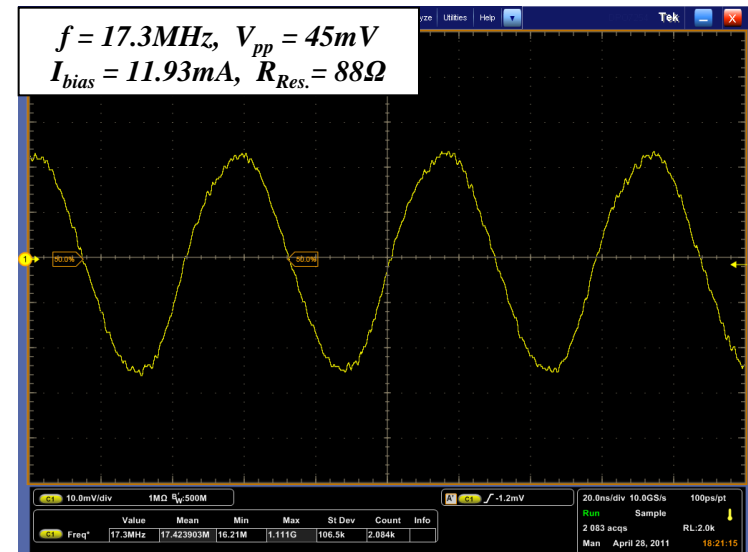
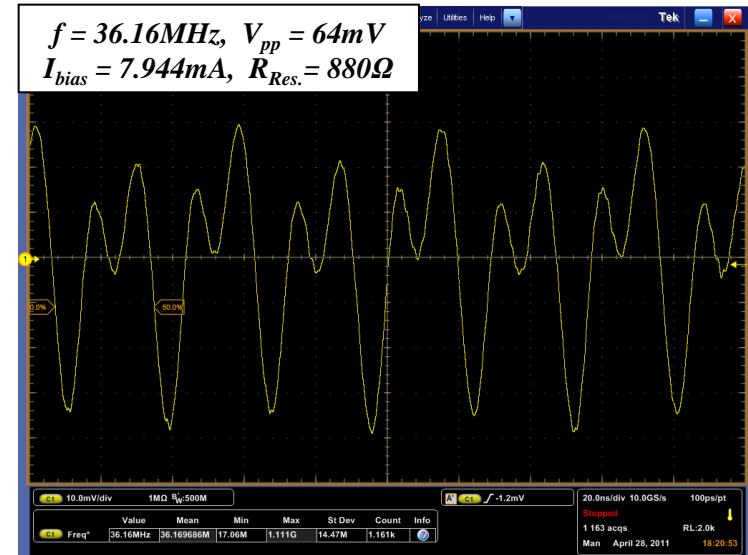
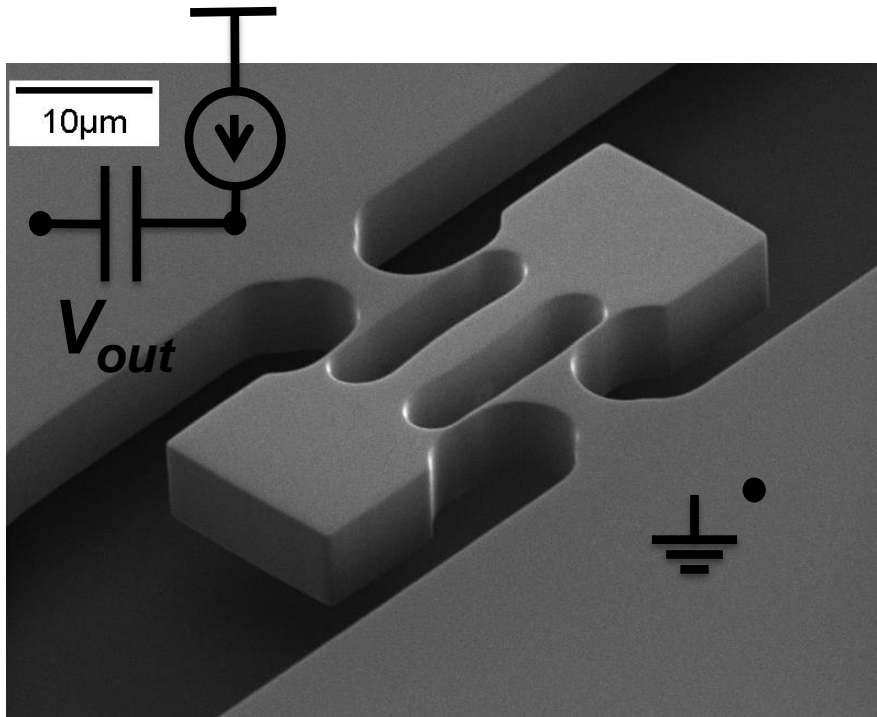
$P = 2.34mW$

Higher Frequency Oscillation

- ❑ Higher oscillation frequency
- ❑ Lower fabrication induced frequency variation



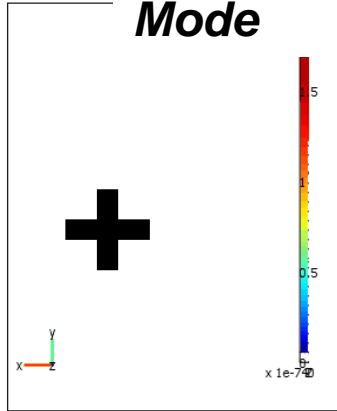
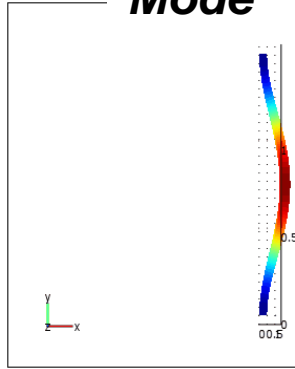
Oscillation Results



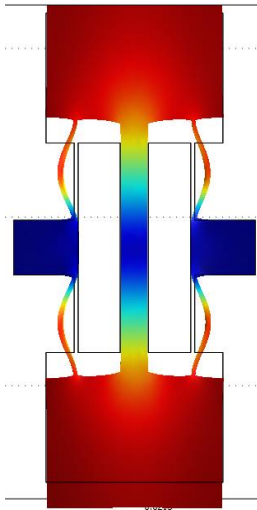
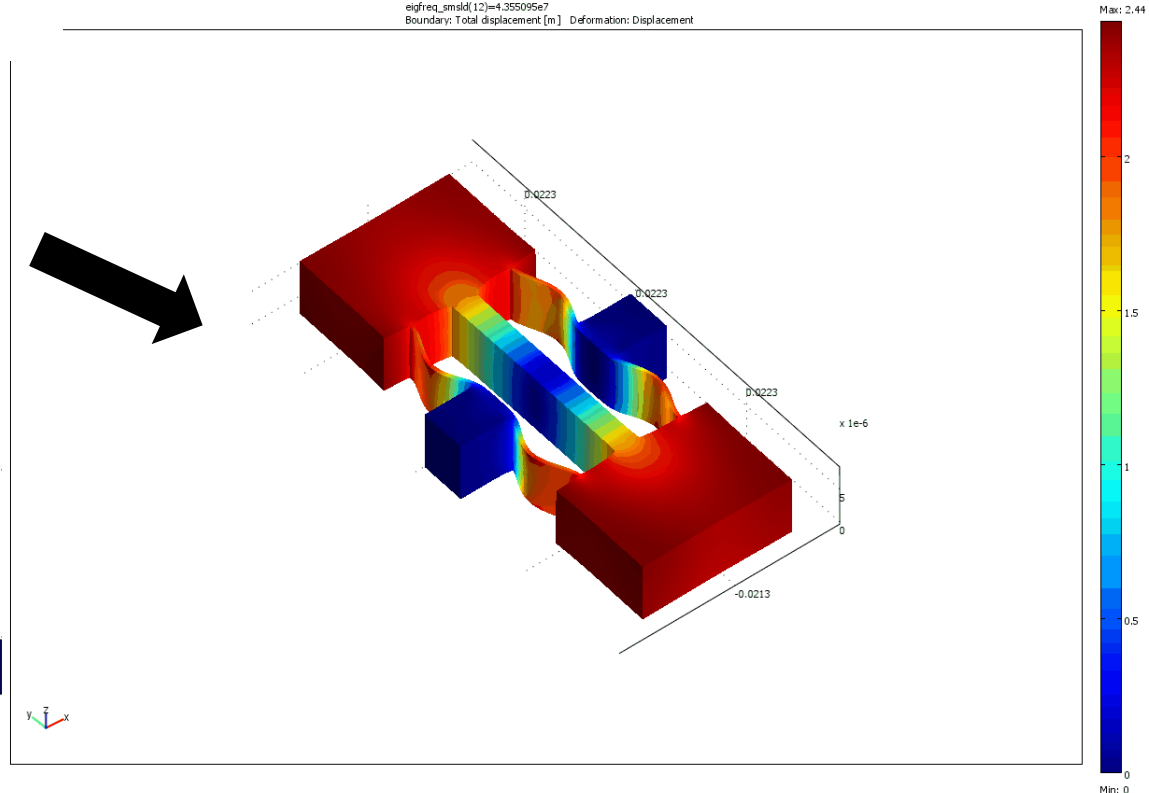
Nonlinear Flexures In Thin Actuators

Flexural Mode

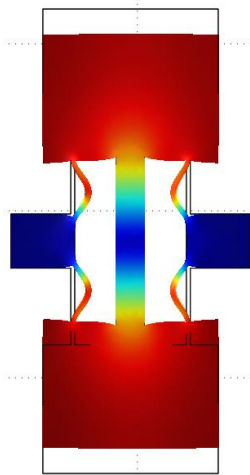
Extensional Mode



+

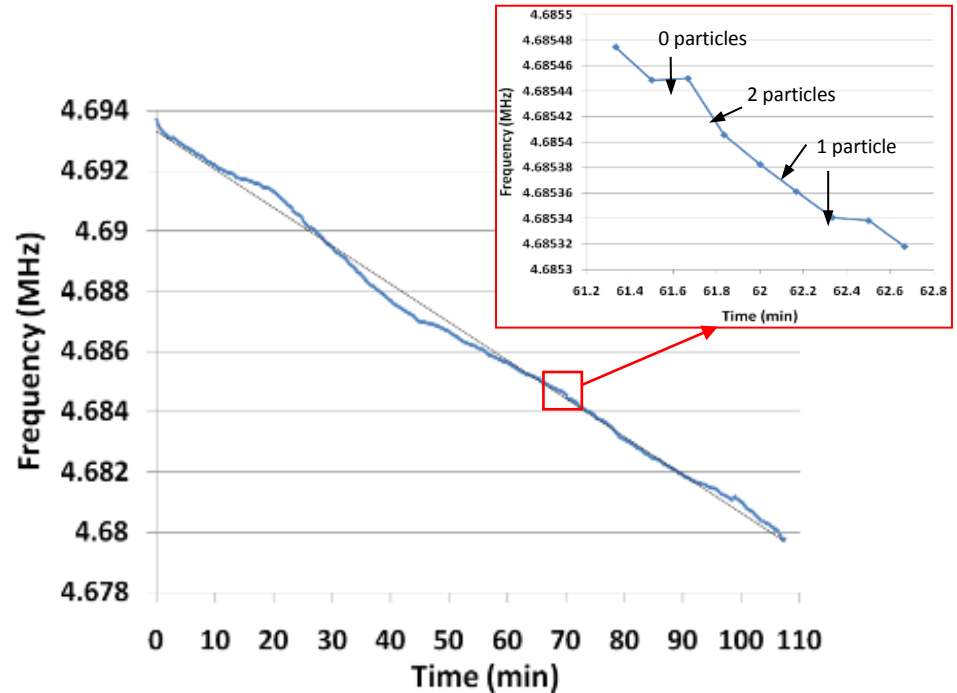
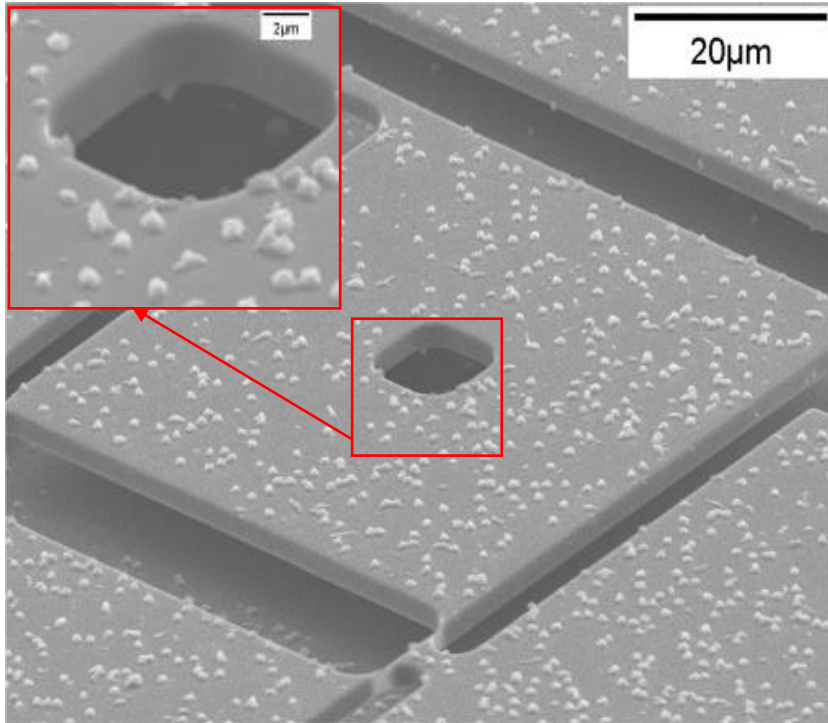


Maximum Elongation



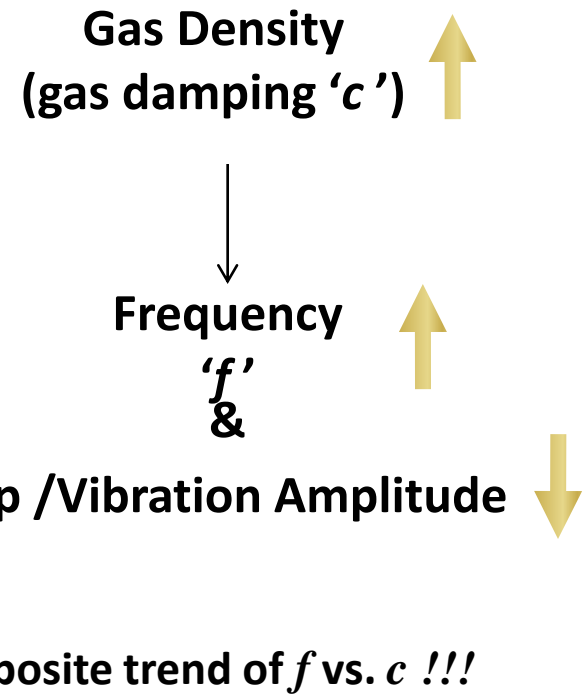
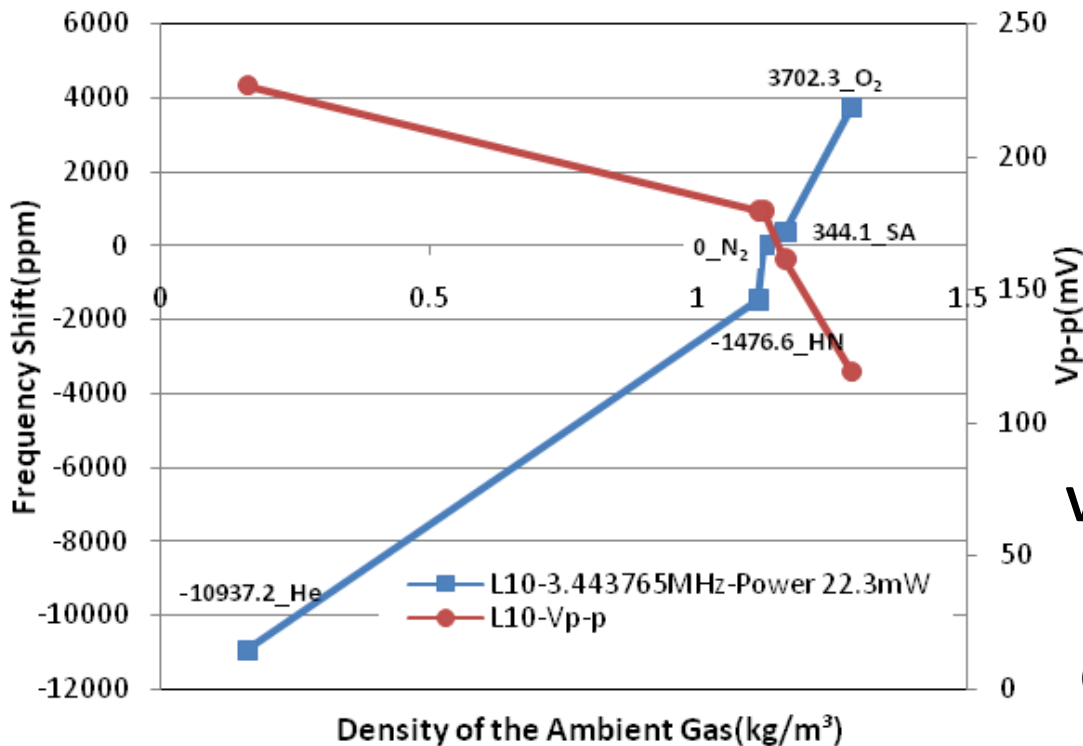
Maximum Compression

Self-Oscillating Sensor Measurement Results



Overall Quantized Frequency Shift of 14.1kHz (3000 ppm)

Response to Different Gases

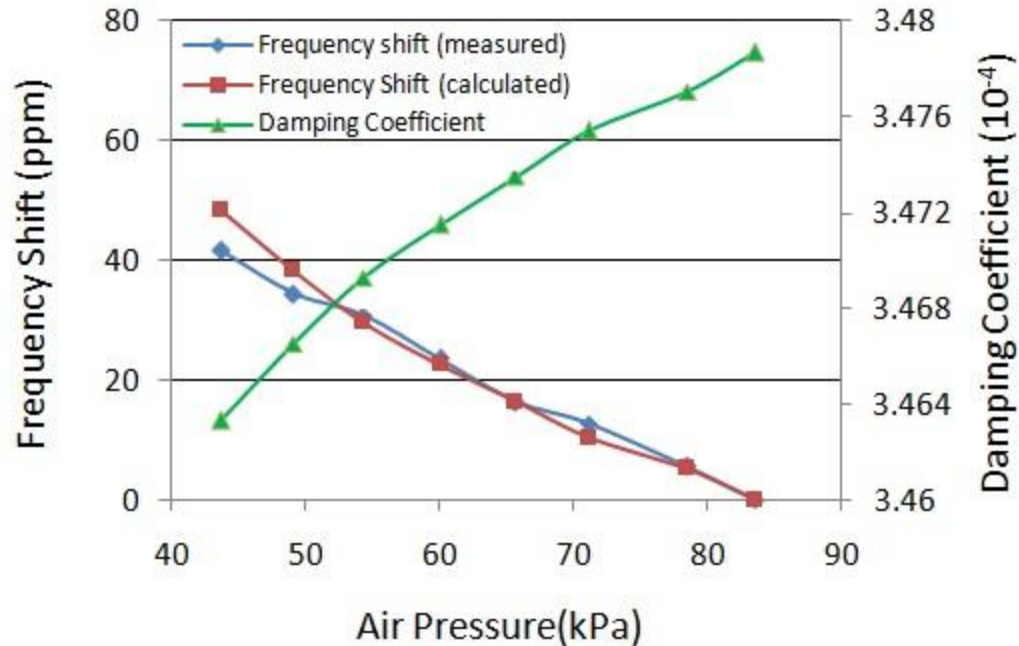


Why?

Measure the frequency shift of TPO in different gases

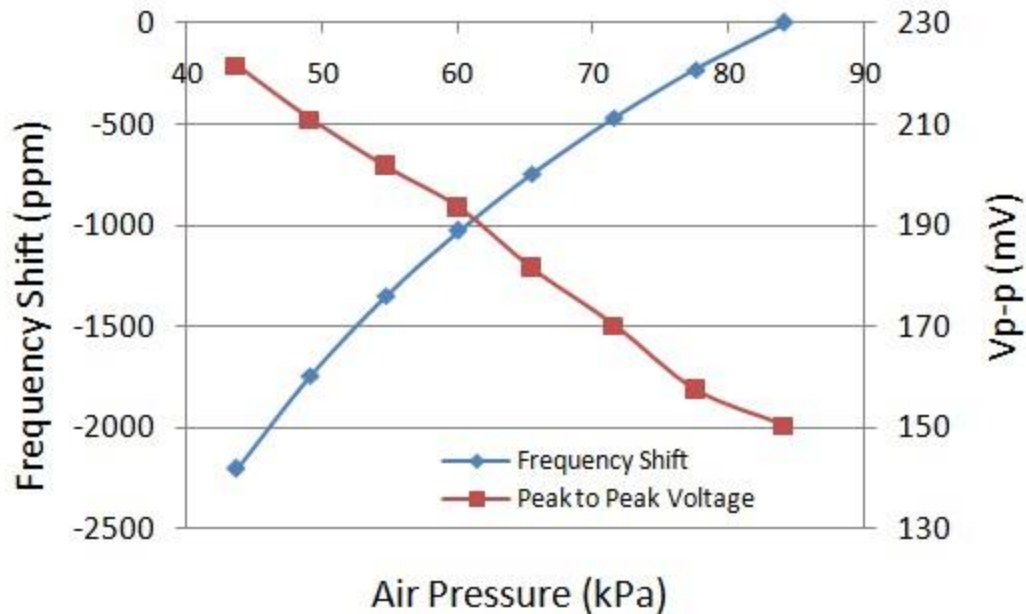
"Gas sensing using thermally actuated dual plate resonators and self-sustained oscillators," Xiaobo Guo, A. Rahafrooz, Yun-bo Yi and S. Pourkamali, 2012 IEEE International Frequency Control Symposium (IFCS 2012).

Measurement Result (TPR)



- Frequency 3.465MHz with power consumption of 0.44mW and a 0.21mA DC
- **Opposite** frequency shift to the TPO under the same pressure change
- Δf **42ppm**, changing the ambient air pressure from 84kPa to 43kPa, **about 50X smaller**
- The damping coefficient in different ambient air pressure is calculated from Eq.(3). They are used to calculate the frequency shift of the TPR.

Pressure Sensing



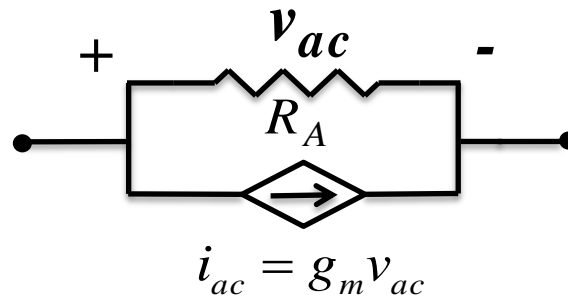
- Frequency 3.456MHz with power consumption 9.10mW
- Higher ambient air pressure, higher damping, lower vibration amplitude (V_{p-p}) with higher k and higher frequency
- Δf -2300ppm, changing the ambient air pressure from **84kPa to 43kPa**

Trans-Conductance Electrical Model

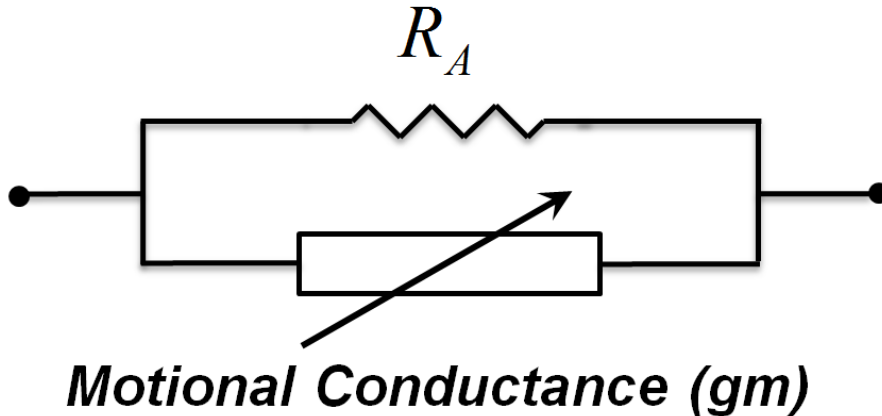


Overall Equivalent Electrical Circuit at resonance

$$H_T \Big|_{s=j\omega_0} = g_m = \frac{i_m}{v_a} = 4\alpha E^2 \pi_l Q \frac{AI_{dc}^2}{KLC_{th}\omega_m}$$



Oscillation Condition in Thermal Resonators



$$g_m = 4\alpha E^2 \pi_l Q \frac{A I_{dc}^2}{KLC_{th} \omega_m}$$

$$g_m + R_A^{-1} < 0 \quad \Rightarrow \quad -g_m R_A > 1 \quad \Rightarrow \quad P_{dc} > -\frac{KLC_{th} \omega_m}{4\alpha E^2 \pi_l QA}$$

$$\Rightarrow P_{dc_{Min}} = \frac{KLC_{th} \omega_m}{4\alpha E^2 |\pi_l| QA}$$

Oscillator Optimization

Scaling a Resonator:

$$P_{dc_{Min}} = \frac{\frac{A}{L} \cdot LA \cdot \sqrt{\frac{A}{LM}}}{4\alpha E^2 |\pi_l| QA} \propto \frac{A^2 L^2}{M^{\frac{1}{2}}} \propto S^2$$

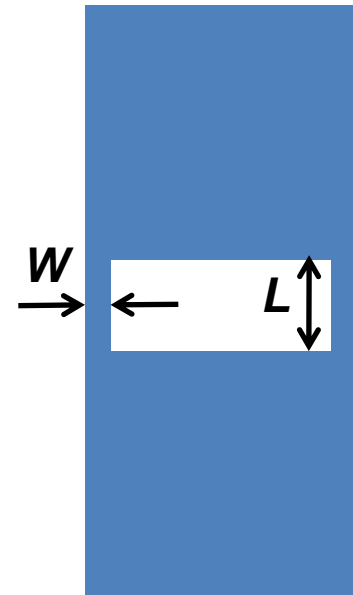
Scaling factors for parameters:

- $\frac{A}{L} \propto S^3$
- $LA \propto S^{\frac{1}{2}}$
- $\sqrt{\frac{A}{LM}} \propto S^{\frac{1}{2}}$
- $M^{\frac{1}{2}} \propto S^{\frac{3}{2}}$

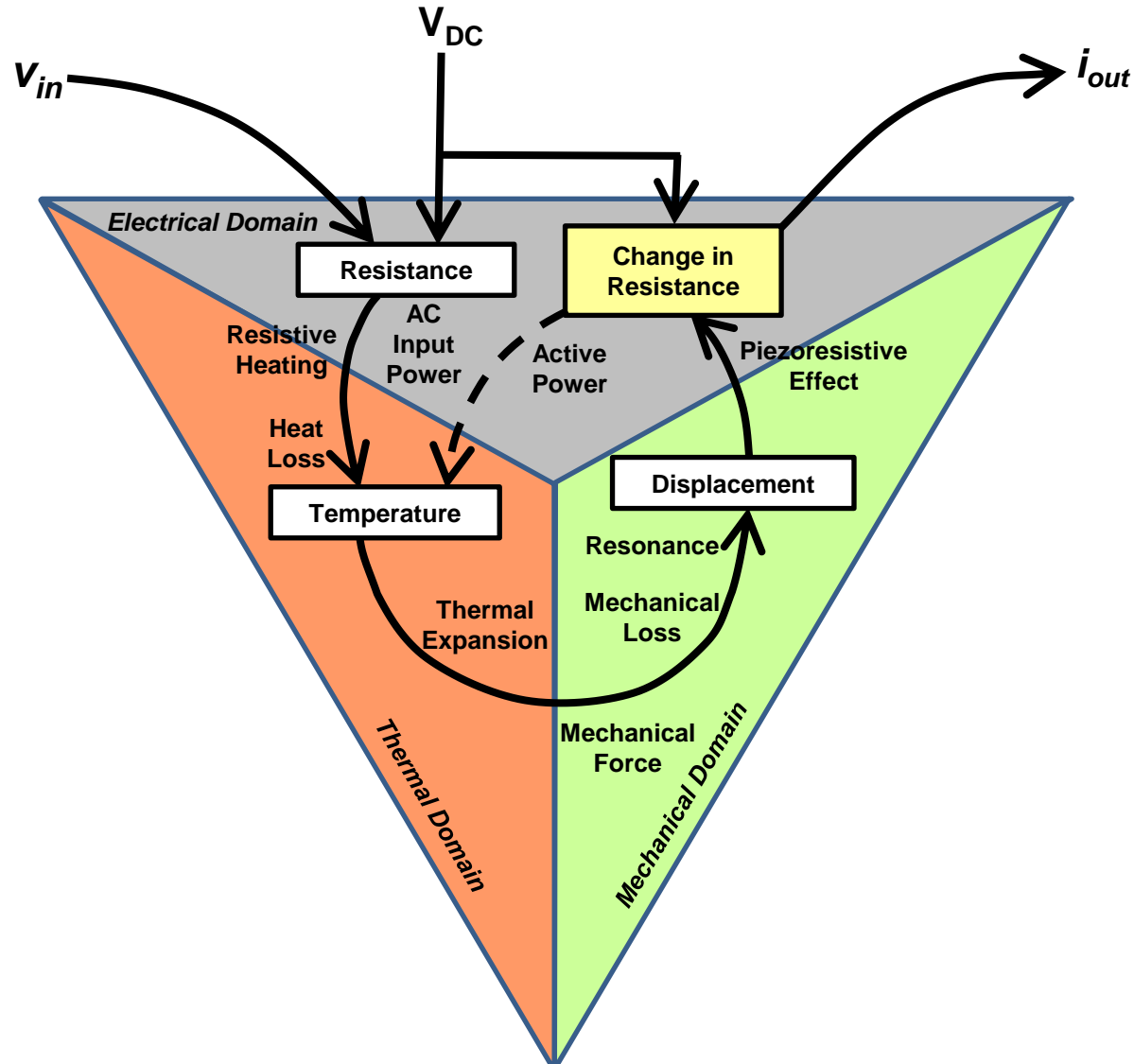
S: scaling ratio

Optimizing at Constant Frequency:

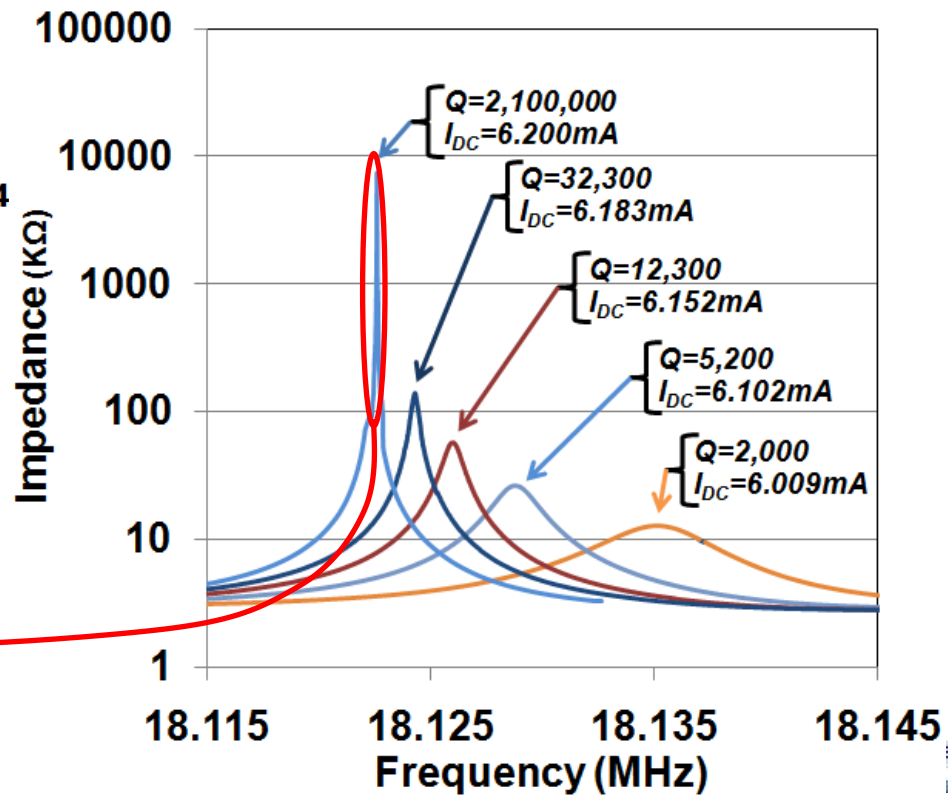
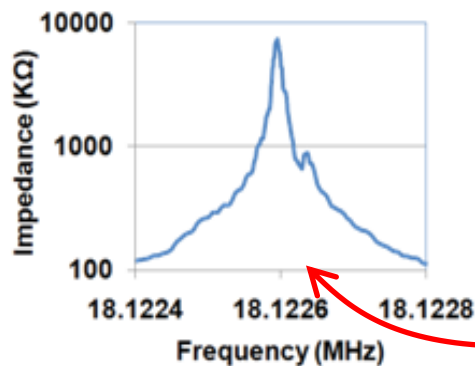
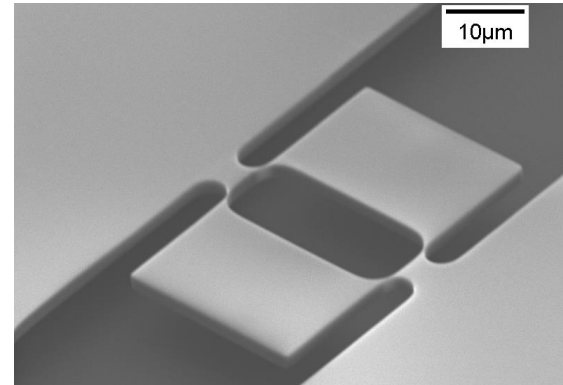
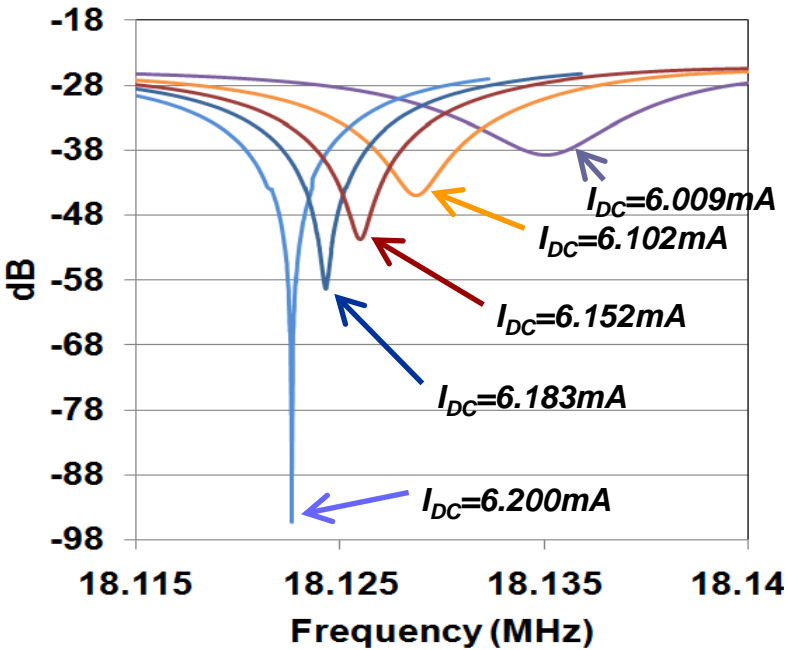
$$P_{dc_{Min}} \propto LA$$



Internal Thermal-Piezoresistive Feedback

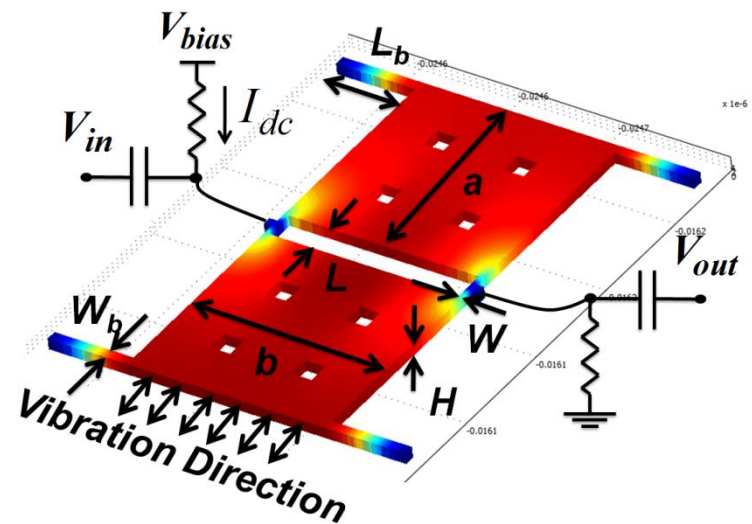
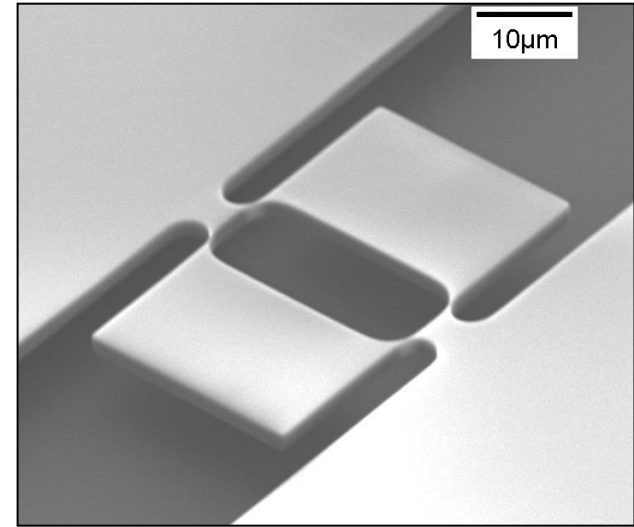
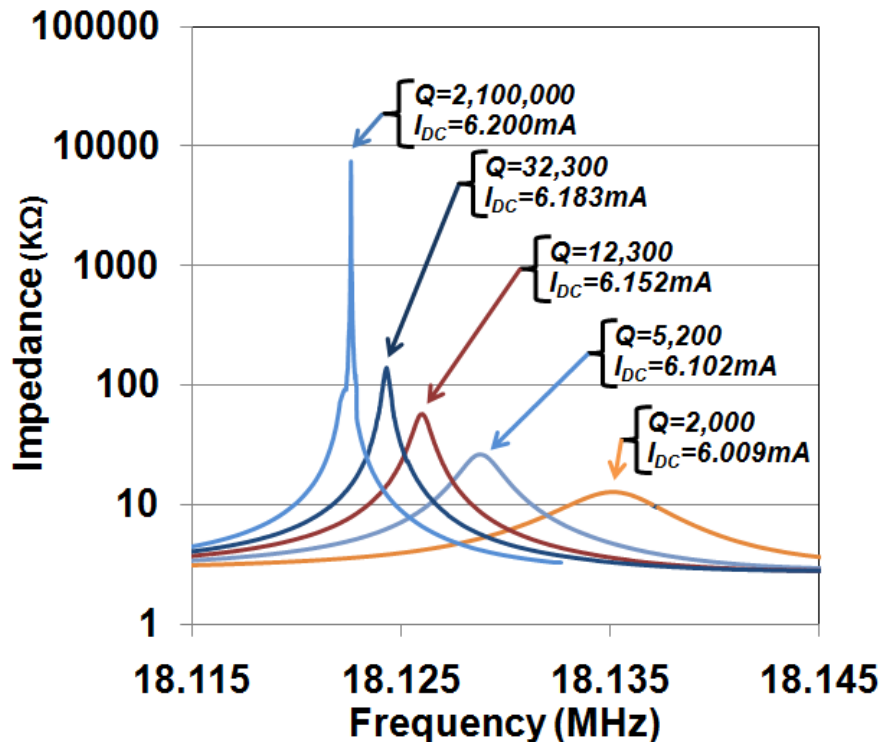


Self-Q-Enhancement

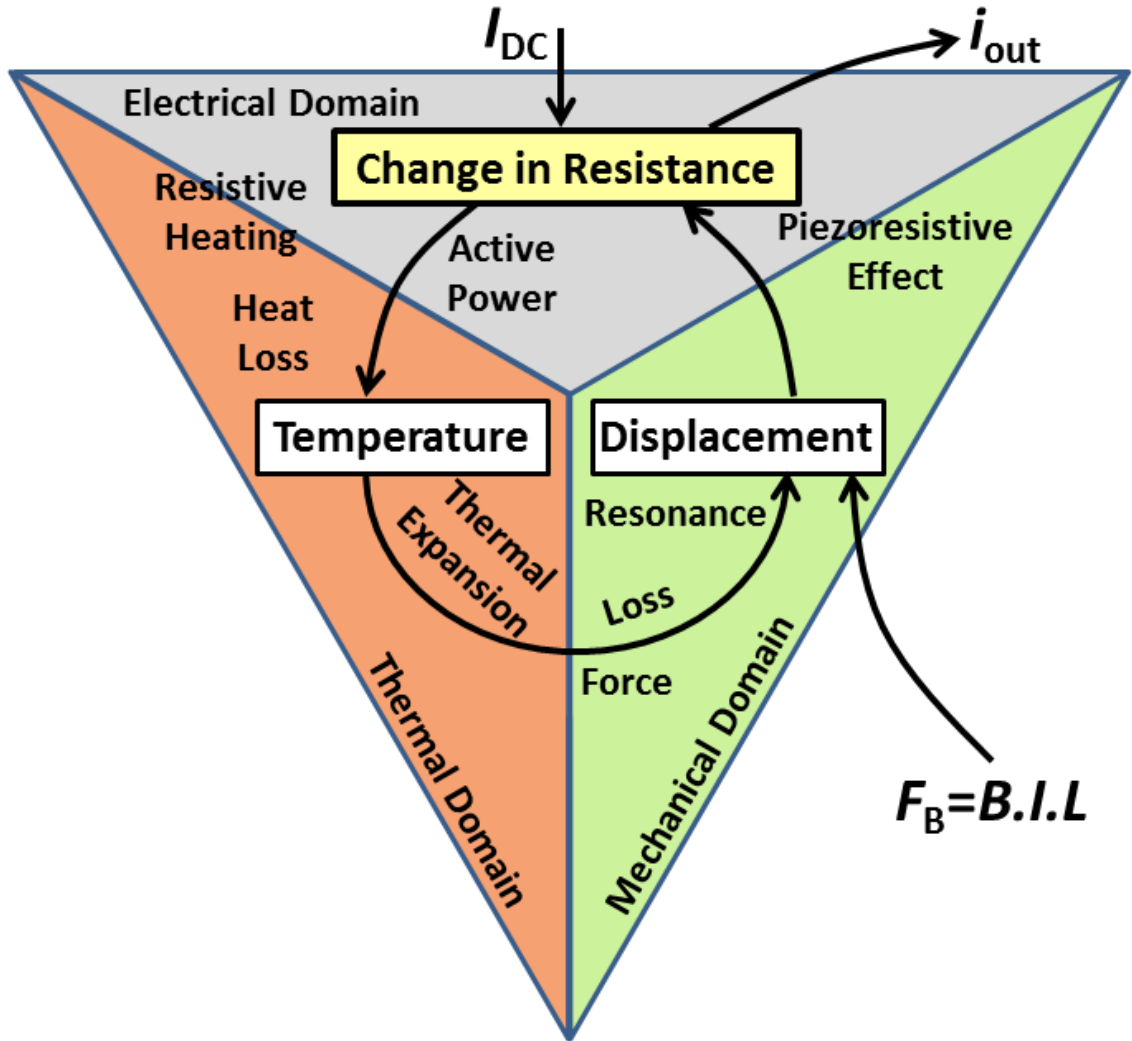
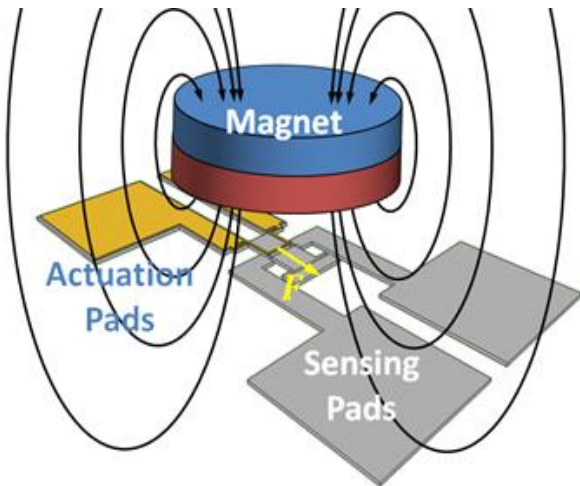
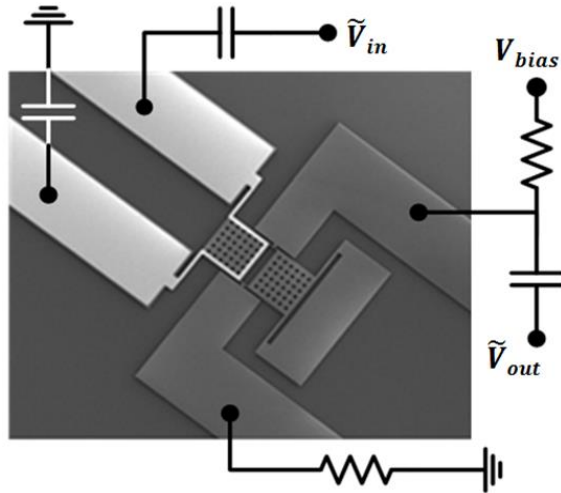


Self-Q-Amplification

□ Internal self-amplification can also be used for resonator Q-amplification

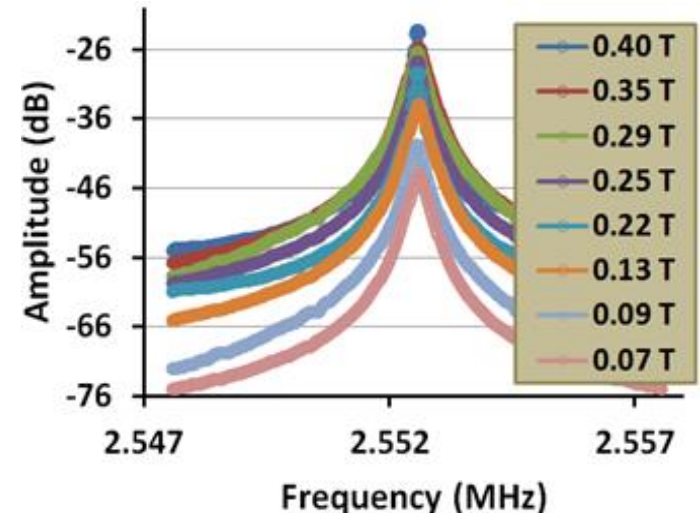
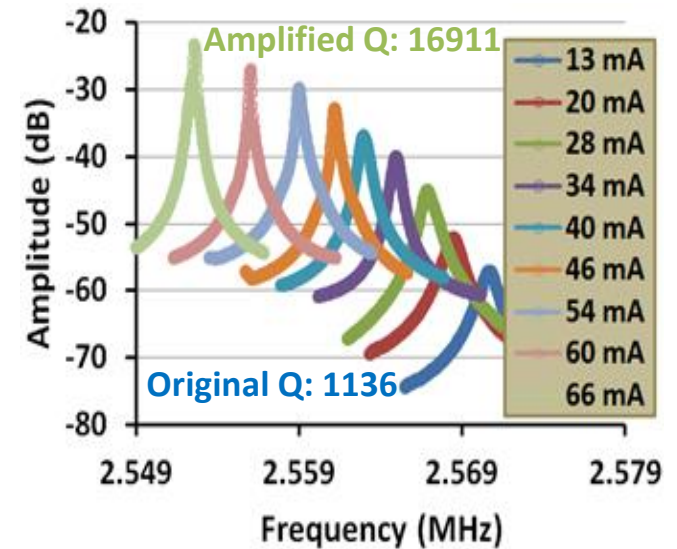
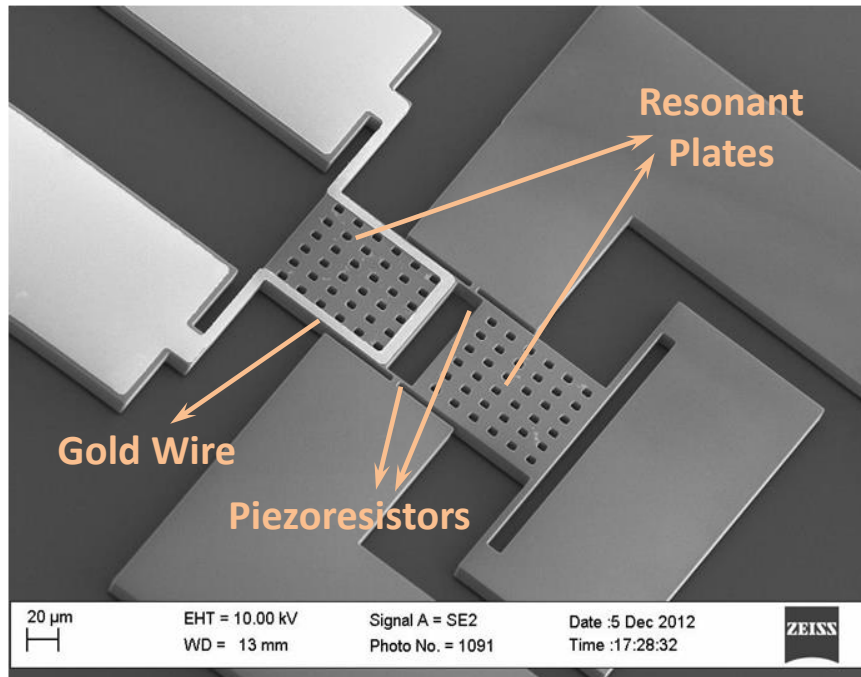


Magnetically Driven Resonator with Internal Amplification



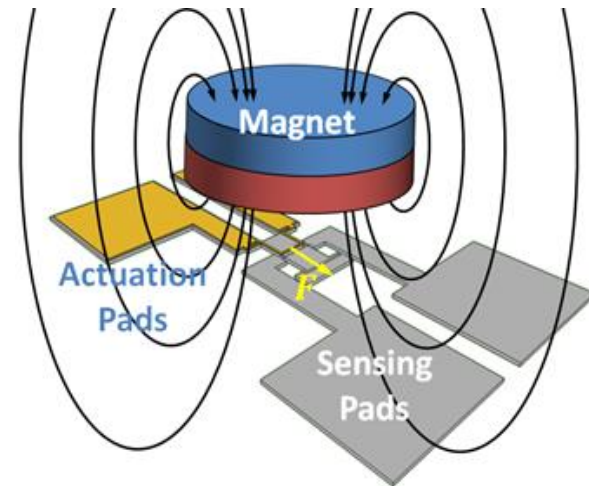
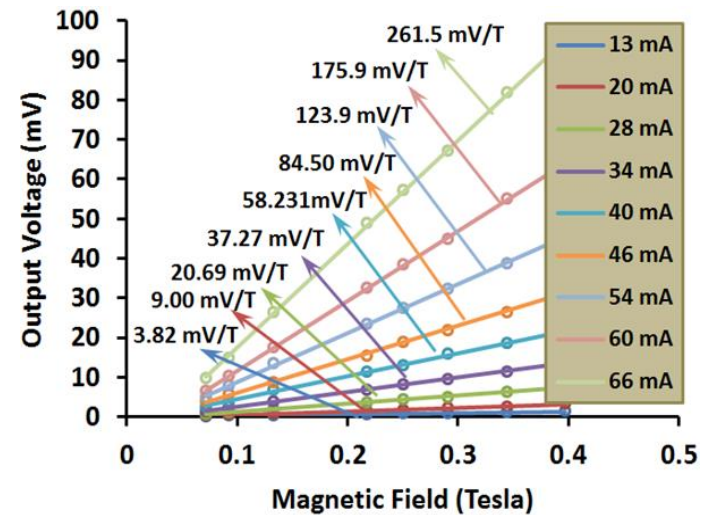
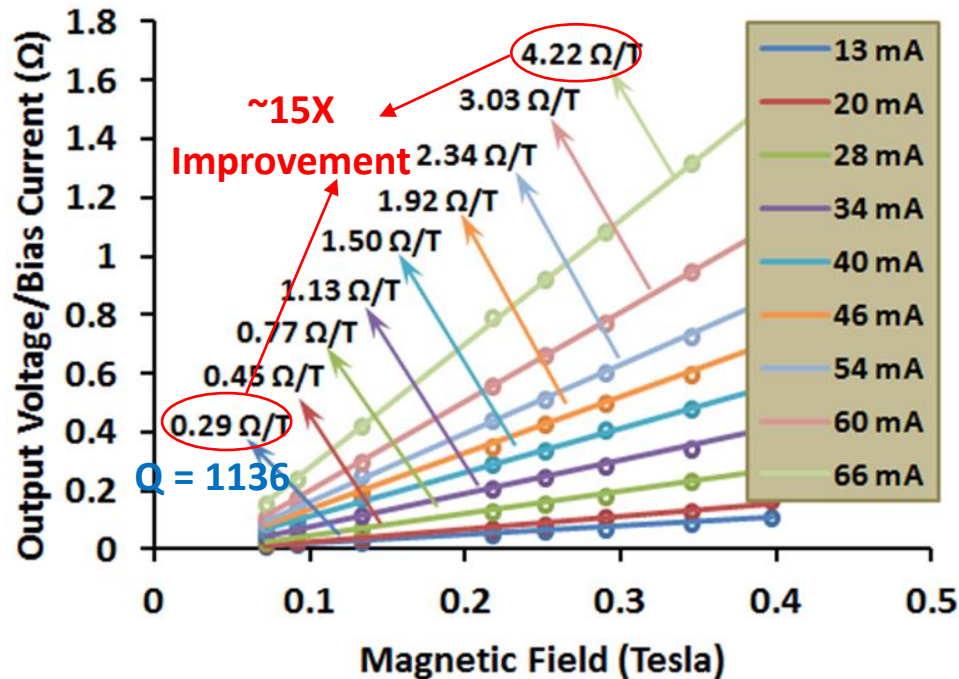
Lorentz Force Magnetometer with Internal Amplification

- ❑ Internal Amplification increases vibration amplitude for the same input force leading to a more sensitive sensor
- ❑ Sensitivity per bias current increases proportionally with the amplified Q

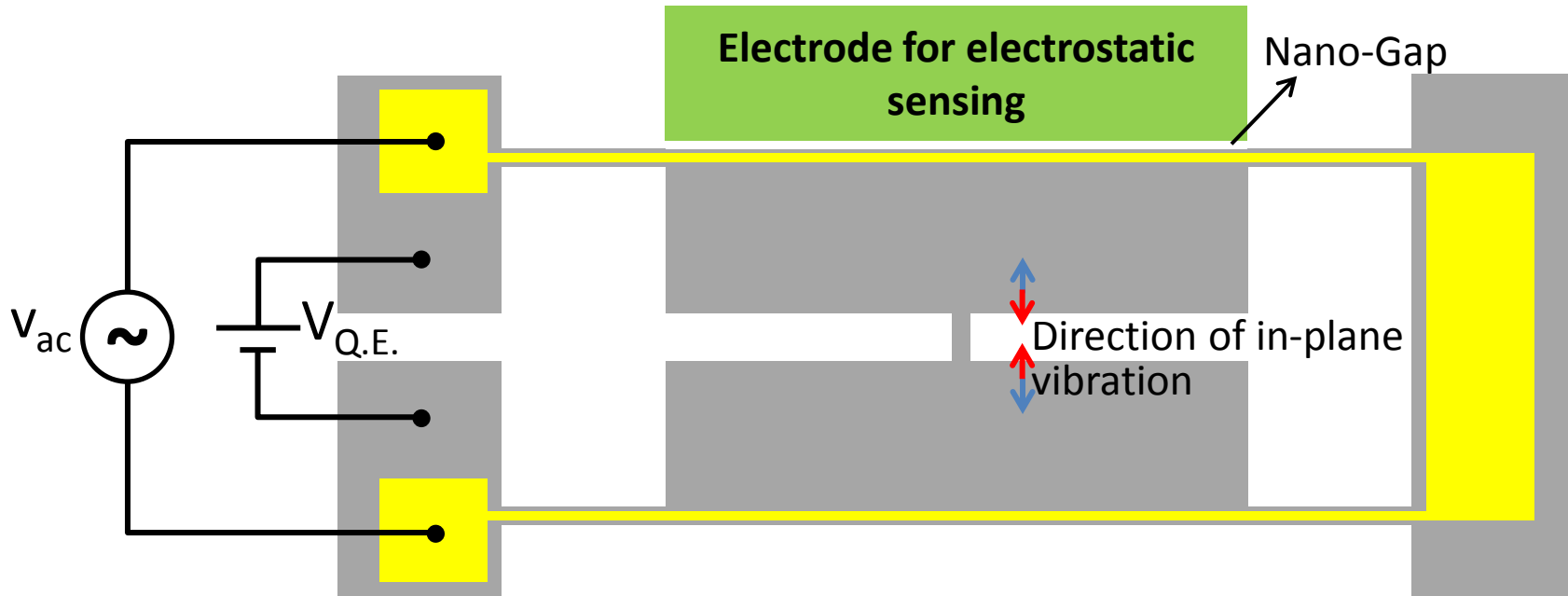


Lorentz Force Magnetometer with Internal Amplification

- Up to **15X** improvement in sensitivity per bias current demonstrated
- This can potentially be orders of magnitude



Towards Quantum Level Sensitivity?!



- Use thermal-piezoresistive interaction to amplify resonator Q by 1000-10000X
- Effective Q up to 40,000,000 already demonstrated for a 4.5MHz resonator
- This can be done by setting $V_{Q.E.}$ to a value slightly short of self-oscillation
- An AC current at the exact same frequency can excite the resonant mode in presence of a weak magnetic field
- Resulting displacement is amplified by the effective Q factor
- A nano-gap and electrostatic sensing can then pick up the resonator vibrations

Acknowledgements

- ❑ Thanks to our sponsors: NSF, State of Colorado, DOE, MSP Corp., and DU
- ❑ My colleagues and collaborators: Professors Wilson, Voyles, Yi, Purse (DU), Abdolvand (Oklahoma State Univ.), Bright (CU Boulder), Tabib-Azar (U. of Utah)
- ❑ My former/current graduate students: Amir Rahafrooz, Arash Hajjam, Babak Tousifar, Xiaobo Guo, Emad Mehdizadeh, Ayesha Iqbal, etc.



Colorado

Office of Economic Development
and International Trade

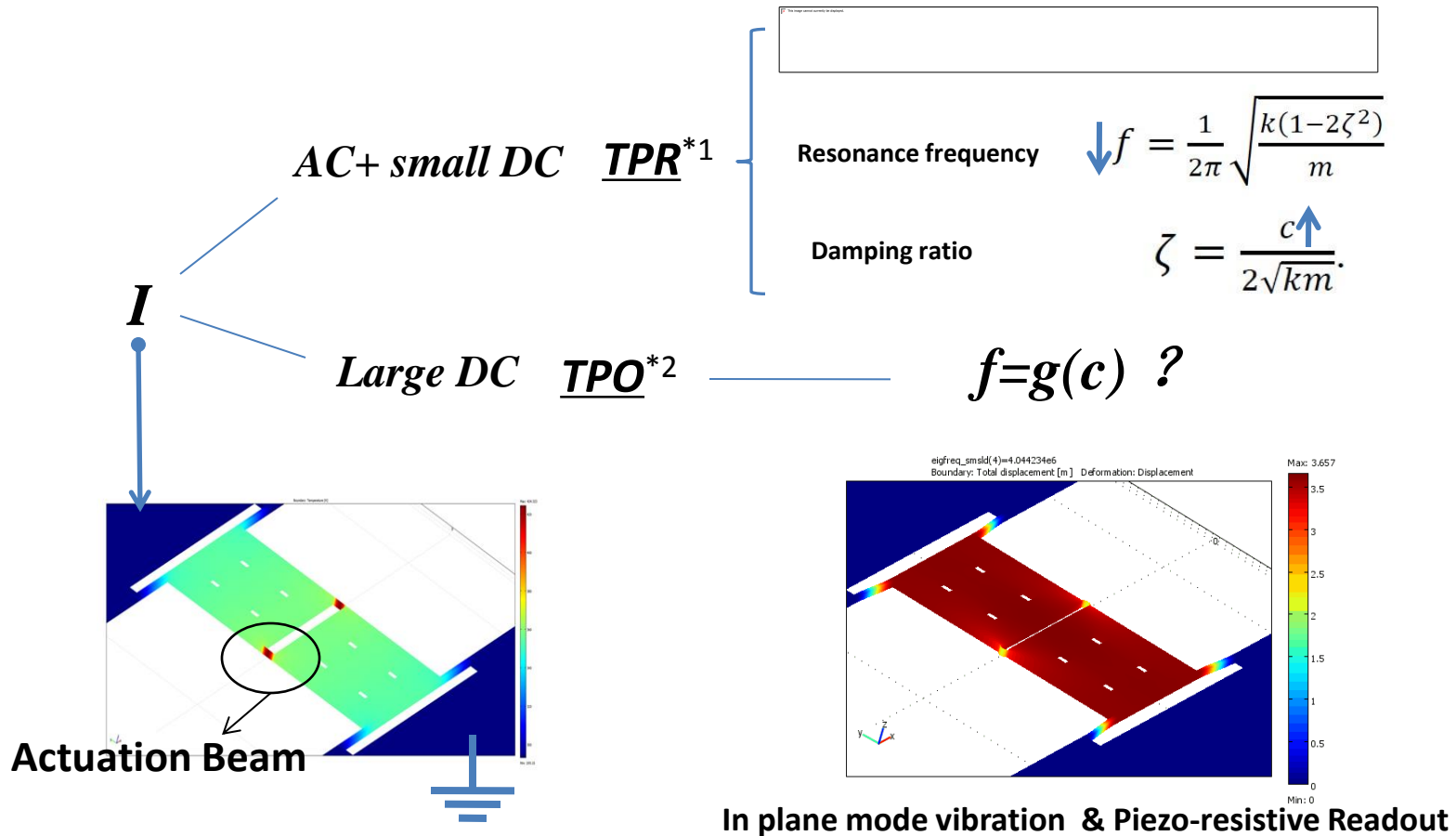


UNIVERSITY OF
DENVER



Thank You for Your Attention

Operation Mechanism of Resonator



*1. "High frequency thermally actuated electromechanical resonators with piezoresistive readout," A. Rahafrooz, and S. Pourkamali, IEEE Transactions on Electron Devices, 58,4(2011).

*2. "Fully Micromechanical Piezo-Thermal Oscillators," A. Rahafrooz, and S. Pourkamali, IEEE International Electron Device Meeting (IEDM), Dec.(2010).

Coupled Equations

$$m\ddot{x} + c\dot{x} + k(x - \alpha l \Delta T) = 0$$

Structural

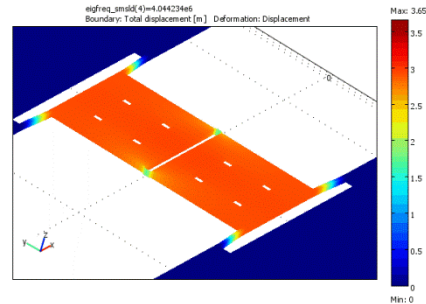
Thermal Stress

Thermal

Piezo-resistive

$$\sigma = \frac{k(x - \alpha l \Delta T)}{A_{sec}}$$

$$\Delta R = \pi_l \sigma R_0$$



Joule Heat

$$\Delta W = I^2 \Delta R$$

$$\Delta \dot{T} = \frac{\Delta W}{C_t}$$

Electrical

Final Solution

Combine these equations together, resulting:

$$\Delta\ddot{T} + \left(Nk\alpha l + \frac{c}{m}\right)\Delta\dot{T} + \frac{(cNk\alpha l + k)\Delta T}{m} = 0 \quad (1)$$

Where $N = I^2 \pi_l R_0 / (c_t A_{sec})$.

Assume $\Delta T = \Delta T_0 e^{i\omega t}$. Eq. (7) becomes

$$-i\omega^3 - \left(Nk\alpha l + \frac{c}{m}\right)\omega^2 + (cNk\alpha l + k)\frac{i\omega}{m} = 0 \quad (2)$$

Solution – part 1

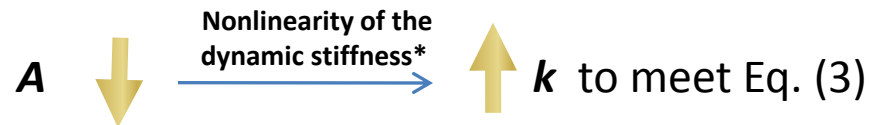
$$-i\omega^3 - \left(Nk\alpha l + \frac{c}{m}\right)\omega^2 + (cNk\alpha l + k)\frac{i\omega}{m} = 0 \quad (2)$$

For Eq. (9) to be satisfied, **the real part** of it should be equal to zero, resulting in:

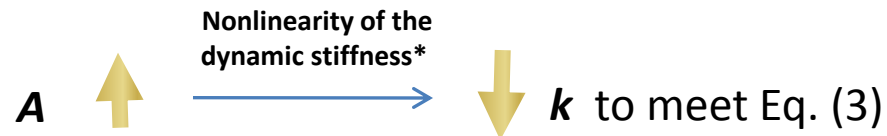
$$c = -mNk\alpha l \quad (3)$$

The damping c is compensated by the term “ $-mNk\alpha l$ ”

If the real part > 0 ,



If the real part < 0 ,



*Nonlinearity of the dynamic stiffness $F = k_1x - k_2x^3$

Solution – part 2

$$\boxed{-i\omega^3} - \left(Nk\alpha l + \frac{c}{m}\right)\omega^2 + \boxed{(cNk\alpha l + k)\frac{i\omega}{m}} = 0 \quad (2)$$

For Eq. (9) to be satisfied, the imaginary part of it should be equal to zero, resulting in:

$$\omega^2 = \frac{(cM\alpha l + 1)k}{m} \quad (4)$$

Since $cM\alpha l \ll 1$ Eq. (4) can be simplified to

$$\omega^2 \approx \frac{k}{m} \quad (5)$$

Can it Catch up with SQUIDs?

❑ Magnetic Force: $F = 2 \cdot B \cdot I \cdot L$

▪ $B = 10^{-12} \text{T}$, $I_{ac} = 100 \text{mA}$, $L = 500 \mu\text{m} \rightarrow F = 10^{-15} \text{N}$

❑ For resonator mechanical stiffness of $K = 400 \text{N/m}$, displacement amplitude: $x = Q_{eff} \cdot F / K$, Assuming $Q_{eff} = 40,000,000$,
 $x = 10^{-11} \text{m}$

❑ For a capacitive gap of $g = 100 \text{nm}$, electrostatic bias voltage of 5V , device thickness of $10 \mu\text{m}$, and resonant frequency of 1MHz :

$$i_{out} = 2 \epsilon_0 A V \omega x / g^2 = 2.8 \text{nA}$$

❑ 28pA is within the detectable range for output of low frequency resonators (e.g. gyroscopes have output signals in the same range)

❑ For example a Trans-Impedance Amplifier with trans-resistance of $1 \text{M}\Omega$ turns this into a 2.8mV signal

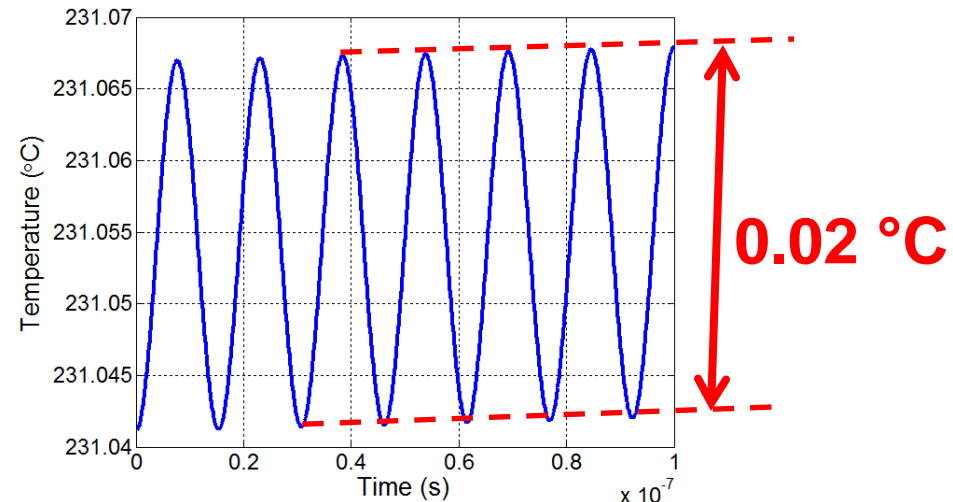
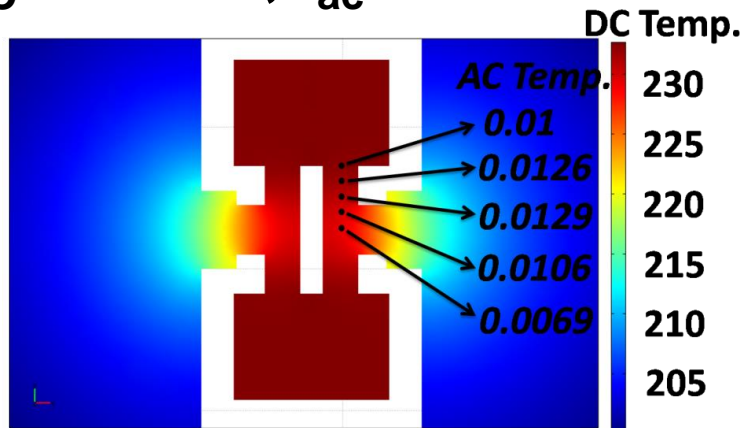
Calculation of Actuator Thermal Capacitance

$$g_m = 4\alpha E^2 \pi_l Q \frac{AI_{dc}^2}{KLC_{th}\omega_m}$$

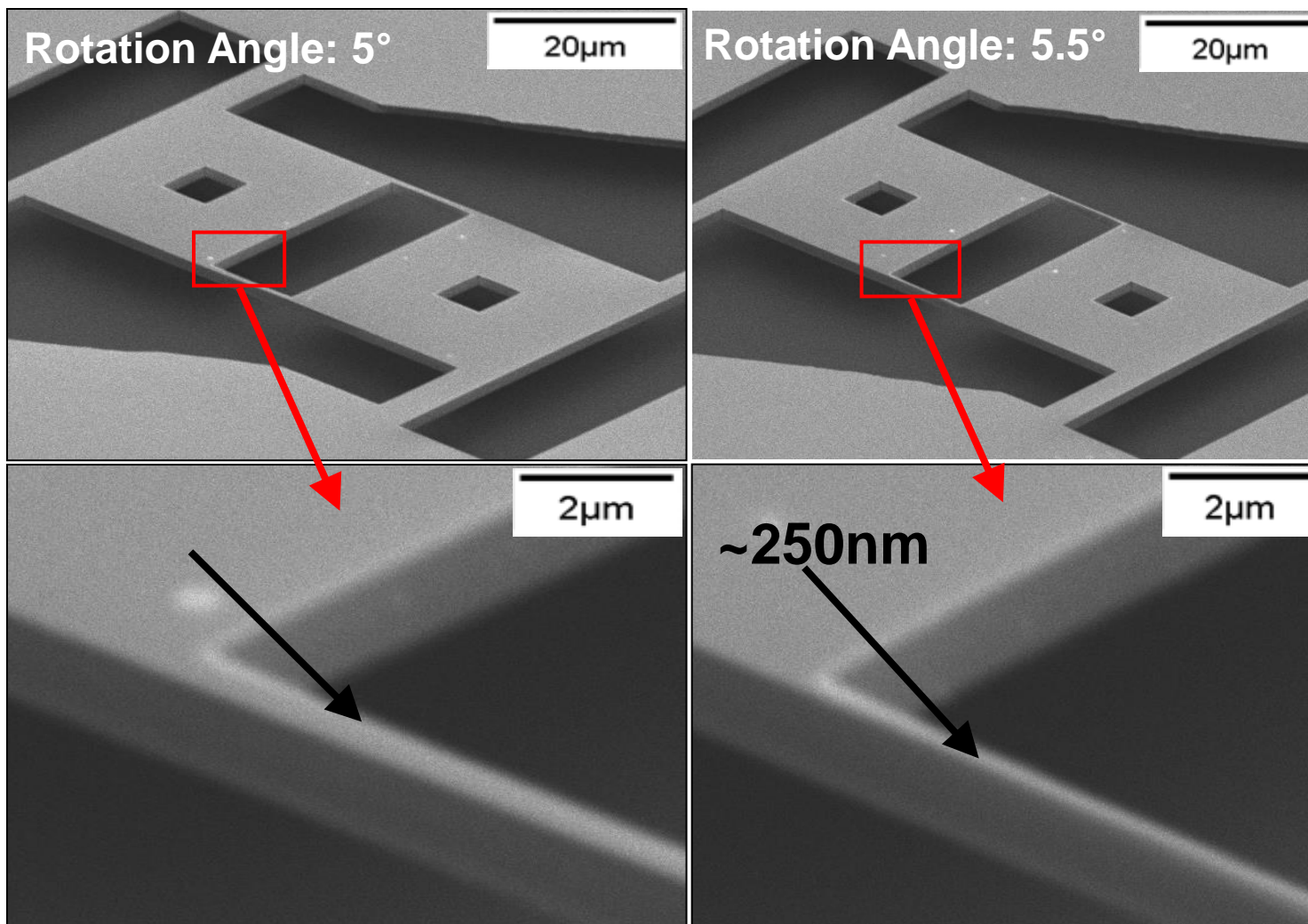
To calculate the g_m , all the parameters except the effective thermal capacitance of the actuators (C_{th}) are known.

$$C_{th} = \frac{I_{dc} i_{ac} R_A}{T_{ac} \omega_m}$$

$I_{DC} = 60\text{mA}$, $i_{ac} = 5\text{mA}$ @ 61MHz

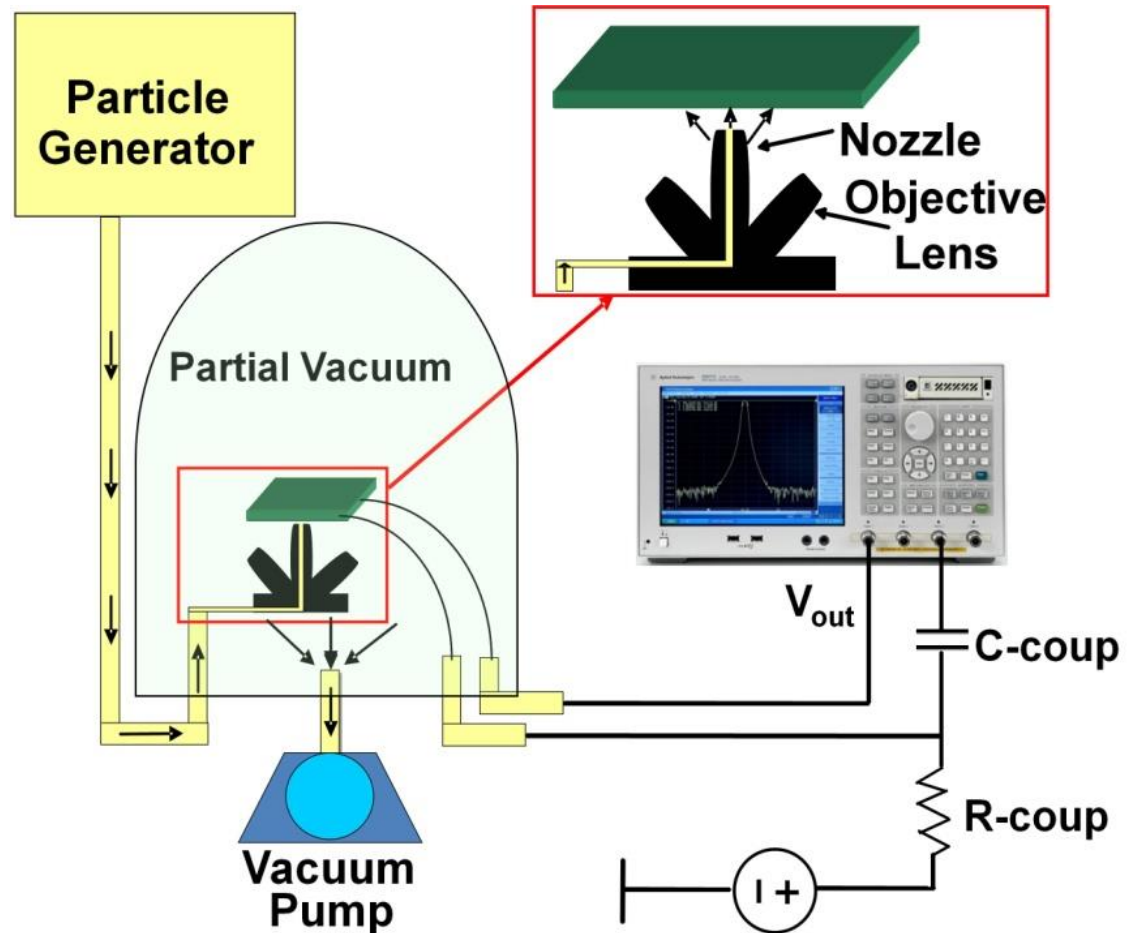


Fabrication Results



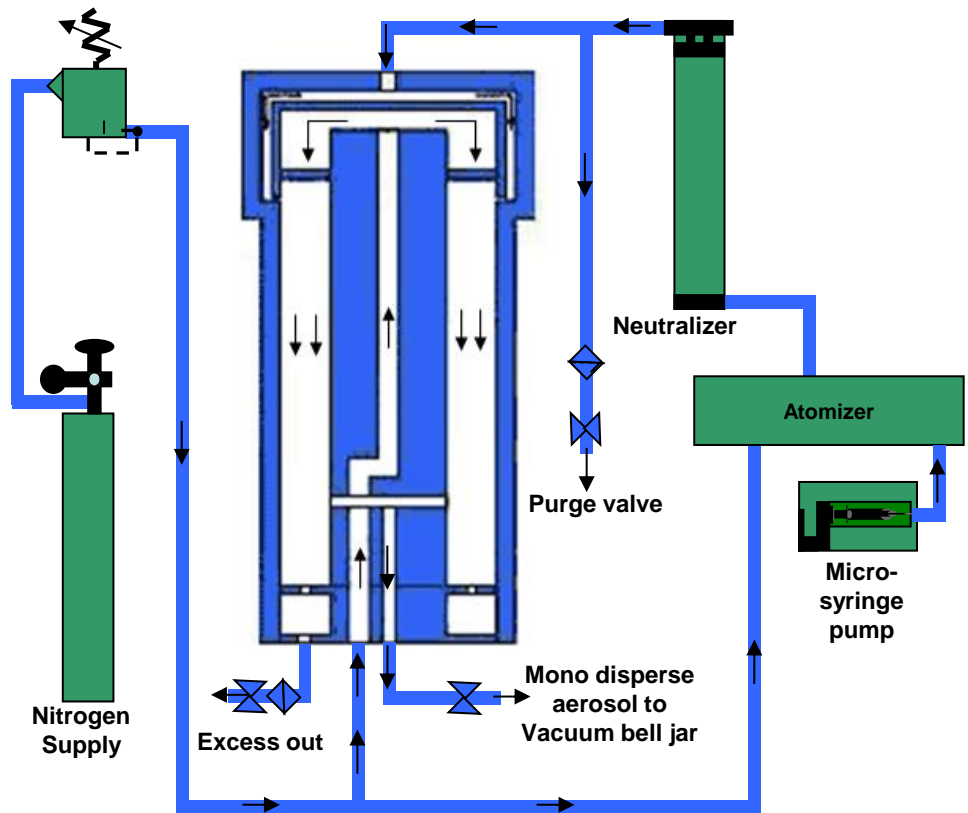
Test Setup for Mass Sensitivity Characterization

Particles deposited on the resonators while monitoring their frequency shift

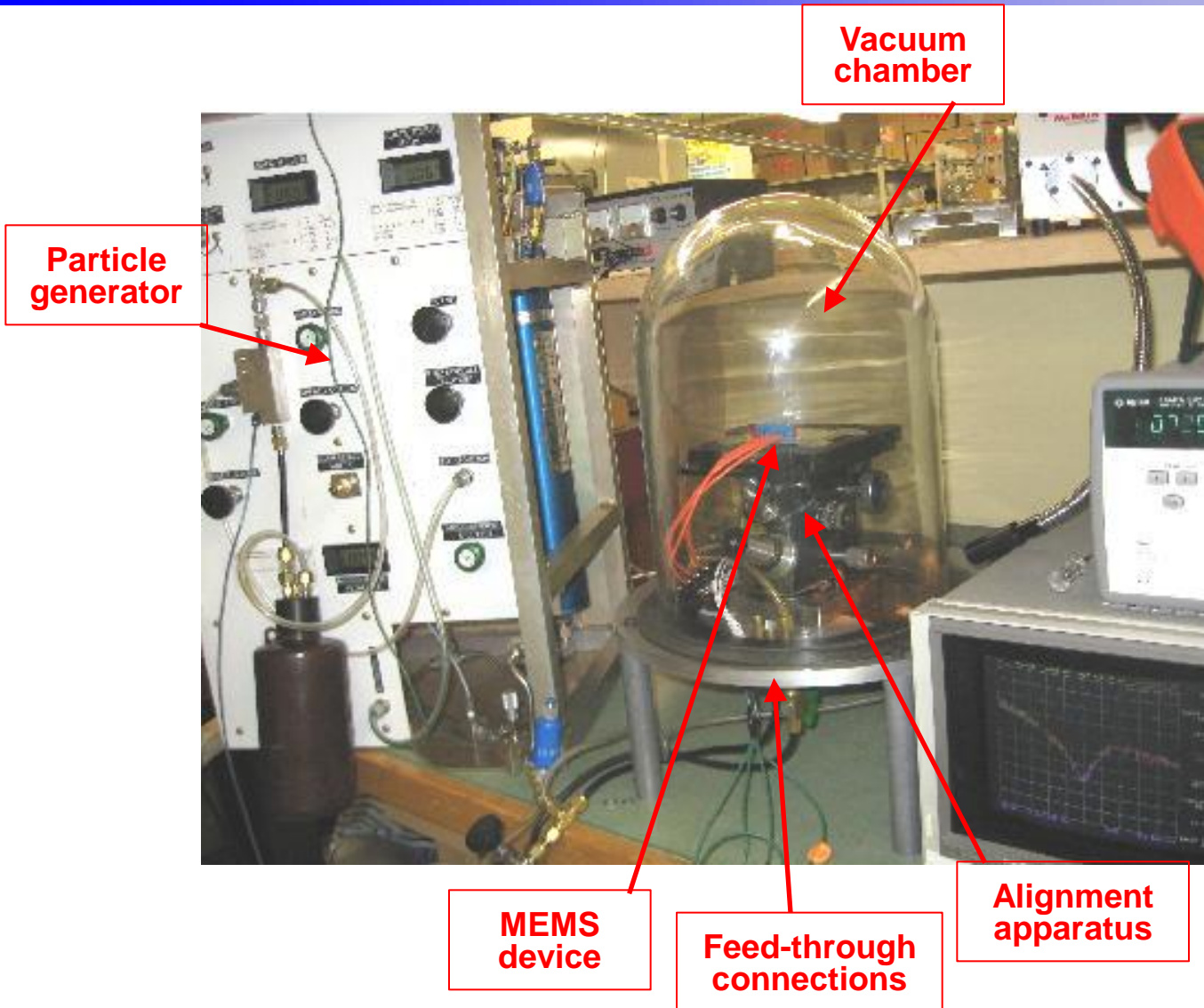


Generation of Artificial Particles

- Aerosol particles with known size and composition generated



Test Setup

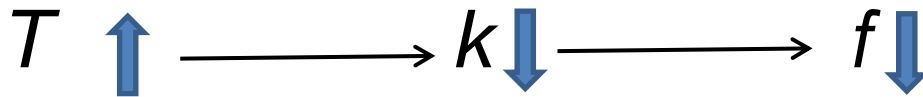


Cause of Negative TCF

- Main cause is negative temperature coefficient of Young's modulus (TCE)

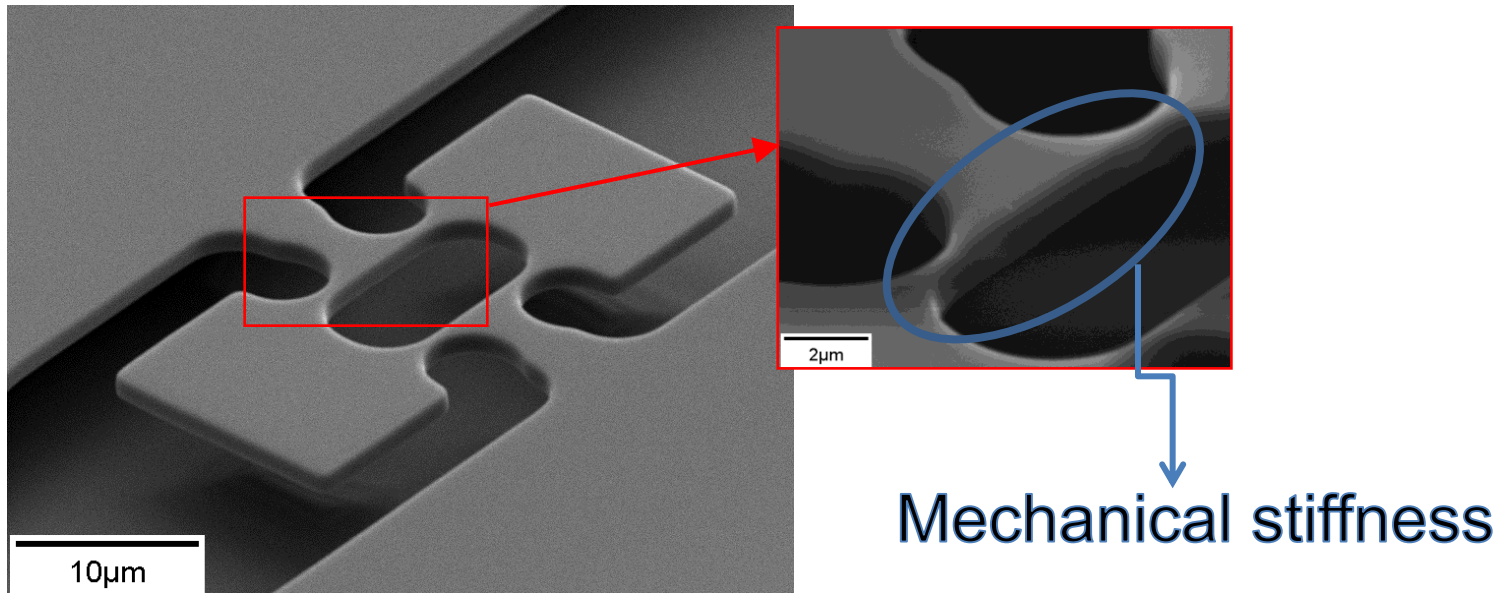
$$f = \frac{1}{2\pi} \sqrt{\frac{k}{m}}$$

K is stiffness and m is mass



High Concentration N-type Doping

- ❑ Effect of high concentration N-type doping on the temperature drift

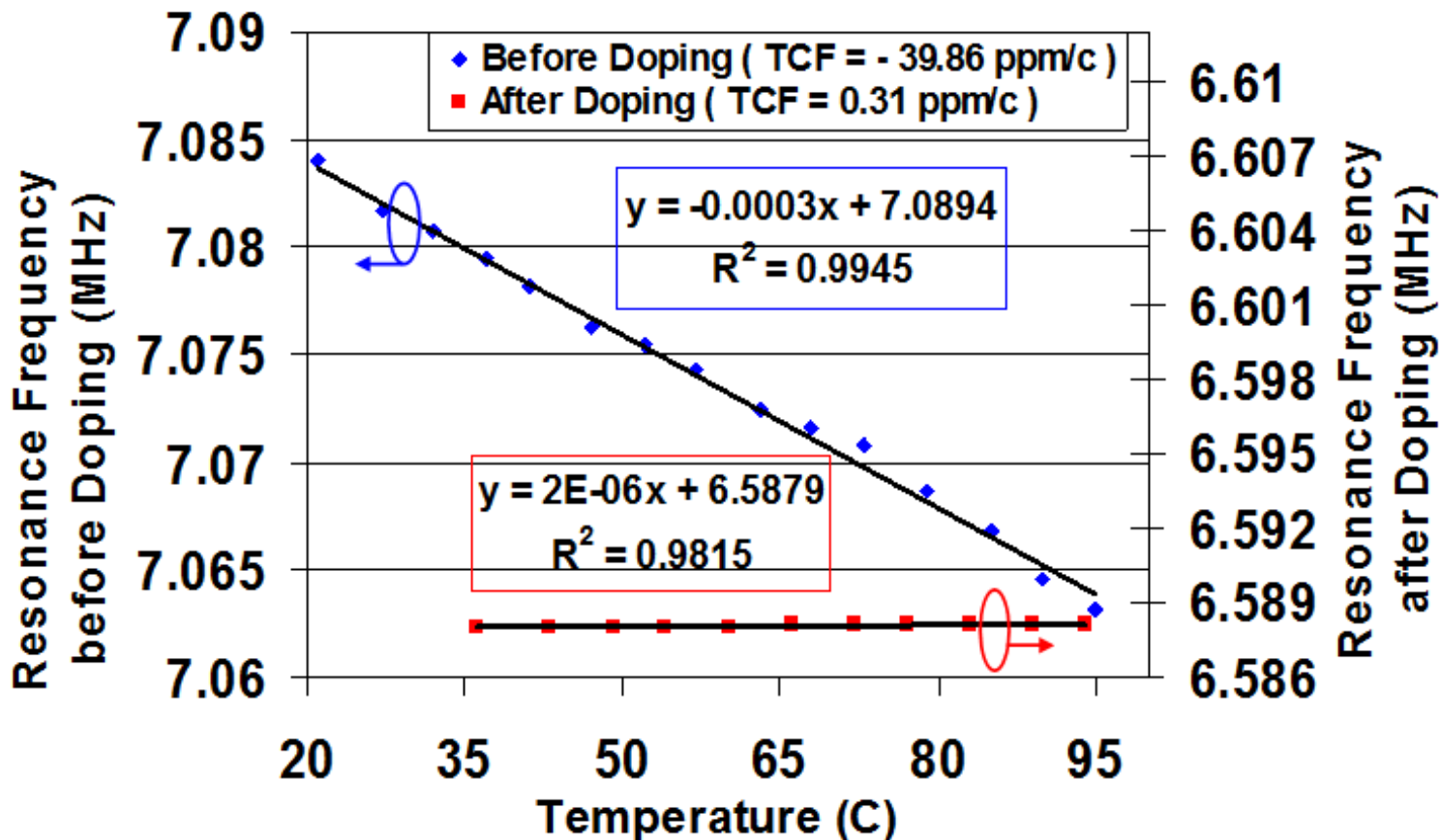


- ❑ Only short doping and drive-in steps were required for reaching high concentrate dopant levels

Measurement Results

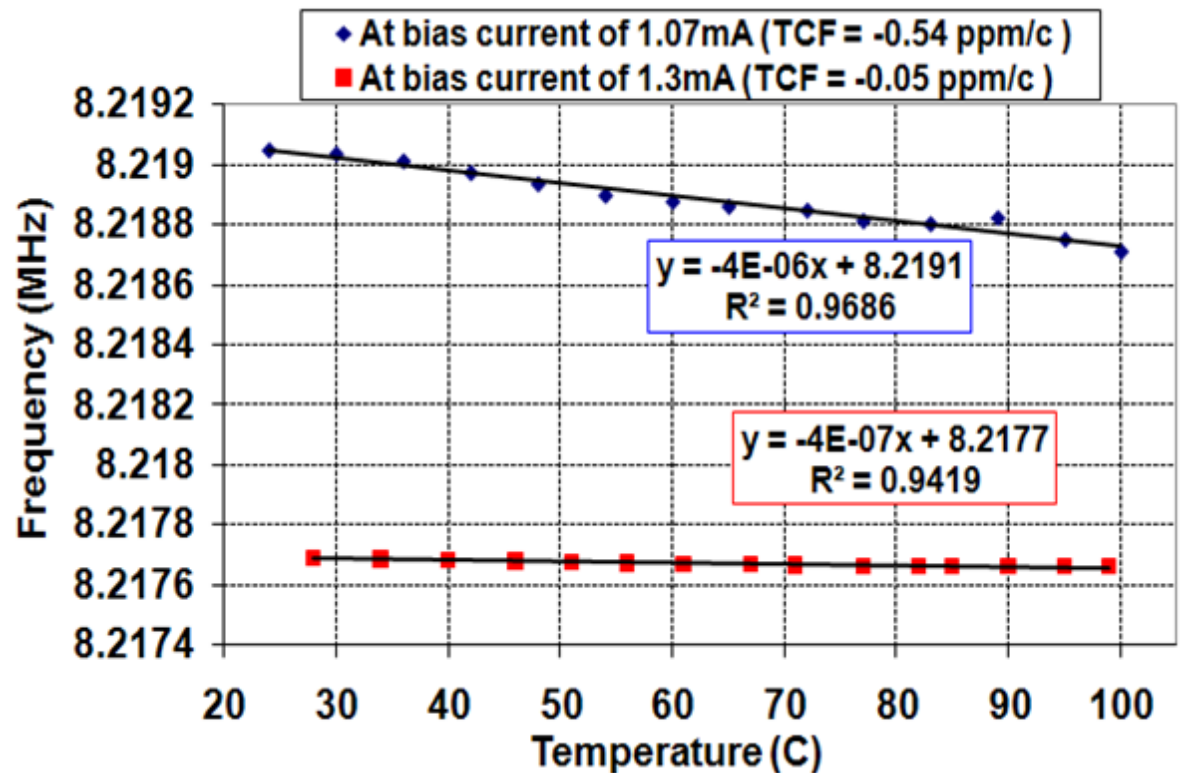
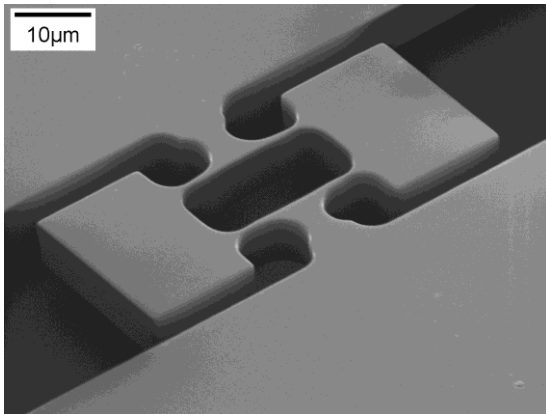
TCF **before** doping = **-39.86ppm/°C**

TCF **after** doping = **0.31ppm/°C** (Positive TCF)



TCF Dependence on Bias Current

□ TCF as low as: **-0.05ppm/°C**



PLL (lysine units in kg/mol)-g(grafting ratio: PEG chains per lysine unit)-PEG (mass of PEG in kg/mol)

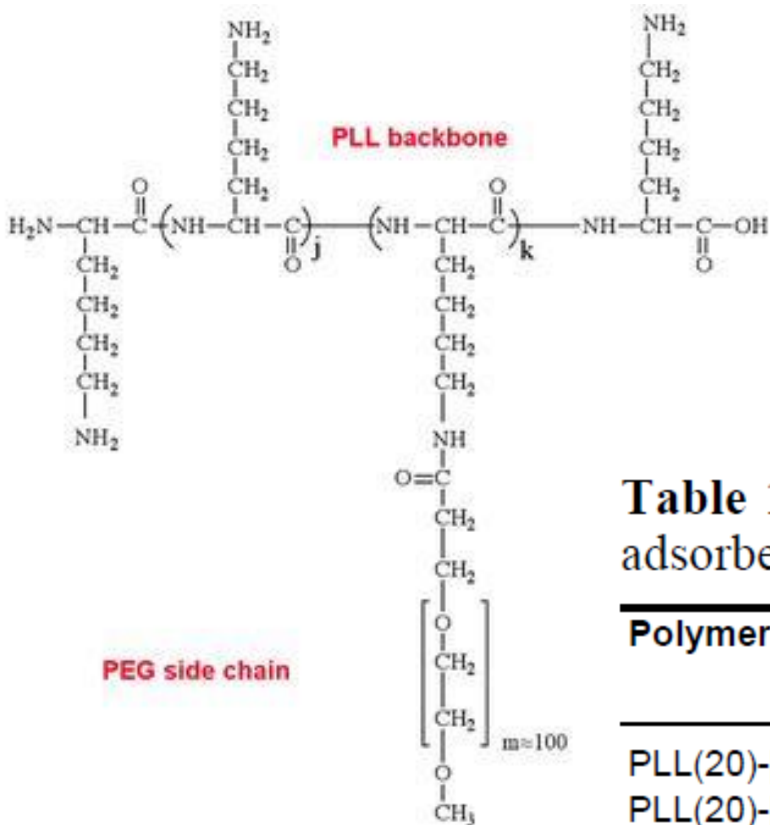
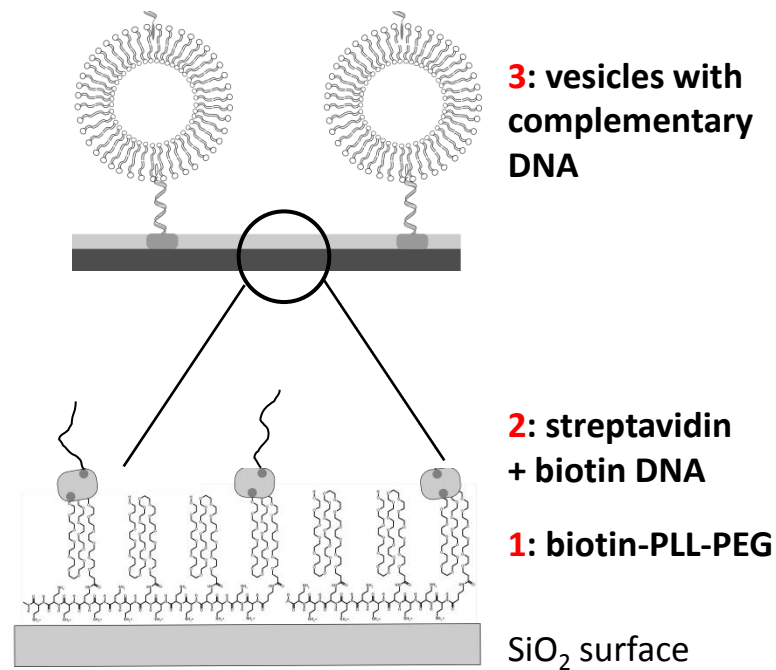
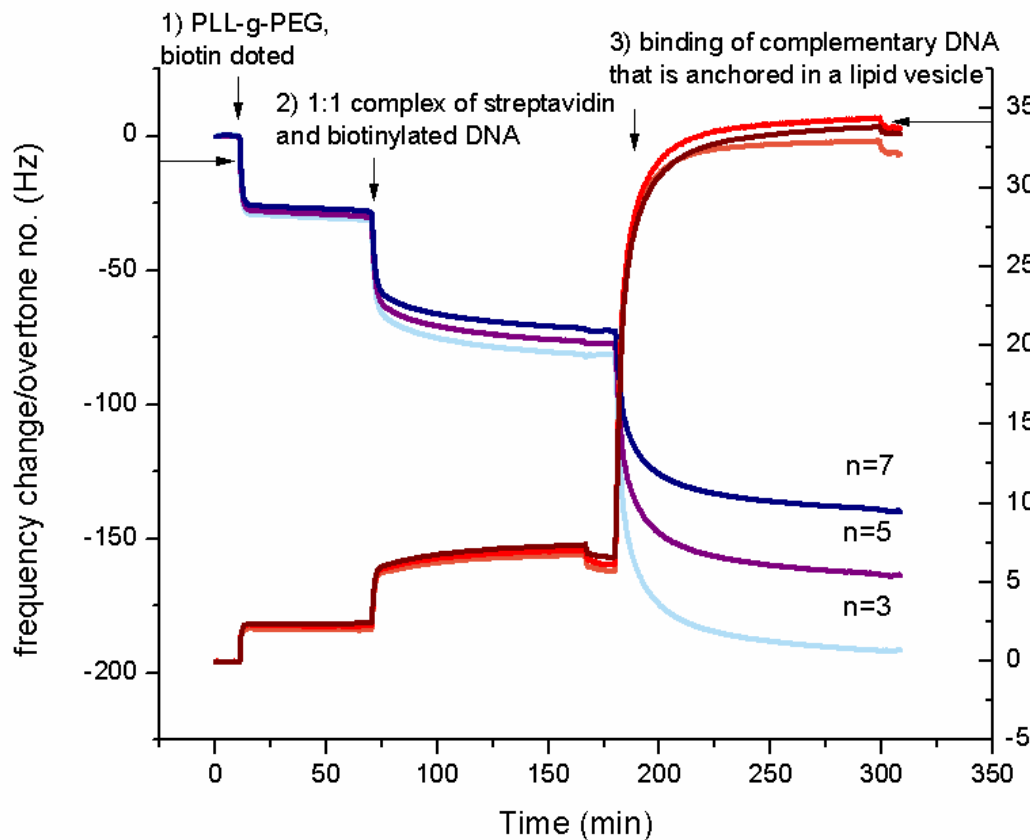


Table 1: Thickness d and hydration of PLL-g-PEG layers adsorbed on SiO_2 .

Polymers	salt [mM]	d [Å]	SLD [Å ⁻²]	hydration [vol.-%]	χ^2 -
PLL(20)-[3.5]-PEG(2)	10	38.6	5.05E-06	82	0.053
PLL(20)-[3.5]-PEG(2)	1	39.7	5.48E-06	90	0.052
PLL(300)-[2.1]-PEG(2)	10	46.3	5.33E-06	87	0.062
PLL(300)-[3.2]-PEG(2)	10	49.1	5.56E-06	91	0.060
PLL(300)-[3.2]-PEG(2)	1	50.6	5.59E-06	92	0.082
PLL(300)-[2.1]-PEG(5)	10	38.2	5.44E-06	89	0.068

Numbers derived from neutron scattering experiments.

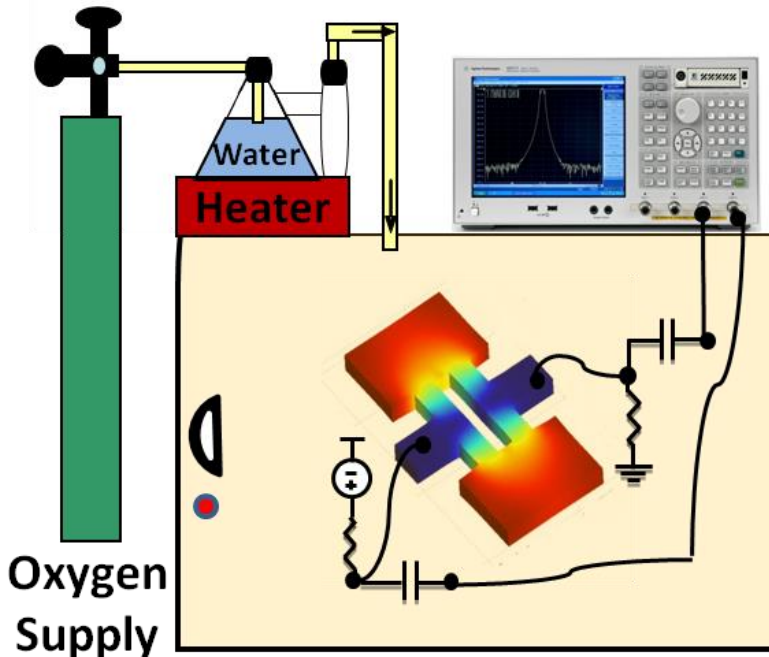
QCM-D response at three overtones for stepwise build up of depicted surface architecture



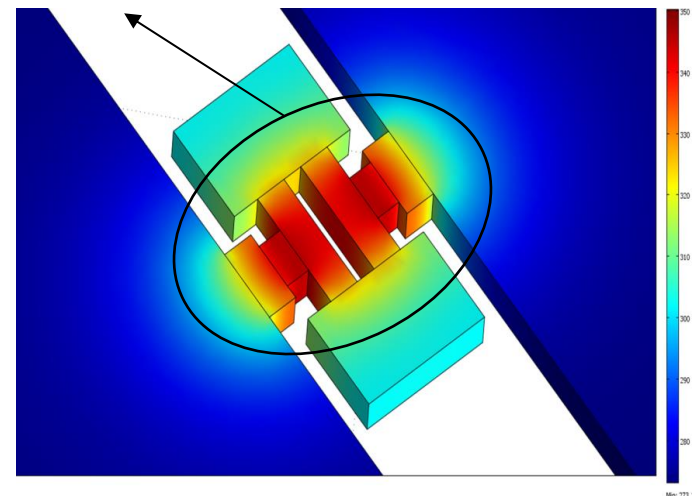
Localized Thermal Oxidation for Frequency Trimming and Temperature Compensation of Micromechanical Resonators

- Resonance frequency of silicon MEMS resonators is dependent on physical dimensions of the resonating structure
- Post-fabrication frequency trimming via pulsed-laser-deposition, material diffusion and electrostatic frequency trimming → Deficiencies such as frequency inaccuracy
- Presented approach based on thermal oxidation of the surface of the beams

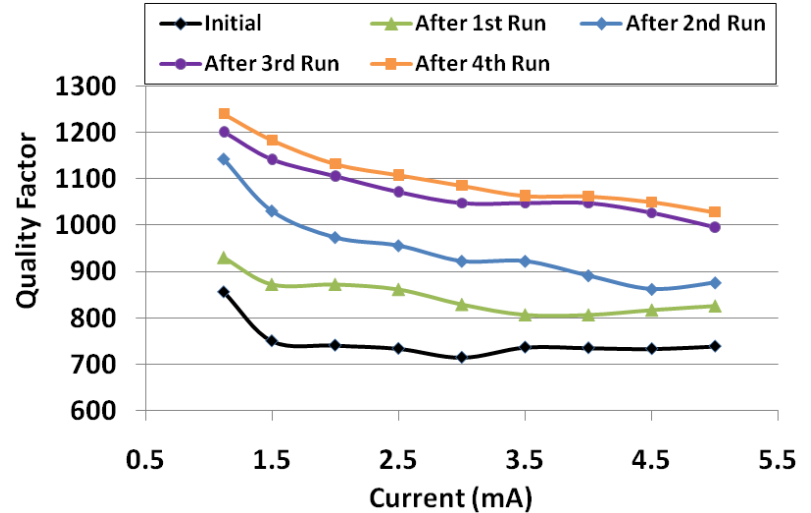
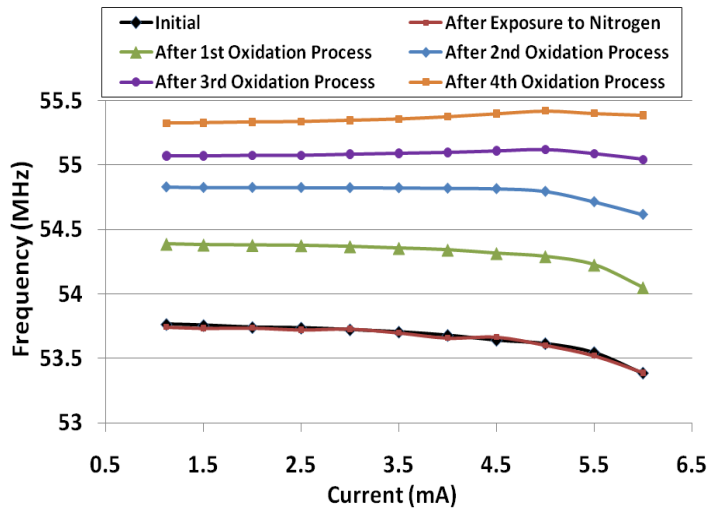
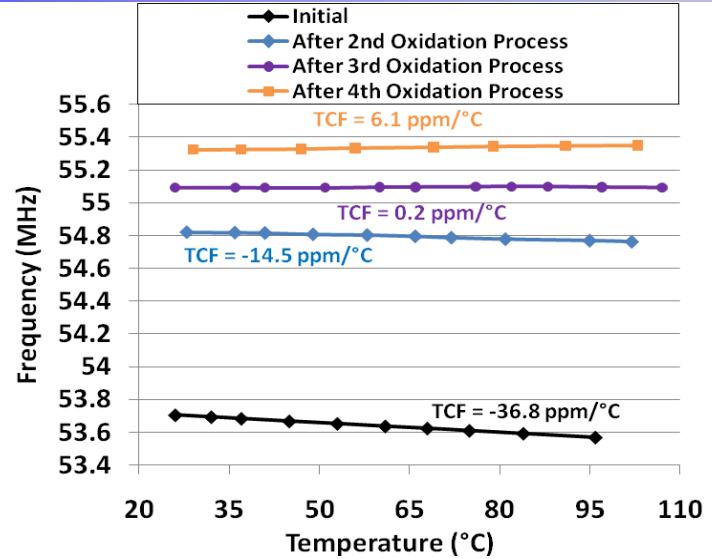
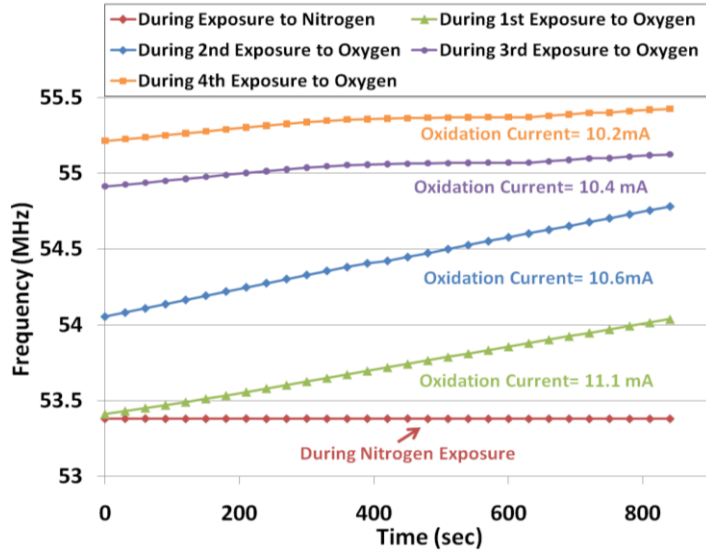
Presentation in MEMS 2012 Conference:



Silicon dioxide forming on the hot surfaces



Measurement Results



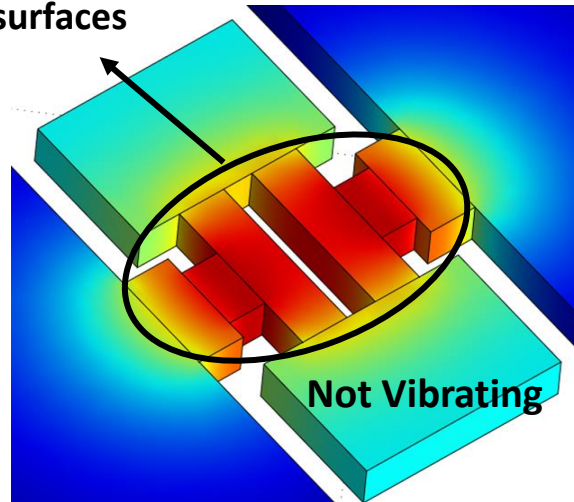
Self-controlled Frequency Trimming Technique for Micromechanical Resonators

Presentation in Hilton Head 2012 workshop:

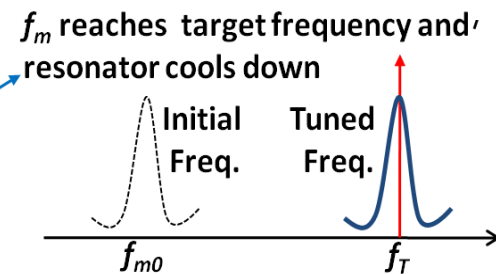
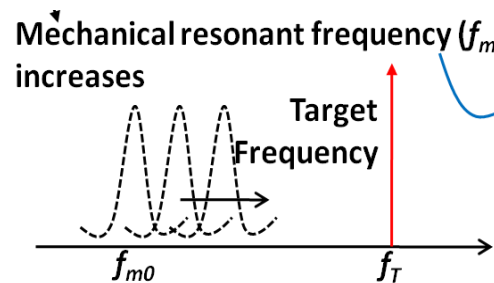
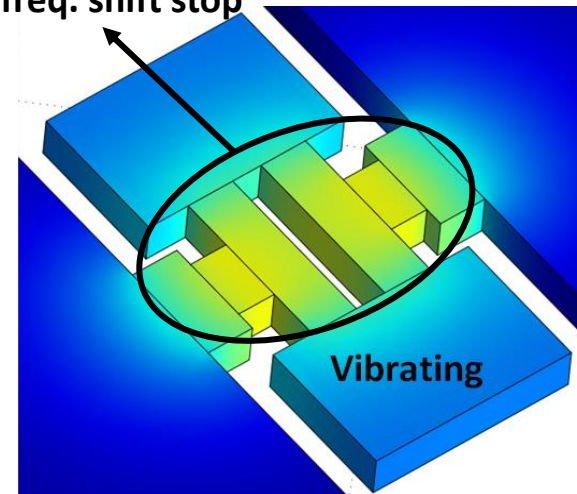
Schematic demo of the autonomous frequency trimming technique

- The cooling effect at resonance, allows the localized oxidation to stop automatically as soon as the resonator frequency reaches the targeted actuation frequency

Silicon dioxide forming on the hot surfaces

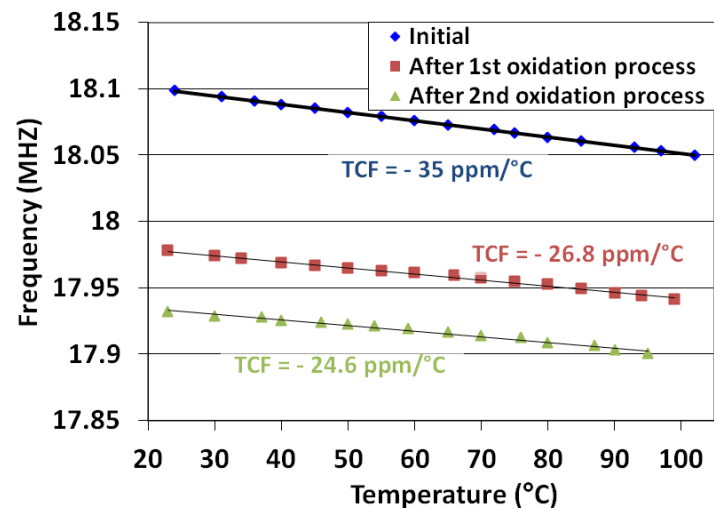
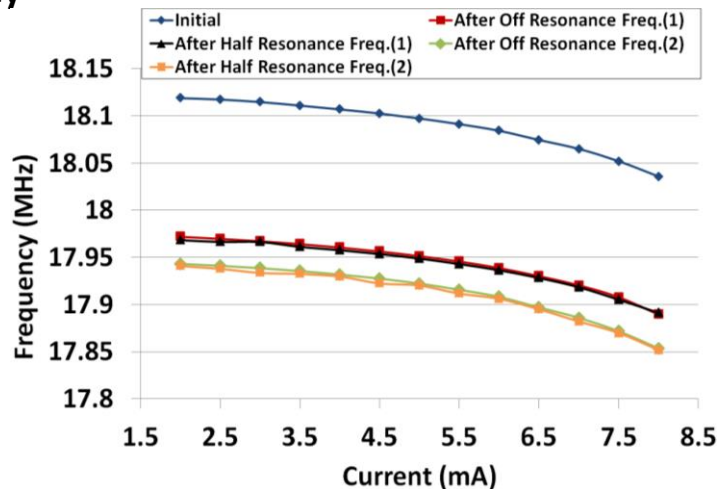
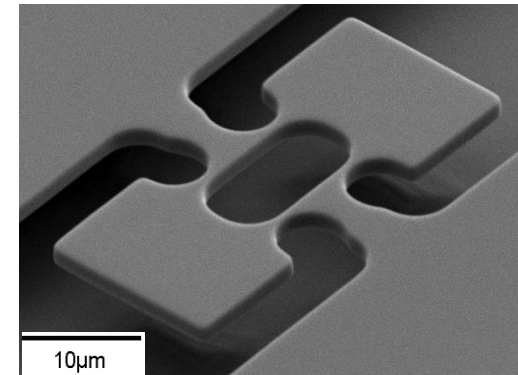
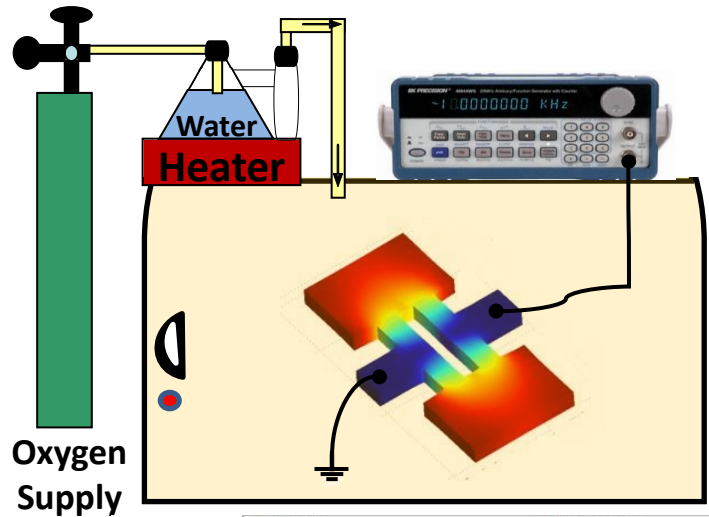


Silicon dioxide formation and freq. shift stop



Measurement Setup and Results

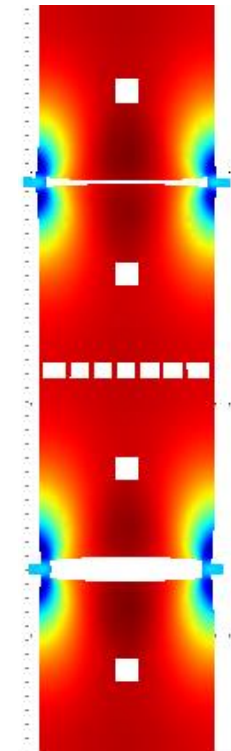
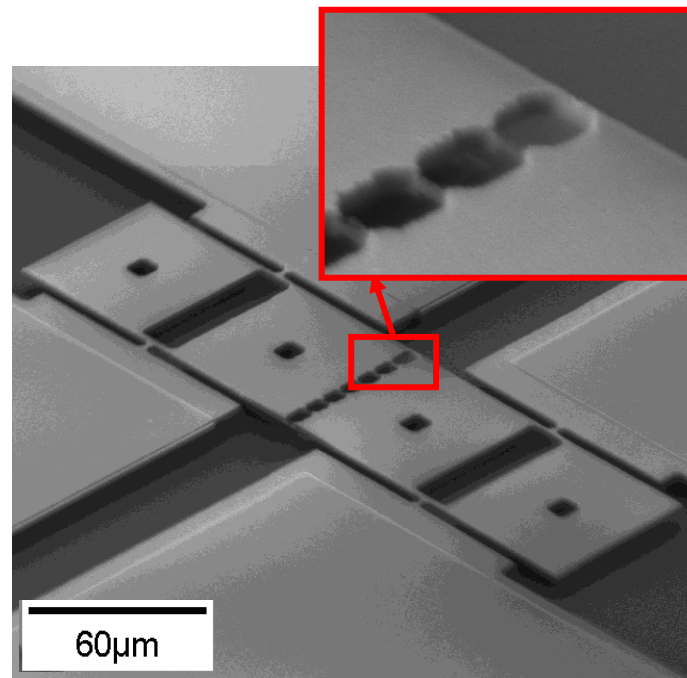
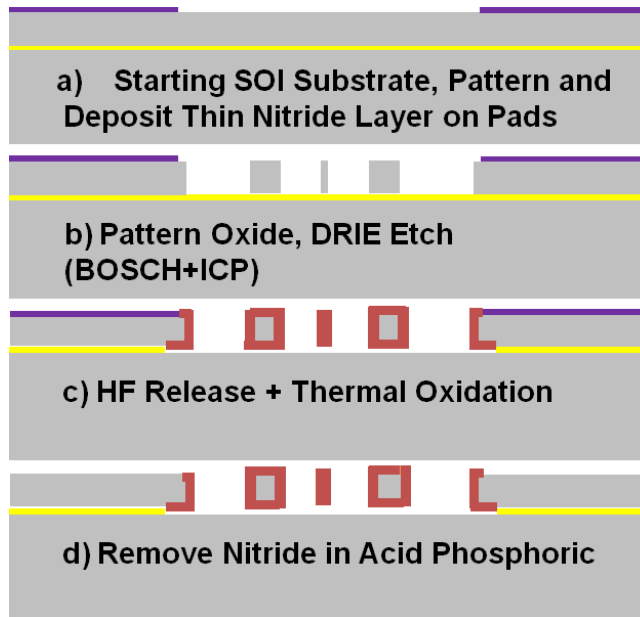
- Changes in dimensions and Young's modulus as well as internal stress caused by oxidation results in a permanent change in the resonant frequency of the device



Input-Output Insulation in Thermal-Piezoresistive Resonant Microstructures using Embedded Oxide Beams

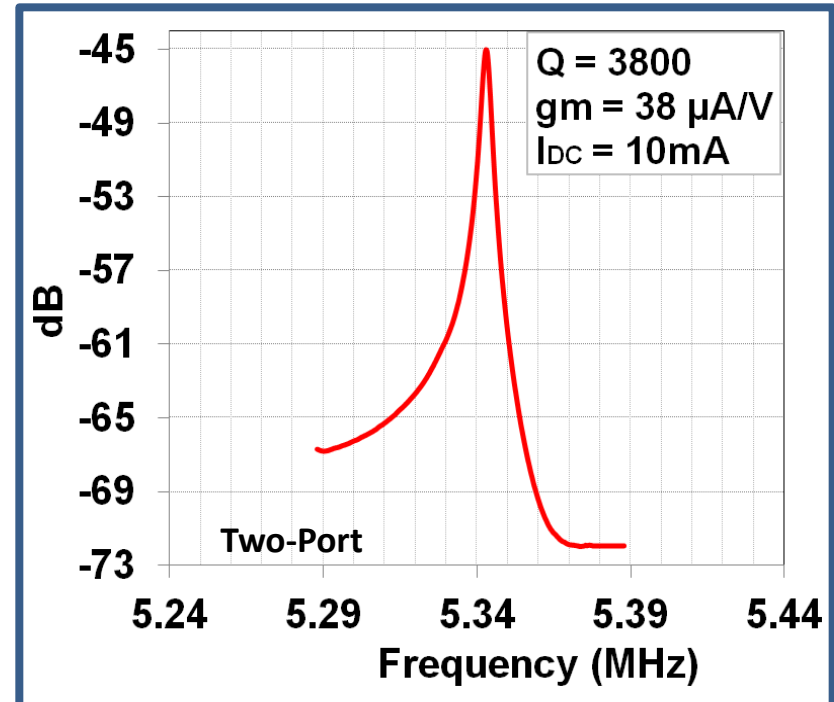
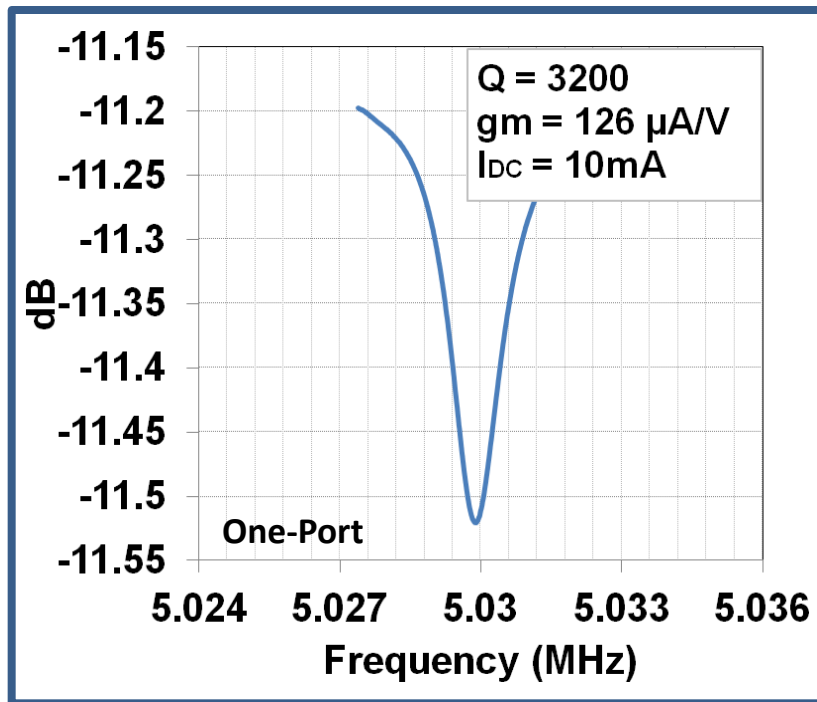
Presentation in International Frequency Control Symposium 2012:

- Thermally actuated MEMS resonators with electrically insulated input and output ports
- Significantly reduced feed through current makes it possible to use such resonators in electronic circuits as frequency selective components
- Eliminates the data processing required to extract the motional conductance and Q factor of such resonators from measurements



Measurement Results

- The downward resonance peak in the one-port device is due to the negative piezoresistive coefficient of the structural material (N-type Si), while the out of phase motion of the two sections in the two-port device results in an upward resonance peak
- The resonance peak for the two port resonator has much larger amplitude due to elimination of feed-through



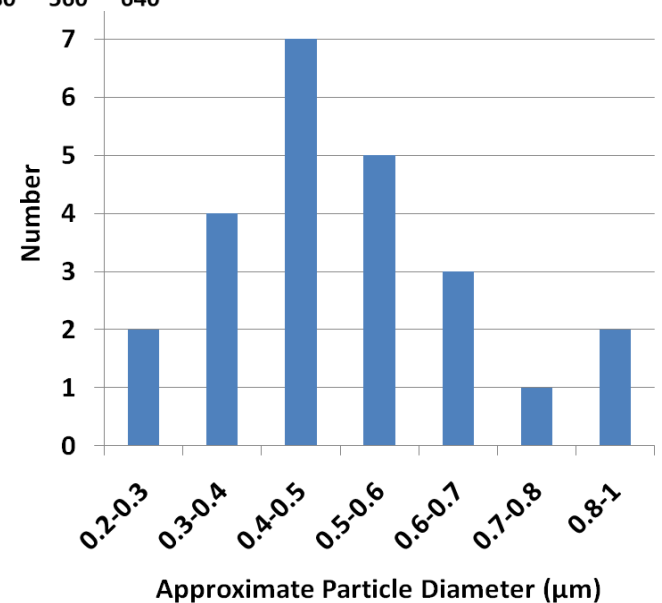
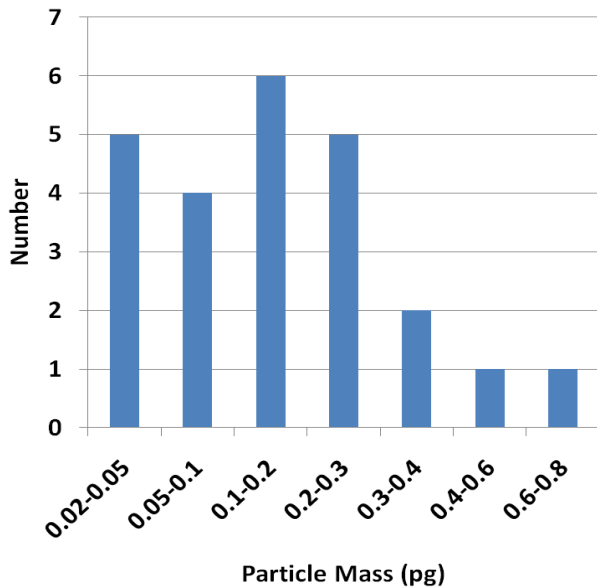
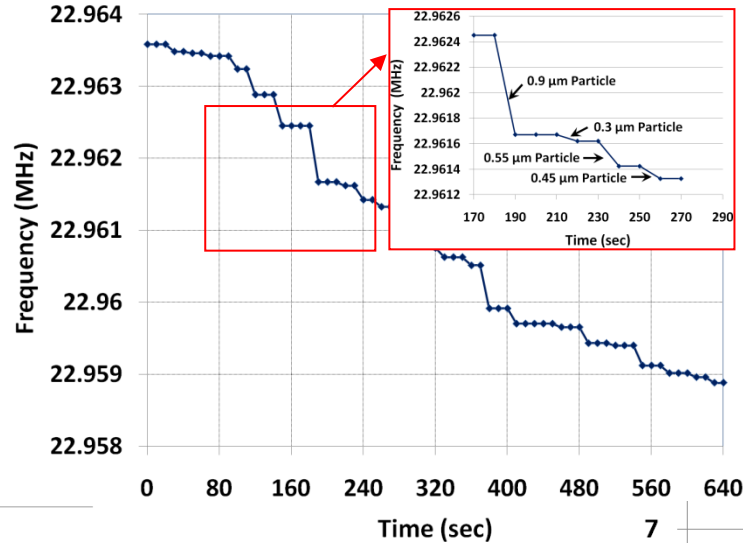
Silicon Nonowire Fabrication Technique

- ❑ Silicon nanowires have great potentials in nanoelectronics and nano-electro-mechanical systems:
 - Huge piezoresistive coefficients
 - Large dependence of electrical conductivity to molecular adsorption
 - Extremely high mass sensitivity of nanowire resonators

- ❑ Costly and time consuming processes: no controlled batch-fabrication capability in any of the proposed fabrication methods

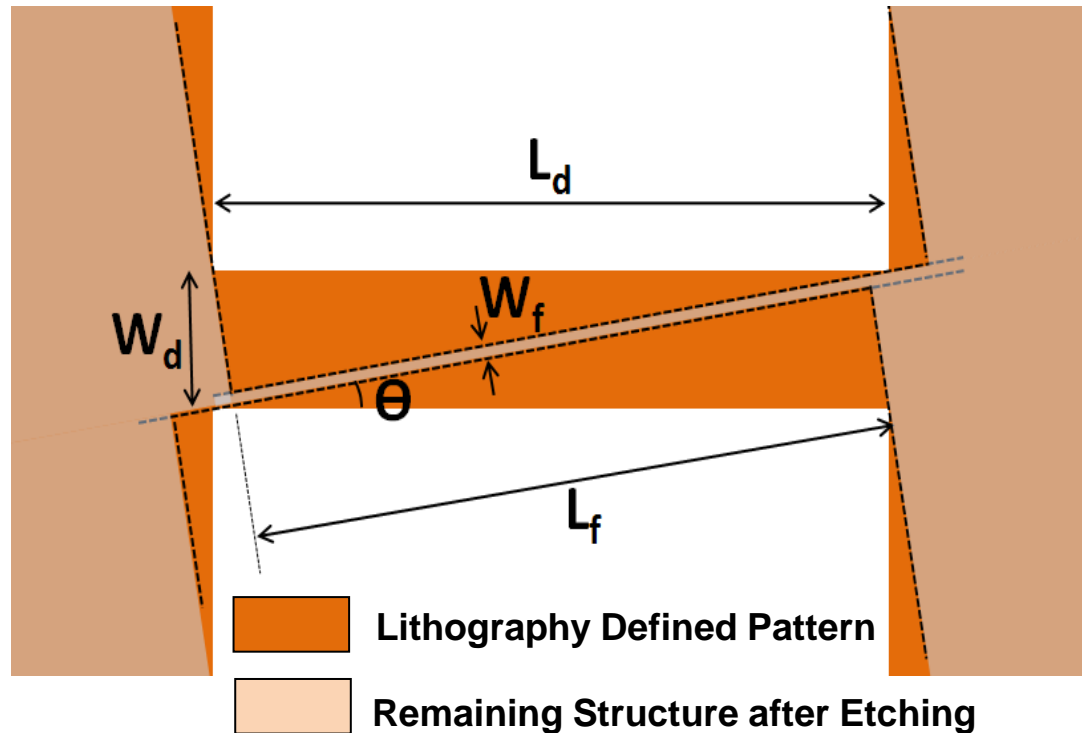
- ❑ Our Method: low cost, controllable process, the ability to be integrated in N/MEMS structures such as high frequency thermal-piezoresistive resonators

Arbitrary Airborne Particle Measurements

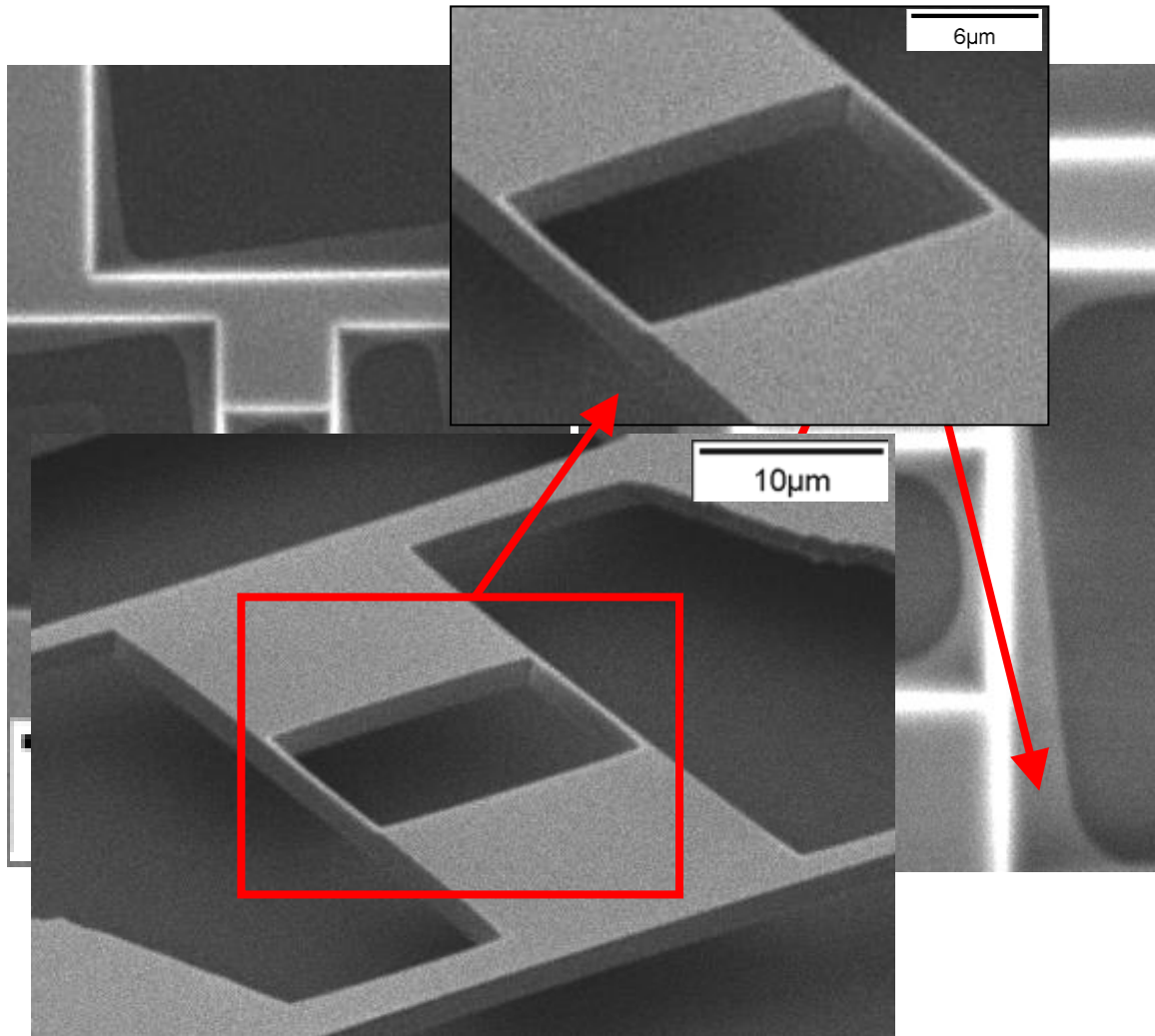


Controlled Batch Fabrication Of Crystalline Silicon Nonowires

- ❑ Using the Anisotropic wet etching of silicon in alkaline solutions (e.g. KOH or TMAH)
- ❑ Rotational misalignment between the photo-lithography defined patterns and the crystalline orientation of silicon



Fabrication Results



Fabrication Results

